Prepared for:

Rijkswaterstaat, Dienst Getijdewateren

Coastal Genesis Project

Morphodynamic Modelling for a tidal inlet in the Wadden Sea

"Het Friesche zeegat"

Progress Report, H 840-50, Part II

December 1991

delft hydraulics

Morphodynamic Modelling for a tidal inlet in the Wadden Sea

"Het Friesche zeegat"

Zheng Bing Wang

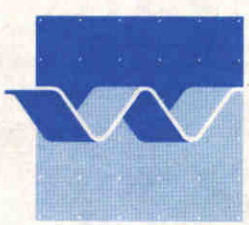

delft hydraulics

CONTENTS

LIST OF FIGURES

LIST OF FIGURES

1 INTRODUCTION

Morphological development in coastal and estuarine areas is a fascinating natural phenomenon, on which our understanding is still limited. Knowledge about this process can be improved by observations in nature and by model studies. In the present study a model is set up in order to investigate the morphological processes in the tidal inlets in the Wadden sea.

In recent years, substantial effort has been put into the numerical modelling of morphological changes in complex three-dimensional situations. For tidal inlets, estuaries and coastal waters, however, this has not yet resulted in sufficiently reliable morphological predictions at intermediate time scales (10-30 years). On the other hand numerical morphological models, based upon elementary hydrodynamic laws, have proved very useful to give insight in the actual coastal morphodynamics.

There are various mathematical models for morphological development in coastal and estuarine areas (Gerritsen, 1990, Steijn, 1991, De Vriend, 1991). These models can be classified into two categories, viz. models based on empirical relations and dynamic models. The equations in the first category of models are based on the observations in nature and they are purely empirical. The empirical relations only work with general morphological features e.g. cross section area of channels, volume of the delta etc., but do not provide detailed information about for instance the shape of a channel. They do not work with detailed information about the flow field but work with integrated information such as tidal volume. The sediment transport rate is often not in the empirical relations. On the other hand the dynamic models are based on the mathematical description of the motion of water and sediment. They work with detailed flow field information and provide detailed information about the variation of the bed level in time and space. Calculation of the sediment transport field is an essential part of the dynamic models. The empirical models have already proved their value for solving practical problems whereas experience with the application of the dynamic models is still very limited. However, the dynamic models can be more useful for learning about the processes in a morphological system.

The main purpose of the study is to obtain a better understanding of the morphological system in the tidal inlets, rather than to make specific predictions of the morphological development in a particular tidal inlet. Therefore the model will work with a schematised geometry and bathymetry rather than with the detailed geometry and bathymetry of one particular inlet.

For this purpose a morphodynamic model for "Het Friesche Zeegat", a tidal inlet system in the Wadden Sea (fig.1.1), is developed as a pilot model (Wang 1991). Since 1969, this tidal inlet system, with an area of about 450 km^2, has undergone significant morphological changes due to the closure of

the Lauwerszee. As a consequence the tidal volume has been reduced by about 34%.

The morphological development of this tidal inlet system since the closure of the Lauwerszee has been well documented. The deeper parts of the outer delta are eroding, large longshore bars are developing, the tidal channels are shoaling and the eastern water shoal is shifting eastward.

The study which is done in the framework of the Working Group "Interrupted Coast" of the Coastal Genesis Programme, will be carried out in several phases:

1. model definition;
2. initial runs;
3. development from "plane" bed;
4. equilibrium situation before 1969;
5. development after 1969.

Phase 1 and part of phase 2 of this program were carried out in 1990 and reported by Wang (1991). The present report describes the results from the research carried out in 1991.

The present study is carried out with the DELMOR model, of which a brief description of the mathematical formulations is described in chapter 2. In chapter 3 the main characteristics of the model set up during phase 1 are summarised. An extended description of the model set up is given by Wang (1991). Phase 2 of the program was already started in 1990 and it is finished in 1991 by carrying out a number of additional runs. The results of these initial runs are reported in chapter 4. Chapter 5 describes a number of long-term morphological runs carried out with "plane" bed as initial bathymetry (phase 3). Further a sensitivity analysis has been carried out and described in chapter 6. For this sensitivity analysis initial computations as well as long-term computations were carried out. A first start of phase 4 is also made in 1991 but no computations have been carried out yet. Finally the main findings of the study up to now are summarised and discussed in chapter 7.

The present progress report, prepared for Rijkswaterstaat, is written by Dr.ir.Z.B. Wang. The author is indebted to Dr.ir.H.J. de Vriend from DELFT HYDRAULICS and Drs.T. Louters from Rijkswaterstaat for their support during the research. The members of the Working Group "Interrupted Coast" of the Coastal Genesis Programme are acknowledged for the discussions which have been very valuable for the present study. Ing. R. Bruinsma is involved in carrying out the computations.

2. THE MATHEMATICAL MODEL

2.1 Simplifying Assumptions

The morphological evolution around a tidal inlet is the result of a very complicated interaction of tide, wind, waves and sediment. Since our understanding of the physical process and the behaviour of the model is still limited, the following simplifications are made:

- the effect of wave action on the flow and on the sediment transport is neglected,
- density currents are not taken into account,
- the sediment is non-cohesive, and
- the sediment consists of one single fraction.

In the case of the Wadden Sea the density flow is not important because of the small fresh water inflow. The wave action, however, can play an important role in the whole system. Still, most of the empirical relationships describing the equilibrium state of the principal morphological units in tidal inlets systems do not include any wave influence, whereas they appear to be well applicable for Wadden Sea inlets (Gerritsen, 1990). This is an indication that even a model which disregards the wave influence could describe important aspects of the morphological behaviour. Moreover, the influence of wave action on the sediment transport can be included in a crude approximation by modifying the bed shear stress.

2.2 General Outline of the Model

The model is based on DELMOR, a program package to simulate morphological evolutions, which was developed by DELFT HYDRAULICS. The program consists of the following basic modules:

- A 2.5D current module, which is based upon TRISULA (Stelling and Leendertse, 1991) solving the complete shallow water equations.
- A quasi-3D sediment transport module describing bed load and suspended load transport due to current and waves. For the time being sediment transport due to waves can only be incorporated by modifying the bed shear stress.
- A sediment balance module yielding the sedimentation and erosion rate

and the new bed level.

The modules are coupled as indicated in fig.2.1, with a "quasi-steady' morphodynamic time-stepping mechanism, i.e. during the flow computation the bed level is assumed to remain invariant and during the computation of the bed level (with a time step of a number of tidal periods) the flow and sediment transport are assumed invariant to the bed level changes. This approach was first described by De Vries (1959) for morphological computations in rivers. More complicated procedures for morphological computations in tidal regions have been studied by Haugel(1978), and Latteux (1987). However, the experience in the application of these procedures is still very limited. Therefore this study will be limited to the straightforward procedure shown in fig.2.1, which implies the following basic assumptions:

- the time scale of the bed level change is much larger than the time scales of the flow and of the sediment transport, and

- the sediment concentration is so small that the presence of sediment in the water has a negligible influence on the flow.

2.3 The Current Module

The flow computation is based on the so-called 2.5D approach. First the depth averaged flow field (the main flow) is computed by solving the shallow water equations. This is done with TRISULA, a program package of DELFT HYDRAULICS for shallow water flow simulation.

The vertical structure of the flow is determined afterwards. The velocity profile in the direction of the main flow is assumed logarithmic. In the cross-stream direction the secondary flow model of Kalkwijk and Booij (1986, also see De Vriend, 1981) is applied. Computations have shown that the secondary flow has significant influence on the sediment transport (Wang, 1991, Wang et al., 1991).

The secondary flow model takes into account the influence of the curvature of the main flow stream-line and of the geostrophic acceleration (assuming Ekman depth >> water depth). The vertical profile of the cross-stream velocity component is assumed to be linear (fig.2.2). The intensity of the secondary flow I, which is defined as the cross-stream velocity averaged over the upper half of the water depth, is computed from

$$L_s \frac{dI}{ds} + I = I_e \qquad (2\text{-}1)$$

In this equation, s is the horizontal coordinate in the main flow direction and L_s is the relaxation length of the secondary flow:

$$L_s = \frac{1-2\alpha}{2\alpha\kappa^2} h \qquad (2\text{-}2)$$

with

$$\alpha = \frac{\sqrt{g}}{\kappa C} \qquad (2\text{-}3)$$

g = gravity acceleration
κ = Von Karman Constant
C = Chezy coefficient
h = water depth

I_e is the intensity of the fully developed secondary flow:

$$I_e = \frac{2U_s h}{\kappa^2 R_s} + \frac{fh}{\kappa^2} \qquad (2\text{-}4)$$

with:
U_s = depth averaged main flow velocity,
R_s = radius of curvature of the stream-line,
f = coefficient for geostrophic acceleration (Coriolis force).

2.4 The sediment transport module

The sediment transport is divided into a bed load and a suspended load part. The bed load transport is calculated with a transport formula, e.g. van Rijn's (1984a). Further the downslope gravitational effect on the magnitude of the transport is taken into account via

$$S_b = S_{be} \left(1 - \alpha_b \frac{\partial z_b}{\partial s}\right) \qquad (2\text{-}5)$$

Herein

S_b = bed load transport rate,
S_{be} = bed load transport rate according to the transport formula,
α_b = constant coefficient,
z_b = bed level.

The downslope effect on the direction of the bed load transport is included via

$$tg(\phi) = tg(\delta) - \gamma \frac{\partial z_b}{\partial n} \qquad (2\text{-}6)$$

Herein

δ = angle between bed shear stress and s-direction,
ϕ = angle between the bed load transport and s-direction,
n = horizontal coordinate in the lateral direction,
γ = coefficient depending on the Shield parameter.

The suspended load transport is modelled by a quasi-3D approach based on an asymptotic solution of the 3D convection-diffusion equation for the sediment concentration. This approach was first presented by Galappatti (1983, also see Galappatti and Vreugdenhil, 1985) for the 2D-vertical case and later extended by Wang (1989) to the 3D case.

First, the depth averaged sediment concentration C is computed by solving the following equation

$$\frac{\partial C}{\partial t} + U\frac{\partial C}{\partial x} + V\frac{\partial C}{\partial x} - \frac{\partial}{\partial x}(D\frac{\partial C}{\partial x}) + - \frac{\partial}{\partial y}(D\frac{\partial C}{\partial y}) = \frac{C_e - C}{T_a} \qquad (2\text{-}7)$$

in which

t = time
U, V= depth averaged flow velocity in x- and y-direction
x, y= horizontal Cartesian coordinates
D = horizontal diffusion coefficient

In the right-hand part of equation (2-7) C_e is the equilibrium depth-averaged concentration which is calculated from a transport formula, e.g. Van Rijn's (1984b). T_a is the adaptation time derived from the quasi-3D model, which expresses the relaxation effect of the suspended sediment concentration. Computations have shown that the relaxation effect is important in the present case (Wang, 1991).

$$T_a = \tau \frac{h}{W_s} \qquad (2\text{-}8)$$

In which W_s is the fall velocity and τ is a coefficient depending on W_s/U_* (fig.2.3) where U_* is the bed shear stress velocity.

The quasi-3D model also provides information on the vertical structure of the sediment concentration, which depends on the parameter W_s/U_* and on the defect-concentration C_e -C. The resulting 3D concentration field c (t,x,-

y,z) can be used to determine the transport rates, using

$$S_x = \int_{z_b}^{z_b+h} (uC - D\frac{\partial C}{\partial x})\, dz \qquad (2\text{-}9)$$

$$S_y = \int_{z_b}^{z_b+h} (vC - D\frac{\partial C}{\partial y})\, dz \qquad (2\text{-}10)$$

Where

S_x, S_y = suspended transport rate in x- and y-directive,
u, v = flow velocity in x- and y-direction.

Since the flow velocity profile as well as the sediment concentration profile are constructed from standard profile functions which can be determined a priori, equations (2-9) and (2-10) can be parameterized. The parameterized equations are used in the program.

2.5 The Bed Level Module

The bed level is calculated from the mass balance equation for sediment:

$$\frac{\Delta Z_b}{NT} + \frac{\partial T_x}{\partial x} + \frac{\partial T_y}{\partial y} = 0 \qquad (2\text{-}11)$$

where

ΔZ_b = bed level change in N tidal period,
N = an integer number,
T = tidal period,
T_x, T_y = residual sediment transport computed over one tidal period.

3. Schematisation

3.1 Introduction

The model was set up last year. A description of the schematisation is given in Wang (1991). In this chapter the main features of the model schematisation are summarised.

3.2 Planform

The real situation of the tidal inlet is shown in fig.1.1. The basin behind this inlet is roughly rectangular of shape and covers an the area of about 195 km^2 (DELFT HYDRAULICS, 1979). The gorge between the two barrier islands has a width of about 10 km. Both barrier islands are approximately parallel to the coast of the main land. The western island has a width of about 2 km and the width of the eastern island is about 3 km. The geometrical schematisation is such that the main features of the system are represented, whereas details are determined by the shape of the computational grid rather than by the actual geometry. The longshore extent of the sea area should be about 30 km and the cross-shore extent should be some 10 km, in order to let the model include entire outer delta without being affected by the adjacent tidal inlets.

3.3 Computational Grid

In order to decide upon the computational grid, various designs have been tested in preliminary computations (Wang 1991). In these preliminary computations the bed level was kept constant throughout the area, at 5 m below mean sea level. Based on these preliminary computations the grid shown in fig.3.1 was chosen. As shown in this figure the sea area in this model is a semi-circle and the two barrier islands are schematised into rectangles with semi-circular heads.

3.4 Bathymetry

The bed level measured in 1970, shortly after the closure of the Lauwerszee, is shown in fig.3.2. This bathymetry will be used to test the flow field and sediment transport modules. The objective of the study, however, is to learn more about the morphodynamic processes and about the behaviour of the dynamic model. One of the questions in this respect is whether or not the model will be able to establish the natural bathymetry, starting from a certain initial bathymetry. Therefore the model will mainly be used

with a schematised initial bathymetry. The horizontal bed used in the preliminary runs can be considered as one of these bathymetries. The results of one of these preliminary runs will be discussed in he next chapter. However, a horizontal bed is not a good choice as an initial bathymetry in a long-term run, because the volume of the basin is too large. Hence it will take a very long time for the basin to develop any-thing near a natural condition. Therefore another schematised bathymetry was introduced (fig.3.3). In this bathymetry the total volume of the tidal basin is about the same as in the natural condition. For generating this bathymetry the following information is used (DELFT HYDRAULICS, 1979).

- the area of the tidal basin at high water is 195 km^2
- 25% of the tidal basin lies below low water
- the average tidal range is 2.25 m
- the tidal volume is 300.10^6 m^3.
- the mean water depth at the gorge is 4.5 m
- the offshore bed slope is $2^o/_{oo}$.

As far as can be assumed on the basis of the present knowledge, this schematised bathymetry differs from the natural situation mainly in the absence of the shoal-channel system. This should provide a good test in the model's ability to represent the formation of a shoal-channel system.

Another bathymetry is constructed by applying a smoothing procedure to the realistic bathymetry shown in fig.3.2. The bed level is only smoothed in the lateral direction, i.e. along the grid lines N=constant. The smoothing procedure consists of a diffusion operator which is applied a number of times. The bathymetry constructed according to such a procedure has the advantage that the total amount of sand in the whole system is exactly the same as in the realistic situation. The smoothed bathymetry is shown in fig.3.4.

3.5 Boundary Conditions

At the open sea boundary the water level will be prescribed as boundary conditions for the flow computation. The tidal amplitude as well as the phase angle are allowed to vary along this boundary. Later it will be shown that the residual flow pattern in the region near the open boundary is very sensitive to this boundary condition. All the other boundaries are closed.

The depth averaged sediment concentration at the open boundary is computed from

$$\frac{\partial C}{\partial t} = \frac{C_e - C}{T_e} \qquad (3\text{-}1)$$

This so-called quasi-equilibrium concentration is applied as a boundary condition for equation (2-7).

In the long-term runs the bed level change rate at the open boundary is set to zero.

4. Initial Computations

4.1 Introduction

Initial computations are computations of only one morphological time step. The periodic flow and sediment transport are calculated with the initial bed level during one tidal period. Integration of the sediment transport gives the residual sediment transport field which in turn determines the bed level change rate per tidal cycle.

Initial computations, requiring relatively much less computational efforts than the long-term computations, are very useful during the set up stage of a morphological model and for the sensitivity analysis when many computations are needed.

Within the framework of this project a series of initial computations have already been carried out in 1990. Based on these computations, a computational grid has been chosen and some useful conclusions have been drawn about the effect of the secondary flow and the influence of the relaxation effect of the suspended sediment transport (Wang, 1991). However, these computations were all carried out with schematised bathymetries, viz. either the constant bed level or the bathymetry shown in fig.3.3. The open sea boundary condition for the flow computation was also strongly schematised, viz. one single tidal component with a phase lag between the two ends of the boundary. One of the conclusions drawn from the 1990 computations was that the residual flow field and the residual sediment transport field are very sensitive to the boundary condition at the open sea in combination with the bathymetry. Therefore it is logical to carry out more computations with a more realistic bathymetry and/or more realistic boundary conditions.

4.2 Computations with Realistic Bathymetry

The computations described in this section are carried out with the fine grid and the realistic bathymetry as shown in fig.3.4, which is based on the data from 1970, short after the closure of the Lauwerszee. The open sea boundary condition is still schematised.

4.2.1 Run e32

At the open sea boundary the water level is prescribed. A single tidal component is applied with

tidal period: 12.5 hour,

mean water level: -0.175 m NAP,
tidal range: 2.2 m,
phase lag between the two ends of the boundary: 0.62 hour.

Compared with the computations carried out in 1990 the mean water level is lower and the phase lag is smaller. These modifications are based on DELFT HYDRAULICS (1979).

Other important input parameters are:

Madian grain size of sediment : D50 = 160 μm,
Fall velocity : w_s = 0.01 m/s.

The sediment transport formula of Van Rijn (1984a, 1984b) is applied for calculating the bed load transport rate and the equilibrium suspended sediment concentration. The secondary flow as well as the relaxation effect of the suspended sediment transport are included.

The flow computation is carried out for three tidal periods. During the last two periods, the sediment transport is also simulated. The residual sediment transport during the last period is used for calculating the bed level change rate.

Fig.4.1 through fig.4.5 show the water level and flow velocity at the following five stations (fig.3.1):

Station nr.	M	N
1	8	52
2	21	52
3	31	52
4	21	31
5	21	19

All these five figures show that periodic flow is established after one tidal period. It should further be observed that the water depth at station 5 is very shallow and it is only flooded during a small time interval within the tidal period.

The sediment concentration and transport in the same stations are depicted in fig.4.6 through fig.4.10. These figures illustrate that the sediment transport mainly occurs during a small period in which the flow velocity is high.

A typical velocity field during flood is shown in fig.4.11. The residual flow field is shown in fig.4.12. The residual current is directed eastward

in the outer delta area. Further outside, in the sea area, a large scale circulation can be observed. In the western part, the residual flow is directed into the model area whereas in the eastern part it is directed outwards. In the gorge and in the tidal basin a system of circulation cells are present. It should be noticed that in this figure the net water flux during the tidal period is shown. In order to obtain the residual flow velocity it has to be divided by the tidal period and the local water depth.

The residual sediment transport during the last period is shown in fig.4.-13. The residual sediment transport rate in the outer area appears to be relatively small. The residual transport is largest in the deep channels in the inner area and around the gorge. This is a major difference with the residual transport field calculated with the schematised bathymetry, where the residual transport is largest in magnitude around the heads of the two barrier islands. Further the magnitude of the residual transport in the Pinkgat area appears to be much larger than that in the Zoutkamplaag area. The net sediment transport through the gorge is outwards.

It should be noted that the residual sediment transport is a small difference between the ebb- and flood-transport, both much larger in magnitude. This can be seen in fig.4.6 through fig.4.10 and it is more clearly illustrated in fig.4.14 through fig.4.17 in which the instantaneous and accumulated sediment transport through 4 cross sections are shown. This is probably the main reason why the residual flow field and the residual sediment transport field are very sensitive to the small changes in boundary conditions and bathymetries. The four cross sections are defined as follows (fig.3.1).

cross section nr	N	M
V03	57	2 - 40 (Mmin - Mmax)
V06	48	2 - 40 (Mmin - Mmax)
V09	31	2 - 40 (Mmin - Mmax)
V12	20	2 - 40 (Mmin - Mmax)

4.2.2 Run e40

The input of this run is exactly the same except that the open sea boundary condition is slightly changed. The open sea boundary is divided in smaller sections and the phase lags between the boundary points are such that the phase is a linear function of the distance from west to east along the barrier islands. In run e32 the water level is a linear function of the distance along the grid line. The tidal period, the mean water level, the tidal range and the total phase lag between the two ends of the boundary remain exactly the same as in the run e32. This small modification in the

boundary condition is made in the hope that the pattern of the residual flow field and the residual sediment transport field in the boundary region can be improved.

The residual flow field and the residual sediment transport field are respectively shown in fig.4.19 and fig.4.20. In the inner region of the model area no significant difference can be observed from run e32, see fig.4.12 and fig.4.13. However, in the boundary region the residual flow pattern as well as the residual sediment transport pattern changed dramatically, although the hoped improvement is not realised. Apparently the minor change in the boundary condition has a very large influence on the residual flow field and residual sediment transport. This stresses the conclusion again that the residual flow and the residual sediment transport in the boundary region are very sensitive to the boundary condition for the flow.

As mentioned earlier, the strong sensibility is probably caused by the fact that the residual flow and/or transport is much smaller than the instantaneouse flow and/or transport rate. A fact supporting this idea is that the instantaneous flow velocity itself is not very sensitive to the boundary condition. Fig.4.21 shows the velocity field at the same time as the one shown in fig.4.11. No significant difference between the two figures can be observed.

4.3 Computations with Realistic Boundary Condition

More attention is required to the open sea boundary condition because of the sensitive dependence of the residual flow field and residual sediment transport field on it. Therefore a simulation (run e03) is carried out for a realistic situation, viz. the situation in a 25 hour period from Jun 8 14:00 to June 9 15:00, 1971. As in run e32 the bathymetry measured in 1970 (fig.3.4) is used in this simulation.

The water level data in the boundary grid points (N=62, M=2 to 14 and M=28 to 40) are produced by Rijkswaterstaat with OOSTWAD, an operational model for tidal flow computation in the Wadden sea. The data are presented with a time interval of 10 minutes. No data is available in the centre section of the boundary (N=62, M=15 to 27).

A Fourier analysis is carried out with the data available. Five components were established from the analysis. The amplitude and phases of the Fourier components at the grid points M=2 (the western end of the model boundary), are shown in fig.4.22. The component a2, which has about the same frequency as the tidal component M2, is far the most important component. Further, the component a4, which is comparable to the tidal component M4, has an amplitude of about 10% of that of a2 and is the most important higher

frequency component.

The variation of the amplitude as well as the phase of the Fourier components along the boundary is shown in fig.4.23. It is remarkable that the mean water level (a0) decreases from west to east.

At the grid point M=21 the Fourier components (amplitude and phase) are determined by a second order interpolation using the available data on the other two sections of the boundary. The centre section of the boundary (m=15 to 27), where no data is available, is then divided into two sections and in each section the boundary condition is determined by interpolation.

Other input data for the simulation is the same as in the run e32 described in the previous section, except that the tidal period is now 25 hours instead of 12.5 hours.

The simulation is carried out for two cycles (i.e. 50 hours). The first period is used for establishing the periodic flow and the output from the second period is presented. The residual flow field determined from the last period of 25 hours is shown in fig.4.24. It appears to be seriously disturbed in the boundary region. In the inner region of the model area the pattern looks very similar to the results from the run E32. Apparently during the determination of the boundary condition some error is induced. The small error in the boundary condition has caused the unrealistic pattern of the residual flow field.

The unrealistic pattern cannot be observed in the instantaneous flow field. Typical velocity fields during flood and ebb are respectively shown in fig.4.25 and fig.4.26.

Some attempts have been made to modify the boundary condition such that the residual flow pattern becomes more realistic, but all of them have failed. One of the attempts involved the closure of the centre part of the boundary where no data is available. In this way the flow in this part of the boundary is forced to follow the boundary direction. This has led to the residual flow field as shown in fig.4.27. After all the attempts it has been concluded that it is very difficult, if not impossible, to make the residual flow field realistic in the whole model area by adjusting the boundary condition for the flow.

The residual sediment transport field is shown in fig.4.28. Compared with that from the run e32 (fig.4.13) it is remarkable that the net sediment transport in the channels is now directed inwards instead of outwards. It should be noted that the component a2 in the boundary condition is far the most important one. This means that there is no large difference between the boundary conditions in the two runs. Nevertheless the residual trans-

port fields from the two runs show significant differences. It has thus to be concluded that the residual sediment transport field is very sensitive to the small changes in the open sea boundary condition. Therefore the open sea boundary condition is a very important factor in the model and it requires more attention in the further study.

The sedimentation erosion pattern from this computation is shown in fig.4.29. It is very scattered as in the run e32. Compared with fig.4.18 the pattern is not much different in the inner region but considerably different in the outer region of the model.

4.4. Concluding Discussions

In summary the following conclusions have been drawn from the initial computations reported in this chapter.

- The residual flow and residual sediment transport are very sensitive to the open sea boundary condition. Small errors in the boundary condition can cause serious disturbances of the residual flow pattern in the boundary region.

- The disturbances appear to be limited in the boundary region. In the inner area of the model the residual flow field is less sensitive to the boundary condition.

- It is very difficult, if not impossible, to correct the boundary condition and make the residual flow field realistic in the whole model region.

- The higher frequency components with relatively small amplitude of the water level variation at the open sea boundary can have significant influence on the residual sediment transport field. This influence is not only restricted to the boundary region but it is important in the whole model area.

The sensitivity of the residual sediment transport field with respect to the open sea boundary condition forms a big problem for the morphological computations. Small errors in the boundary condition, which is nearly impossible to avoid, will cause serious disturbances in the residual sediment transport field and thereby the bed level change in the boundary region. For an initial computation this is not a serious problem since the disturbances appear to be restricted in the boundary region. For the long-term computations, however, the generated disturbances will penetrate into the model area as the computation proceeds. Although more research on the boundary condition is recommended it seems to be that some errors in the

boundary condition is inevitable. Therefore a solutions has to be found in order to avoid that the disturbances at the boundary penetrate into the model area. In the following chapter it is suggested to solve this problem by excluding the boundary region where the disturbances are present from the morphological computation. In other words the morphological model is made smaller than the flow-transport model (see 5.3).

An important message from the computation with the realistic boundary condition is that although the higher frequency tidal components have much smaller magnitude than the semi-diurnal tide they may have significant influence on the residual sediment transport and the morphological development. The importance of the higher frequency components on the morphological computation is a subject in the sensitivity analysis reported in chapter 6.

The computations also show that one tidal period (of 12.5 hours) is enough for the model to establish periodic flow. This information will be used in the long-term computations. After each morphological time step the periodic flow is disturbed due to the bed level change. One tidal period will be used for establishing the periodic flow with the new bathymetry after each morphological time step. This applies to all the morphological computations described in this report.

5. Long-term Computations

5.1 Introduction

A first long-term computation was already carried out in 1990. The computation was carried out with the coarse grid and schematised bathymetry without the central shoal (Engelsmanplaat). The computation showed that significant morphological changes only occur in the gorge area, especially around the heads of the barrier islands, where serious scour and siltation are observed (Wang, 1991, Wang et al., 1991). The computation became unstable after 16 morphological time steps, immediately after the occurence of (permanent) drying at the outer delta.

The instability of the computation was apparently due to the occurrence of drying which was not correctly handled in the program. The program is unable to modify the computational grid during the morphological computation. Therefore a modification has been made in the program in order to avoid permanent drying due to sedimentation. The modification is such that when the bed level becomes higher than a certain critical level due to sedimentation, a local smoothing procedure is applied to bring the bed level below the critical level.

Compared with the realistic bathymetry the schematised bathymetry used in that computation misses an important element, viz. the sand bank "Engelsmanplaat", which divides the inlet under consideration into two gorges. The computation did not show the generation of this sand bank, in contrast to what was hoped, causing some doubt with respect to the applicability of the model. The first computation carried out this year is exactly the same as the one carried out last year except a central bank is added in the initial bathymetry. This computation is described in the following section. As the run is successfully carried out it is repeated with the fine grid with a little modification for the open sea boundary condition for the morphological development (section 5.3). In section 5.4 a computation is described with a initial bathymetry which is derived from the realistic bathymetry measured in 1970 by applying the smoothing procedure described in section 3.4.

All the computations described in this chapter have been carried out with a single tidal component (M2) at the open sea boundary condition for the flow. Further it should be noted that the model has not been calibrated quantitatively concerning the magnitude of the residual sediment transport. Therefore the time in the model should not be directly compared with the real time for the morphological development.

5.2 Influence of the Central Bank

The computation last year is repeated (run W40) but then with a small change in the initial bathymetry by adding a (permanent dry) central bank between the two barrier islands (fig.5.1). All other input of the computation are kept the same.

The improved program is used for the computation, but the smoothing procedure added has not been needed since no permanent drying occurred during the computation. The computation remains stable and 81 morphological time steps were carried out.

In fig.5.2. though fig.5.4 the computed bathymetry after 17 steps (the moment at which the previous computation became unstable), 41 steps and 81 steps are shown respectively.

The morphological development according to this computation appears to be totally different than that in the previous one. The presence of the central bank seems thus to be essential for the morphological computation.

The figures clearly show the development of a tidal delta around the gorge. It is also interesting that a system of channels and sand banks develop during the run. Although the structure of the channel-bank system is still far from the situation in the real world, the results of this computation are very encouraging.

Local scour and sedimentation around the heads of the barrier islands still occur but they are much less than in the previous computation. Further, some disturbances develop at the open sea boundary although they did not make the computation unstable. They are probably caused by the unrealistic residual sediment transport pattern and the improper boundary condition for the morphological computation (the bed level at the boundary is kept unchanging).

The residual sediment transport field at the initial state and at the end of the run are respectively shown in fig.5.5 and fig.5.6. The morphological development appears to have caused more circulation cells in the residual sediment transport field. The magnitude of the net transport appears to be increased in the outer area and decreased in the inner area and around the gorge.

5.3 Fine Grid

The computation described in this section (run WS6) is basically the same as the one reported in the previous section (W40). However, the fine grid is used instead of the coarse grid (fig.3.1). Further a modification is made in handling the open sea boundary condition for the morphological model.

In the previous run it has been observed that the unrealistic residual sediment transport pattern in the boundary region causes disturbances in the bathymetry development (fig.5.4). Adjustment of the boundary condition for the flow would not solve the problem as was concluded in the previous chapter. Fortunately, in the inner region of the model area where the morphological development is of interest, the residual flow and residual sediment transport are not very sensitive to the small errors in the boundary condition. In the outer delta area, the residual flow and residual sediment transport are directed eastward in all the computations (see chapter 4). Therefore it is decided to make the morphological model smaller than the flow and transport model. The tidal flow and sediment transport are calculated in the whole model area, with the open sea boundary at N=62 (fig.3.1), whereas the morphological development is only calculated within a smaller area ($N \leq 53$). In the boundary region ($53 < N \leq 62$), where the residual sediment transport pattern is unrealistic, the bed level is kept constant in time.

Further the time steps are decreased because of the smaller spatial grid size. The time step Δt for the flow and sediment transport computation is set to 1 minute instead of 5 minutes in the previous computation. The morphological time step is set to 400 tidal periods, i.e. about 200 days instead of 720 tidal periods in the previous computation.

The computation is carried out for 84 morphological time steps. The computed bathymetry after 21, 42, 63, and 84 steps are shown in fig.5.7 and fig.5.8. The main features of the morphological development are similar to the previous computation (run W40). However, the present computation provides more details than the computation with the coarse grid and there are considerable differences between the results from the two computations (see e.g. the shape of the outer delta). It seems to be that the fine grid should be recommended for the morphological computations although then much more computational efforts is required.

Considering the boundary region, the effect of the modification of the boundary condition for the morphological computation can clearly be observed. There are still some disturbances at the boundary region of the morphological model, but much less serious than in the previous computations. The disturbances appear to occur only in the outflow part of the

boundary (part where the residual sediment transport is directed outward). Apparently keeping the bed level constant provides a good boundary condition in the inflow part of the boundary but not at the outflow part. This problem requires further investigation.

The residual sediment transport pattern at the initial state and at the end of the computation are respectively shown in fig.5.9 and fig.5.10. Comparison between the two figures show that the morphological development has led to a system of circulation cells in the residual sediment transport field.

5.4 Smoothed Bathymetry

In this computation (run SM4) the smoothed bathymetry shown in fig.3.4 is used as initial bathymetry. As explained in chapter 3 this bathymetry is obtained by a smoothing procedure applied to the realistic bathymetry measured in 1970, shortly after the closure of the Lauwerszee. The smoothing procedure is such that no sand is added or lost from the model area as a whole. Therefore the total amount of sand in this bathymetry is exactly the same as in the realistic situation in 1970. However, Biegel (1991) shows that siltation has occurred in the model area since the closure of the Lauwerszee. Therefore compared with the realistic case, at present there is a small shortage of sand in the model.

Due to the smoothing, the channel-bank structure is modified. The channels become less deep and the small channels even disappear (fig.3.2 and fig.3.4). The main purpose of the present computation is to investigate the ability of the model to restore the channel-bank structure as in the realistic situation.

The computation is only carried out with the fine grid because the coarse grid will not provide sufficient resolution for the channel-bank structure.

The input of this computation is about the same as in the one reported in the previous section. Only the morphological time step is set to 50 days instead of 200 days.

The computations has been carried out for 116 time steps. The computed bathymetry after 41, 66, 91 and 116 steps are shown in fig.5.11 and fig.5.12. The following observations have been made from these pictures.

- The morphological development in the Pinkgat area is much faster than that in the Zoutkamplaag area. In other words the morphological time scale in the Pinkgat area is much smaller than that in the Zoutkamplaag area. This difference in time scale causes a serious problem for the computation. The time step for the computation is determined by

the smallest time scale, which implies that a very long computation is needed in order to see something happening in the area with the largest time scale. The small time scale in the Pinkgat area is the reason why the time step in this computation is made smaller.

- In the Pinkgat area a channel-bank structure develops which is similar in many features as the one in the original real bathymetry, although the details of the structure still differ considerably from the real one.

- Unrealistic deep scours at the heads of the barrier islands, especially at the western one, still occur. This causes another problem in the computation. Further investigation is needed to solve this problem.

- In the Zoutkamplaag the morphological development is much slower. The orientation of the channel only changes slightly and the channel becomes slightly longer. Probably longer computation is needed in order to see significant change in the channel-bank structure.

- In the outer delta area of the Zoutkamplaag two shallow banks develop and between them a flood-channel develops, which is present in the original bathymetry but smoothed out in the initial bathymetry of this computation.

- A small disturbance occurs at the outflow part of the boundary for the morphological computation similar as in the previous computation.

In fig.5.13 and fig.5.14 the residual sediment transport pattern at the initial state and at the end of the computation are shown. From fig.5.13 it can be observed that the transport in most part of the gorge area is ebb-dominant. Further there is apparently a small disturbance inside the Zoutkamplaag channel which causes large residual transport locally. At the end of the computation the disturbance disappears (fig.5.14) and a system of circulation cells develops in the residual sediment transport field. Further the local deep scour at the western island head makes the pattern of the residual transport there rather unrealistic.

Pictures like fig.5.11 and fig.5.12 only give some overall impression of the morphological development. More detailed information can be obtained by an animation showing the bathymetry after each time step. Such an animation is already provided to Rijkswaterstaat.

A more detailed analysis of the computational results is done by examining the development of the bed level along a number of grid lines. In fig.5.15 through fig.5.18 a number of cross sections around the gorge (N=31) are

shown. In each figure the mean water depth along the cross section in the original realistic bathymetry, the smoothed bathymetry (which is also the initial bathymetry in the computation) and the bathymetry after 100 time steps are compared with each other. In this way it can be examined whether or not the model is able to restore the morphological features which were smoothed out in the initial bathymetry. The figures clearly show the unrealistic local scour at the western island head (M=1). Further in the Pinkgat area channels develop with depth already having the same order of magnitude as in the original bathymetry. In the Zoutkamplaag area it can be observed that inside the gorge (N<31) the main channel is eroding, i.e. restoring its depth although the depth is still much smaller than in the original situation. Outside the gorge (N>31) the channel is silting up , which means that the main channel will not restore its original depth. The development of the flood channel near the eastern islands can also be clearly observed from the figures.

It should be noted that the original bathymetry (1970) may be considered as an "equilibrium" bathymetry under the hydraulic condition before the closure of the Lauwerszee. The present computation, on the other hand, is carried out with the hydraulic condition after the closure of the Lauwerszee. Therefore, even if the model was perfect, the original bathymetry would not be restored. More computations will be needed in order to draw the final conclusion.

Fig.5.19 through fig.5.26 show a number of longitudinal profiles in the Pinkgat area (M=4,6,8,10) as well as in the Zoutkamplaag area (M=27, 29, 33, 36). These figures show again that many of the morphological features in the Pinkgat area are already restored while in the Zoutkamplaag it is still far from restored.

5.5 Development before the Closure of Lauwerszee

The tidal inlet system under consideration has undergone significant morphological changes since the closure of the Lauwerszee in 1969. As a consequence the in- and out-going tidal volume has been reduced by about 34%.

One of the subjects of the present research is to study the equilibrium situation before 1969. The ability of the model to generate the equilibrium bathymetry before the closure of the Lauwerszee will be examined. The computations described in the previous sections show that the model is unable to generate exact the same bathymetry as in the real situation after the closure of the Lauwerszee. It can thus be expected that the model will not be able to generate the equilibrium situation before 1969 either. However, simulations with the Lauwerszee open is very important for the

study since they will provide information on the difference of the behaviour of the model in different situations. Comparison between the computations with the Lauwerszee open to the computations so far will also show if the model is able to simulate the effect of the closure of the Lauwerszee.

The schematised bathymetry before 1969 is shown in fig.5.27. Due to the restriction of the used grid the shape of the Lauwerszee is not exactly the same as in the real case (fig.1.1). However, the main characteristics such as the area of the basin at different levels (thus also the volume), the cross section at the connection with the tidal basin at present are about the same as in the realistic case. This means that the discharge through the connection will be well represented in the model. As the morphological development within the Lauwerszee is not of interest in the present study the schematisation as shown in fig.5.27 is allowed.

In 1991 no computation with the present model has been carried out yet. The computations with the Lauwerszee open are planned to be carried out in 1992.

5.6 Concluding Discussions

In summary three long-term computations are described in this chapter. All of them concern the situation after 1969, i.e. with the Lauwerszee closed. The first two computations (W40 and WS6) are about the same. Both are carried out with the schematised "plane" bed (fig.3.3) as initial bathymetry, but run W40 is carried out with the coarse grid whereas run WS6 is carried out with the fine grid. Run SM4 is carried out with the fine grid and with the smoothed bed (fig.3.4) as initial bathymetry.

Comparison between run W40 and the run carried out last year (Wang, 1991) shows that the plane form of the model domain in the gorge is a critical element in the model schematization. This corresponds with observations in river dynamics, where the width/depth ratio is critical to the channel stability. On the other hand, it is somewhat worrying, that the model itself does not bring the gorge into the required shape. Further research is needed here.

The main characteristics of the morphological development computed with the fine grid are similar to those from the computation with the coarse grid. However, there are still considerable differences between the results from the two computations concerning the details. In fact the coarse grid is unable to provide the required resolution as the grid size is of about the same order of magnitude as the channel width in the real case. Therefore the fine grid is recommended for the further computations.

The boundary condition for the morphological computation at the open sea still requires more research. The modification of this boundary condition in run WS6 with respect to run W40 clearly gives improvement of the morphological development at the boundary region. However, at the outflow part of the boundary disturbances still occur. Apparently keeping the bed level unchanged at the outflow boundary is not a good boundary condition for the morphological model.

The computations show unrealistic local scours at the islands heads, especially at the western one. This is apparently due to the unrealistic schematisation of the geometry there. These scours, although restricted to a small local area, cause a serious problem for the long-term morphological computations. Therefore this problem should be paid more attention to in the study.

The run with the smoothed bed as initial bathymetry (SM4) shows that a structure of shoals and channels with similar characteristics as in the original bathymetry forms during the computation. The computation shows also that the morphological time scale in the Pinkgat area is much smaller than that in the Zoutkamplaag area. This difference in time scale causes another serious problem in the morphological computations. The time step of the computation is restricted by the small time scale so a very long computation is needed in order to simulate the development in the area with the larger time scale.

All the computations show that at the end of the computation more circulation cells develop in the residual sediment transport field than at the initial state (with the schematised bathymetry).

The model is still far from being able to give a quantitative description of the natural process. In fact the time in the model cannot be compared with the real time, because the sediment transport rate have not been calibrated to any field data. Further the structures of shoals and channels formed by the model are still far from those in the realistic case. However, the results obtained so far are encouraging enough to continue research in this direction.

6. Sensitivity Analysis

6.1 Introduction

In this chapter the influences of a number of factors are investigated by a sensitivity analysis. Each time one of the computations reported in the previous two chapters is used as reference and a new run is carried out with one of the aspects in the input changed. Comparison between the results from the two computations gives insight into the influence of the changed factor.

Only physical factors are concerned in the analysis. Influences of the numerical factors such as the grid size and time step were investigated last year when the model was set up. The following factors have been investigated:

- the storms,
- the spatial roughness variation,
- the higher frequency tidal components,
- the bed level sink and/or sea level rise.

In each of the following sections one of these factors is considered.

6.2 Influence of Storms

In the computations up to now, the tide has been considered as the only driving force for the flow. However, in reality many other factors also influence the flow and the morphological development. One of these factors is the wind.

No doubt, the flow and sediment transport at storm situation will be completely different than that at nice weather situation. The question is then, how important is the wind driven flow for the long-term morphological development? In order to answer this question an initial computation is carried out with the same input as the computation WS6 reported in 5.3, but then a storm is included with a wind velocity of 22 ms^{-1} from north-west.

It should be noted that wind does not only influence the depth-averaged flow velocity but it also influences the vertical structure of the flow. Further, at storm situations, the action of short waves usually plays an important role. However, in the present model, short waves and the influence of the wind on the vertical structure of the flow is not implemented yet. This means that only the influence via the depth-averaged flow velocity will be simulated in the computation. Therefore the results of the

present computation should be considered as a first indication of the significance of the wind influence.

The computed residual sediment transport field is shown in fig.6.1. Compared to fig.5.9 the pattern looks completely different. The residual transport is not concentrated anymore around the two islands heads. At the west islands the transport is directed inward whereas at the eastern islands it is directed outward. In the outer area the large scale circulation as in fig.5.9 is not present anymore, and the residual transport is directed eastward in the whole area.

Concerned with the relative importance of the storms it can be observed from the two figures that the order of magnitude of the residual sediment transport in the two situations is about the same. Based on this observation it can be concluded that the storm situation is probably not very important for the morphological development since storms only occur during a small portion of the time.

6.3 Spatial Variation of the Roughness

The local roughness of the bottom will influence the flow and in more extent the sediment transport. In a morphological model like the one under consideration, the roughness of the bottom is usually roughly schematised by using a constant Chezy coefficient or a constant roughness hight over the whole model area. In reality neither the Chezy coefficient nor the roughness hight will be constant over the model area. Therefore the sensitivity of the model with respect to the spatial variation of the roughness is investigated here.

The investigation is done by comparing the results of two computations, one with constant Chezy coefficient ($C=55\ m^{0.5}s^{-1}$), i.e. run SM4 reported in section 5.4 and the other with a constant roughness hight ($k_s=0.05$ m). The computed residual sediment transport from the second computation is shown in fig.6.2. Compared with fig.5.13 very little difference can be observed This means that the different way of schematisation does not influence the residual sediment transport pattern very much. Although the realistic spatial variation of the roughness is not considered in the present analysis, it is concluded that the spatial variation of the roughness is probably not very important for the morphological computations, especially when the schematic computations in the present study are concerned.

6.4 The Higher Frequency Tidal Component

In all the three long-term morphological computations reported in chapter 5 only a single tidal component is taken into account. This is based on two considerations. First, the M2 component is far the most important component in the present case. Second, the higher frequency components like M4 are usually generated in the shallow water regions. If the open sea boundary is located far enough from the region of interest the required M4 component will be generated even when only a M2 component is prescribed at the boundary (Van Dongeren, 1991). However, the initial computations described in chapter 4 indicate that the higher frequency tidal components at the boundary, especially the M4 component, may be of significant importance. Unfortunately this information has not been incorporated in the long-term computations reported in the previous chapter because they were carried out parallel with the initial computations. Therefore the computation reported in 5.5. is repeated with the modification in the boundary condition that a M4 tidal component is included. The amplitude and phase of the M4 component are based on the data reported in 4.4.

The computation is carried out for 45 morphological time steps. The difference between the final bathymetry computed in this run and the bathymetry after 45 time steps in run SM4 is shown in fig.6.3. The difference is considerable as can be observed from the figure. In fig.6.4 the water depth change from the two computations along the main channels in Pinkgat and Zoutkamplaag are compared with each other. Especially along the Pinkgat channel, where the morphological time scale is relatively small, the difference between the two computations is very large. Therefore it is concluded that the higher frequency tidal components at the boundary, especially the M4 component, are important for the morphological development. They should not be neglected anymore in the computations.

6.5 Bed Level Sink and/or Sea Level Rise

Bed level sink in the Wadden Sea may occur due to for instance gas winning in the area. For the morphological development this has the same effect as sea level rise and they can also be treated in the same way in the computations.

It is assumed that the time scale of the bed level sink and/or sea level rise is much larger than the tidal period. This process can thus be taken into account in the model by a simple modification of the bed level module. At each time when the bed level change is calculated the bed level sink and/or sea level rise is simply added to the water depth.

An interesting question arises about the interaction between the sea level

rise and/or the bed level sink with the morphological development under influence of the flow. Is it possible to consider the two processes separately and calculate the total long-term bed level change simply by superposition?

The interaction between the two processes will probably depend on the time scales of them. If the time scales of the two processes differ very much from each other, the interaction will probably not be very important. If the two time scales are of the same order of magnitude, more interaction can be expected.

Here a computation is carried out with a bed level sink having a time scale of the same order of magnitude as the time scale of the morphological development due to tidal flow. The computation SM4 (see section 5.5) is again chosen as reference. The bed level change rate in this computation has the order of magnitude of 5 cm per time step. Therefore the bed level sink rate is set to 5 cm per time step in the present computation.

The computation has been carried out for 10 time steps. In fig.6.5 two pictures are shown. The first picture shows the difference between the water depth computed from run SM4 after 10 time steps and that from the present computation. If there were no interactions between the bed level sink and the morphological development due to tidal flow, the difference should be 0.5 m in the whole model area. The picture shows that the difference is between 0.3 and 0.7 m in most part of the region. The second picture shows the influence of the interaction by depicting the difference shown in the first picture minus 0.5 m. It can be observed that the interaction is most important in the region around the islands heads, especially the western one. In most part of the model area the effect of the interaction is negligible.

As explained earlier the model is unable to adjust its computational grid during the computation. In the present case this means that the model area will not expand although in reality more land will be flooded when bed level sink and/or sea level rise occur. Further the computation only lasts 10 time steps, which is relatively short compared with the morphological time scale in the region. Therefore care should be taken in dealing with the conclusion from the present computation. Moreover, taking into account of the interaction between the bed level sink and the morphological development is not difficult at all. Therefore it is recommended to take the effect of the interaction always into account when bed level sink and/or sea level rise are considered.

7. Concluding Discussions

7.1 Summary of the Works in 1991

In 1990 an exploratory numerical model for morphodynamic simulations was set up for one of the tidal inlets of the western Wadden Sea, the Netherlands. It consists of quasi-3D submodels for tidal currents and sediment transport, linked together via a morphological time-stepping procedure based on the sediment balance. In 1991 this model is used for carrying out a series of computations.

An number of initial computations have been carried out with the realistic bathymetry. Schematised as well as realistic boundary conditions for the water level at the open sea have been used in the computations. Together with the computations carried out in 1990 they finnish phase 2 of the study programme, "initial computations".

Phase 3 of the programme, "development from 'plane' bed" has been completed by carrying out three long-term computations. All these computations were carried out with a schematised open sea boundary condition with a single tidal component. Further, a sensitivity analysis has been carried out in order to investigate the influence of a number of parameters in the model.

A start is made for phase 4 of the programme, "equilibrium situation before 1969", by setting up a schematised model with the Lauwerszee open. However, no computation has been carried out yet with this model.

Furthermore, a report (Wang, 1991) was written about the research carried out in 1990, and a paper (Wang et al., 1991) about the results from 1990 and a part of the results from 1991 is published.

7.2 Restrictions of the Model

The primary objective of the study is to test the capacity of the model to simulate natural evolutions in this type of situations. If this leads to a positive conclusion, the model is to be used as an aid in the analysis of the morphodynamic system around tidal inlets.

The model in its present form has some severe limitations, e.g. due to the absence of wind and wave effects. This will probably make it less suited for operational real-life predictions. Still, a model with the tide as the only hydrodynamic agent must make sense as an aid to study tidal inlet systems, because many aspects of their morphologic behaviour correlate very well with tidal parameters.

The influence of waves will be felt mainly at the outer delta, where most of their energy is dissipated. On the other hand, the total volume of the outer delta correlates fairly well with the tidal prism (Eysink, 1991), so it must be merely the shape of the delta that is sensitive to wave action (Hatanaka and Kawahara, 1989). Studies on other deltas (cf. Stive, 1986, and Steijn et al., 1989) have shown that waves do have an important reshaping effect on the delta after a reduction of the tidal prism. This probably explains the formation of a big sandy hook at the tip of the eastern island in the last twenty years (Biegel, 1991).

Even in a wide open inlet like the Friesche Zeegat, wave penetration from the sea into the basin will be limited. Most of the wave energy is dissipated at the outer delta and at the shoals bordering the inlet channels. The effect of sea waves on the channels in the basin will therefore be minimal. This explains why the dimensions of these channels correlate so well with tidal parameters.

Still, waves play a role inside the basin, especially in the evolution of intertidal shoals (cf. De Vriend et al., 1989). This may explain why the relative intertidal area is a function of the size of the basin, rather than the tidal prism (Eysink, 1991).

Apart from waves, also wind and wind-driven currents in the horizontal and the vertical plane play an important part in tidal inlets, as they influence the residual sediment fluxes and the shoal evolution (De Vriend et al., 1991). The latter is in keeping with the above observation. At present, the model is being extended with a quasi-3D description of wind-driven currents.

7.3 Observations and Conclusions

In spite of these limitations and the early stage of the study, the results presented herein lead to a number of observations and conclusions.

From the initial computations, including those carried out in 19990 the following observations and conclusions are made:

- Especially in the gorge, the vertical structure of the flow (secondary flows) has a significant effect on the residual transport and the morphological evolution.

- Also the spatial relaxation effect in sediment transport, expressed by the advection terms in equation (2-7), has a significant effect on the residual transport.

- The residual sediment transport pattern differs strongly from the residual current pattern.

- Especially near the seaward boundary, both patterns are quite sensitive to the combination of the open sea boundary condition and the bathymetry. This becomes even more serious in longer-term computations, as errors originating from the boundaries tend to penetrate into the model domain. The boundary condition in multi-dimensional morphodynamic computations therefore requires further investigation.

- Computations with the realistic bathymetry show that the sedimentation-erosion pattern is very scattered. This is probably due to the small errors in the bathymetry data.

- Although the M2 component is the most important tidal component in the area under consideration, the other smaller tidal components, especially the M4 component, appear to be important for the residual sediment transport field and the morphological development.

- It is nearly impossible to make small corrections to the open sea boundary condition such that the residual flow field and the residual sediment transport field become realistic in the whole model area.

- The strong sensitivity of the residual sediment transport field is due to the fact that the residual transport is a small difference between the much larger ebb- and flood-transport.

From the long-term computations with the schematised "plane" bed as initial bathymetry the following observations and conclusions are made:

- The model describes the formation of the outer delta and a structure of shoals and channels, both at the outer delta and in the basin.

- The planform of the model domain in the gorge is a critical element in the model schematization. This corresponds with observations in river dynamics, where the width/depth ratio is critical to the channel stability. On the other hand, it is somewhat worrying, that the model itself does not bring the gorge into the required shape. Further research is needed here.

- The fine grid is recommended for further computations despite of the fact that then much more computational time is required.

- Disturbances occur at the open sea boundary, especially in the outflow part of the boundary. This indicates that the treatment of the boundary condition for the morphological development is still not

sufficient despite the improvement of the program carried out.

- Unrealistic local scours at the islands heads cause a serious problem for the model.

The long-term computation with the smoothed bed as initial bathymetry led to the following observations and conclusions:

- The model describes the formation of a structure of shoals and channels with characteristics similar to the one which was smoothed out in the initial bathymetry.

- The morphological time scale in the Pinkgat area is much smaller than that in the Zoutkamplaag area. The Pinkgat area is thus morphologically much more active than the Zoutkamplaag area.

All the long-term computations carried out so far show that:

- The morphological development according to the model leads to more circulation cells in the residual sediment transport field.

The sensitivity analysis leads to the following conclusions:

- The residual sediment transport pattern at storm situation is completely different from that at nice weather situation. However, the wind influence is probably much less important for the morphological development than the tidal flow, because of its low frequency.

- The spatial roughness variation has little influence on the residual sediment transport field. Its influence on the morphological development in the present model, which is strongly schematised, can thus be neglected.

- The tidal component M4 having a amplitude of about 10% of that of the M2 component has significant influence on the morphological development.

- The interaction between bed level sink and morphological development under influence of tidal flow is not very important, even under extreme conditions. However, the interaction can be very simply taken into account. Therefore it is recommended to take the interaction into account whenever the bed level sink and/or sea level rise are considered.

7.4 Recommendations for Further Research

Although we are still far from a quantitative description of the natural process, the present results are encouraging enough to continue research in this direction. The results up till now also provide useful information about how the model can be improved.

The small tidal components have been neglected in most of the computations carried out so far. However, there have been clear indications that the small tidal components may be important for the morphological development although there magnitude is smaller than the semi-diurnal tide. Therefore more research is still needed for determining the dominating condition for the morphological development. Quantitative results can only be produced with the model when the dominating condition is known.

In order to obtain quantitative results from the model the magnitude of the residual sediment transport field has to be calibrated such that the morphological time scale in the real case is reproduced by the model. This requires a more thourough examination of the computational results with the help of the field measurements.

The different morphological time scales in the model area form a serious restriction of the model. Therefore attention should be paid to this problem.

More attention should also be paid to the treatment of the boundary condition for the morphological development at the open sea, especially for the outflow part of the boundary, in order to solve the problem with the disturbances at the boundary.

The unrealistic deep scours at the islands heads indicate that the schematization of the local geometry should be reconsidered. This deep scour may also be a consequence of the absence of the wave influence in the model.

Up till now the computed morphological development does not reflect the realistic morphological time scale because the model has not been calibrated quantitatively. More attention should be paid to this point in the further study.

Despite of the needed improvement of the model mentioned above, the general working plan describe in chapter 1 still forms a good guiding line of the study. Next step is to investigate the morphological development before 1969, i.e. with the Lauwerszee open (phase 4).

REFERENCES

Biegel, E.J. (1991), The evolution of the ebb-tidal delta and the tidal basin of the Friesche Zeegat in relation to the closure of the Lauwerszee, Utrecht State University, Inst. Phys. Geogr., Geopro-rept. (in Dutch).

DELFT HYDRAULICS, (1979), Morfologie van de Waddenzee (in Dutch), Report nr. R 1336.

Dongeren, A. van (1991), A model of the morphological behaviour and stability of channels and flats in tidal basins, Master thesis, Delft University of Technology, Faculty of Civil Engineering.

Edelman, T. (1961), Verstoringen in de kustlijn t.g.v. de aanwezigheid van zeegaten (in Dutch), Rijkswaterstaat Nota WWK 61-3, 18 pp.

Eysink, W.D., (1991), Simple morphologic relationships for estuaries and tidal channels, handy tools for engineering, Proc. COPEDEC'91, Mombasa (in press).

Galappatti, R. (1983), A depth-integrated model for suspended transport, Delft University of Technology, Dept. of Civil Eng., Report nr. 83-7.

Gallappati, R. and Vreugdenhil, C.B. (1985), A depth-integrated model for suspended sediment transport, J. of Hydr. Res., vol. 23, nr. 4.

Gerritsen, F. (1990), Morphological stability of inlets and channels of the Western Wadden sea, Rijkswaterstaat, report nr. GWAO-90-019.

Hauguel, A. (1978), Utilization des modeles mathematiques pour L' etude du transport solide sous L' action des courants de Maree, Report E42/78.41, EDF, Direction des Etudes at Recherches.

Hatanaka, K. and Kawahara, M. (1989), A finite element application of sand terrace formation process, Proc. Int. Symp. Sediment Transport Modelling, New Orleanns, 1989.

Kalkwijk, J.P.Th. and Booij, R. (1986), Adaptation of secondary flow in nearly horizontal flow, J. of Hydr. Res., Vol. 24, no. 1.

Latteux, B., (1987), Transport modelling of particulate matter-methodology of long-term simulation of bed evolutions, Lab. Nat. d'Hydraulic, Chatou, France, Rept. HE-42/87.25 (in French).

Postma, J.T. et al (1986), Morfologische en hydraulische gevolgen van de afsluiting van de Lauwerszee (in Dutch), Nota 84.21, Rijkswaterstaat.

Rijn, L.C. van (1984a), sediment transport, part I: Bed load Transport, J. of Hydr. Eng., Vol. 110, nr. 10.

Rijn, L.C. van (1984b), sediment transport, part II: Suspended load Transport, J. of Hydr. Eng., Vol. 110, nr. 11.

Sha, L.P. (1990), Sedimentological studies of the ebb-tidal deltas along the West Frisian Islands, the Netherlands, Doctoral thesis, University of Utrecht, the Netherlands.

Steijn, R.C. (1991), Some considerations on tidal inlets, Report no. H840, DELFT HYDRAULICS

Steijn, R.C., Louters, T., van der Spek, A.J.F and De Vriend, H.J., (1989), Numerical model hindcast of the ebb-tidal delta evolution in front of the Deltaworks, In: Falconer R.A. et al., "Hydraulic and Environmental Modelling of Coastal, Estuarine and River Waters", Gower Technical, Aldershot.

Stelling, G.S. and Leendertse, J.J. (1991), Modelling of convective processes in two- and three-dimensional models, Conf. on Estuarine and Coastal Modelling, to be held in Florida, Nov. 1991.

Stelling, G.S., Wiersma, A.K. and Willemse, J.B.T.M., (1986), Practical aspects of accurate tidal computations, J. Hydr. Eng., 112/9, p. 802-817.

Stive, M.J.F., (1986), A model for cross-shore sediment transport, Proc. 20th ICCE, Taipei, Taiwan, p. 1551-1564.

Struiksma, N., Olesen, K.W., Flokstra, C. and Vriend, H.J. de (1985) Bed deformation in curved alluvial channels, J. of Hydr. Res., Vol. 23, No. 1.

Vriend, H.J. de (1981), Steady flow in shallow channel bends, Doctoral thesis, Delft University of Technology.

Vriend, H.J. de (1985), Flow formulation in mathematical models for 2DH morphological changes, Report no. R1747-5, DELFT HYDRAULICS.

Vriend, H.J. de, Louters, T., Berben, F. and Steijn, R.C., (1989), Hybrid prediction of a sandy shoal in a mesotidal estuary, In: Falconer R.A. et al., "Hydraulic and Environmental Modelling of Coastal, Estuarine and River Waters", Gower Technical, Aldershot.

Vriend, H.J. de, (1991) Modelling in marine morphodynamics, Proceedings of the second international conference on computer modelling in ocean engineering, Barcelona, 1991.

Vries, M. de (1959), Transients in bed-load transport in open channels (basic considerations), Report no. R3, DELFT HYDRAULICS.

Wang, Z.B. (1989), Mathematical modelling of morphological processes in estuaries, doctoral thesis, Delft University of Technology.

Wang, Z.B. (1991), A morphodynamic model for a tidal inlet, Report H840, DELFT HYDRAULICS.

Wang, Z.B., Vriend, H.J. de and Louters, T. (1991), A morphodynamic model for a tidal inlet, Proceedings of the second international conference on computer modelling in ocean engineering, Barcelona, 1991.

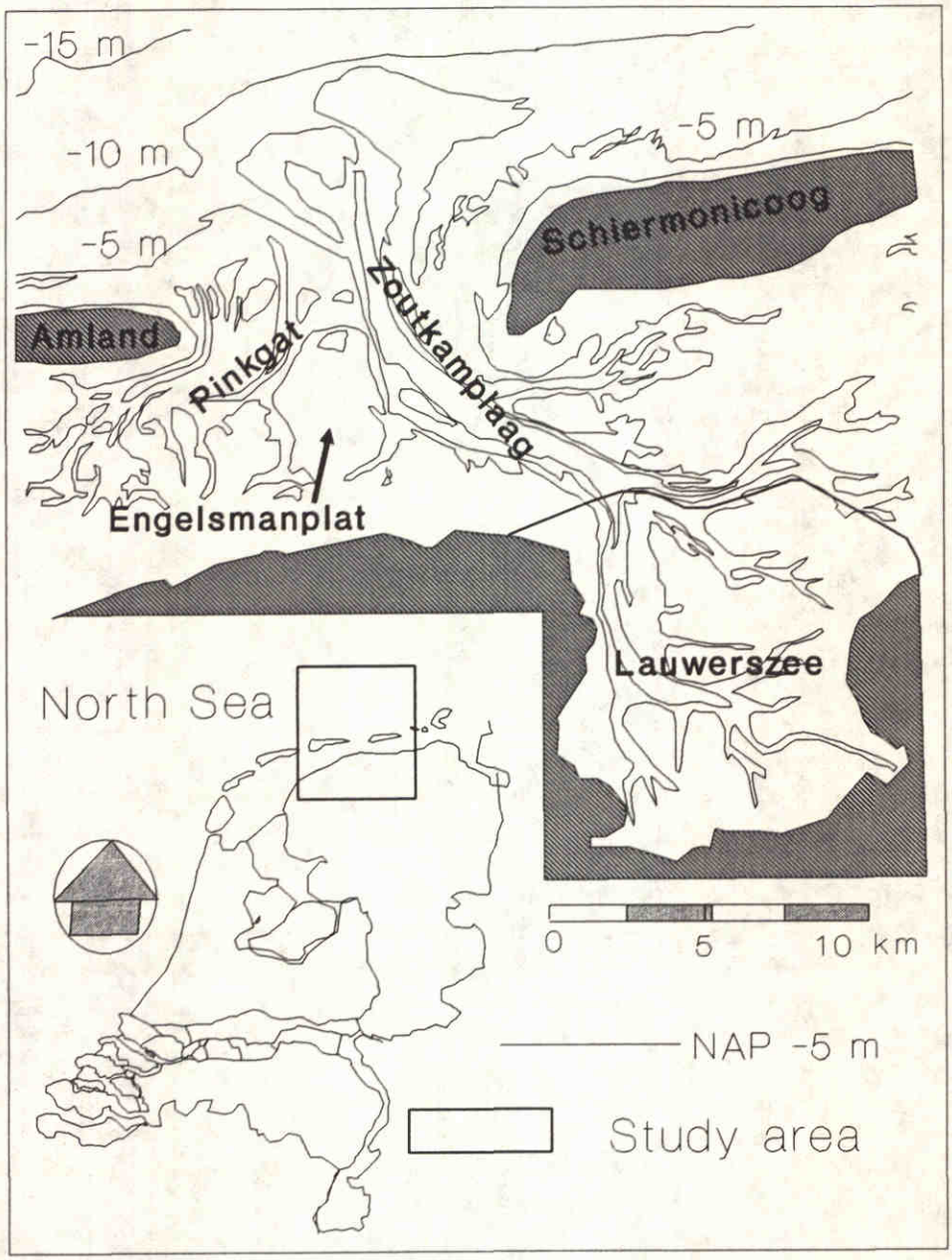

The study area : "Het Friesche Zeegat"

Kustgenese Project

DELFT HYDRAULICS | h840.50 | Fig.1.1

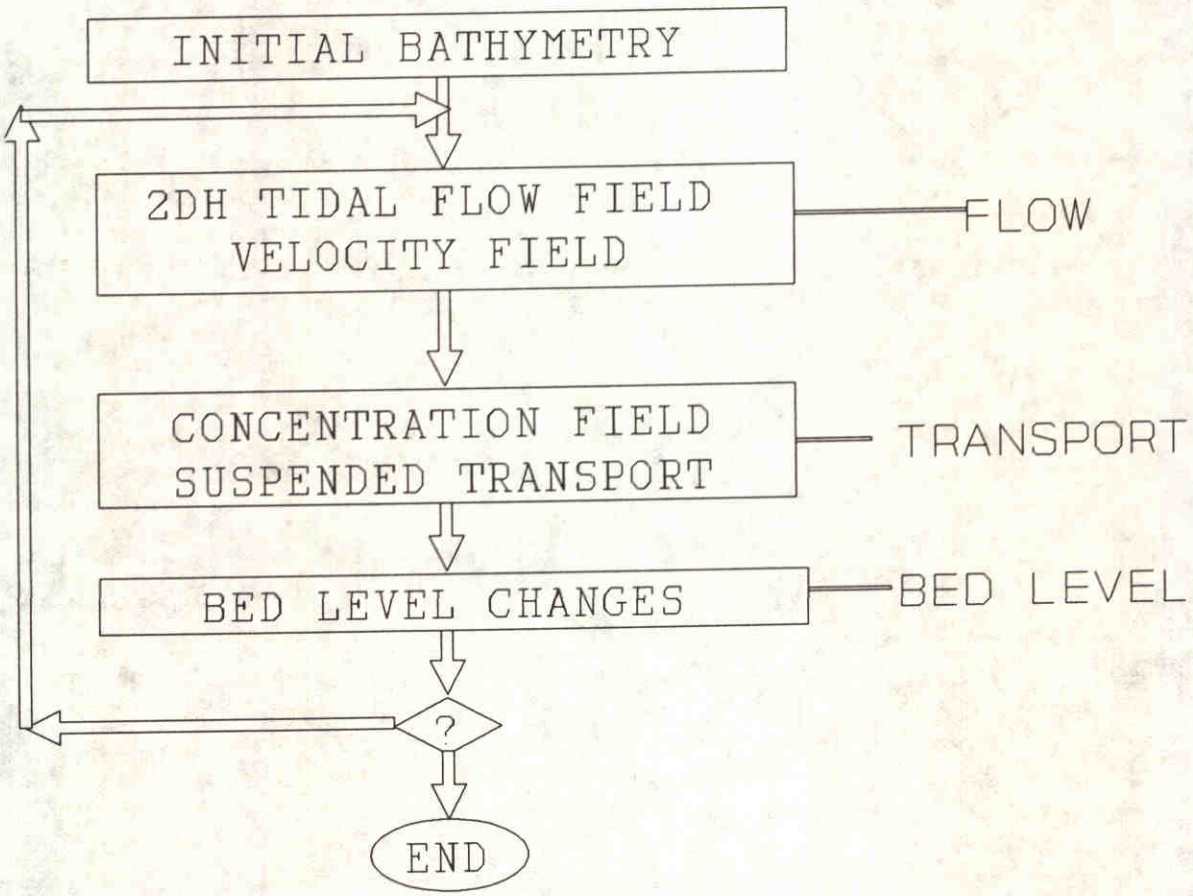

The computational procedure
in the DELMOR model

Kustgenese Project

DELFT HYDRAULICS | h840.50 | Fig.2.1

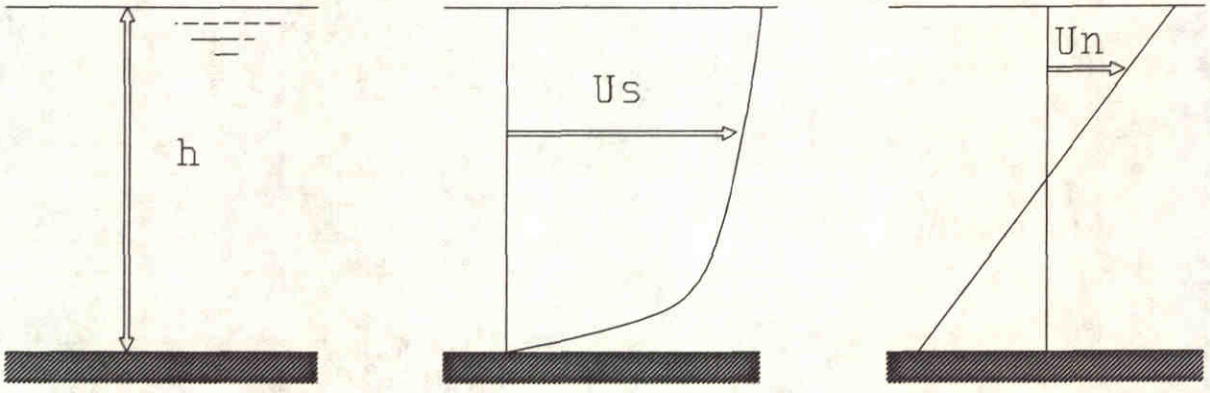

Velocity profiles
of the main flow and secondary flow

Kustgenese Project

DELFT HYDRAULICS

h840.50

Fig.2.2

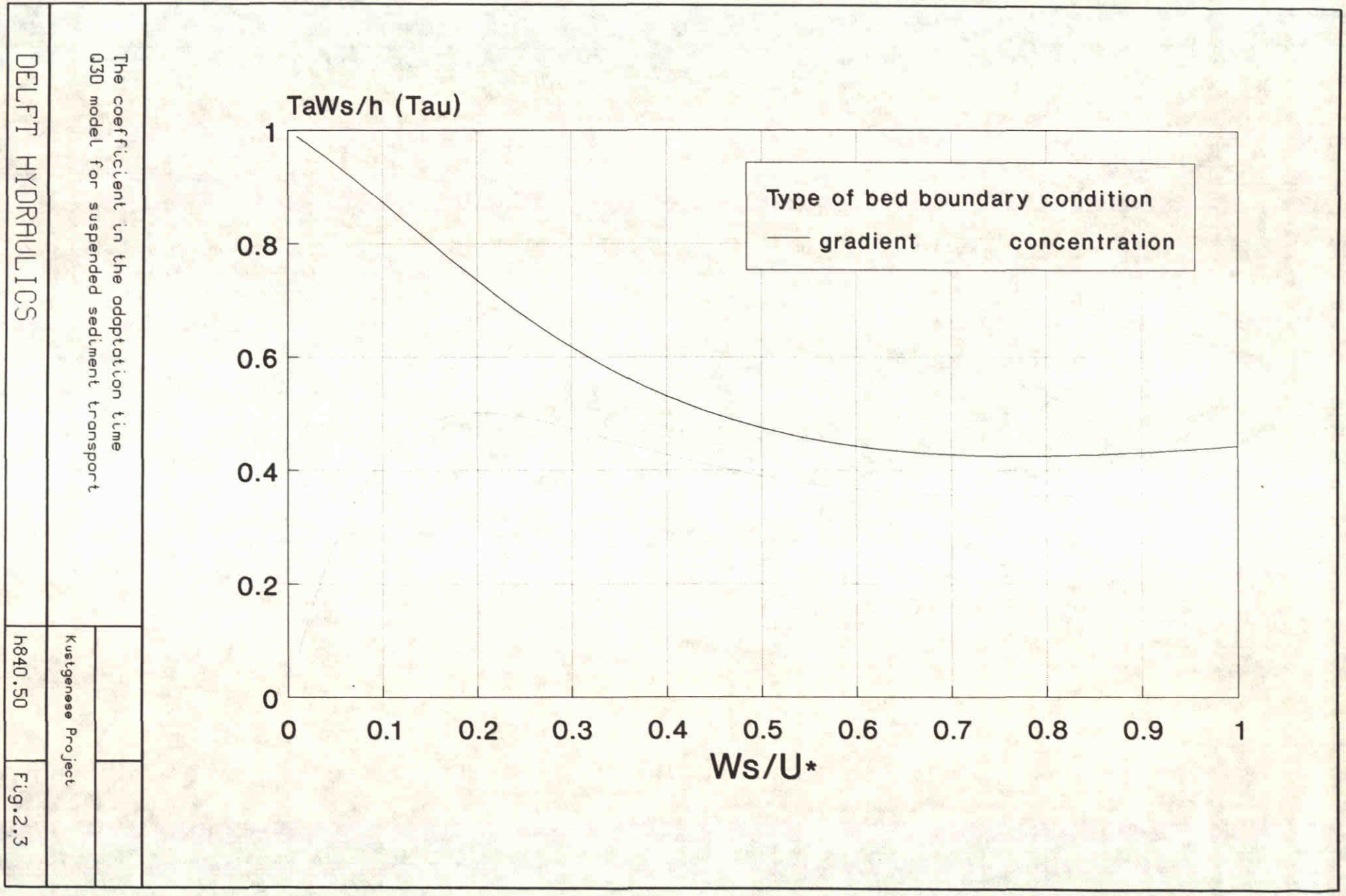

DELFT HYDRAULICS

The coefficient in the adaptation time
Q3D model for suspended sediment transport

Kustgenese Project

h840.50

Fig.2.3

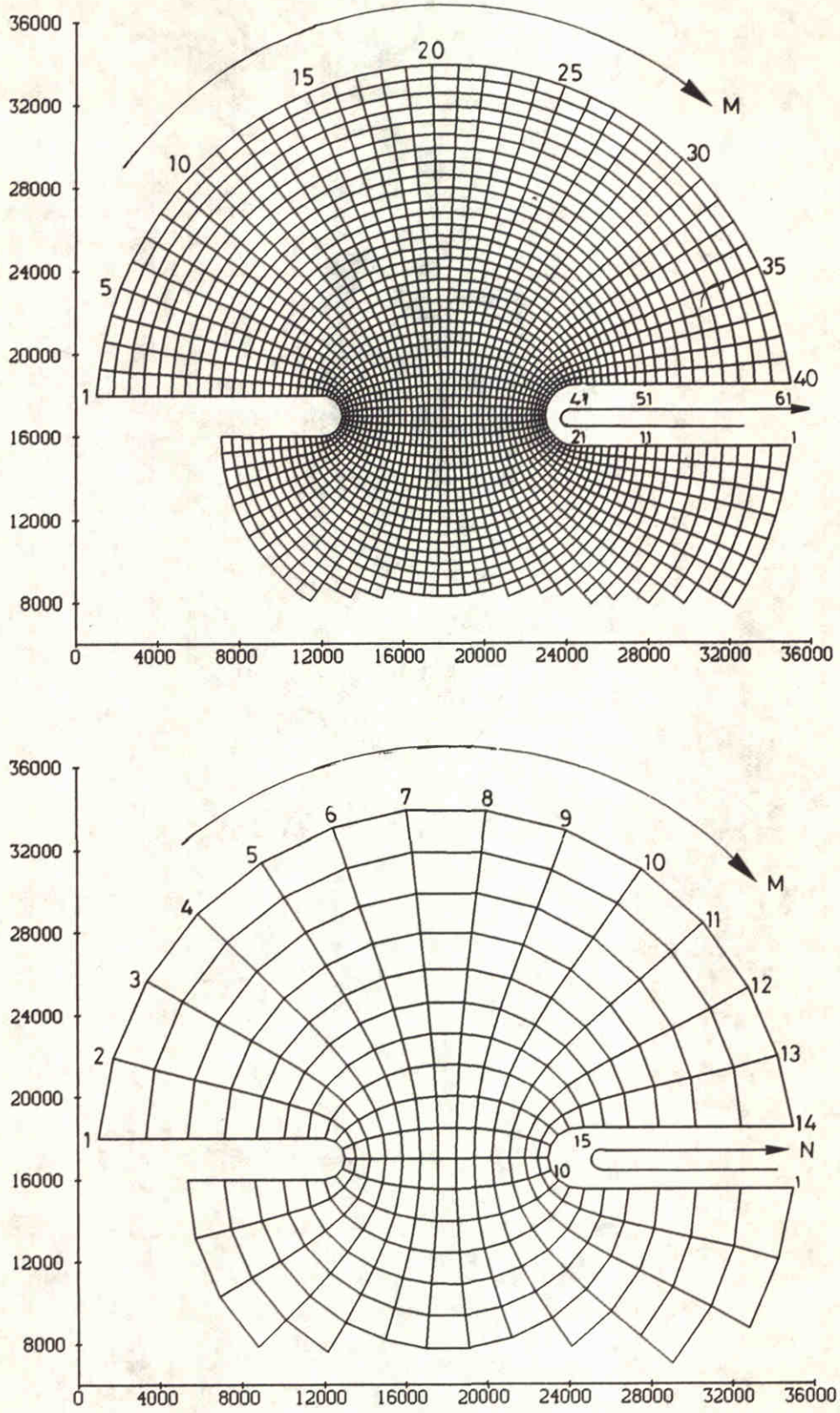

The computational grid
Top: fine grid
Bottom: coarse grid

Kustgenese Project

DELFT HYDRAULICS

h840.50

Fig.3.1

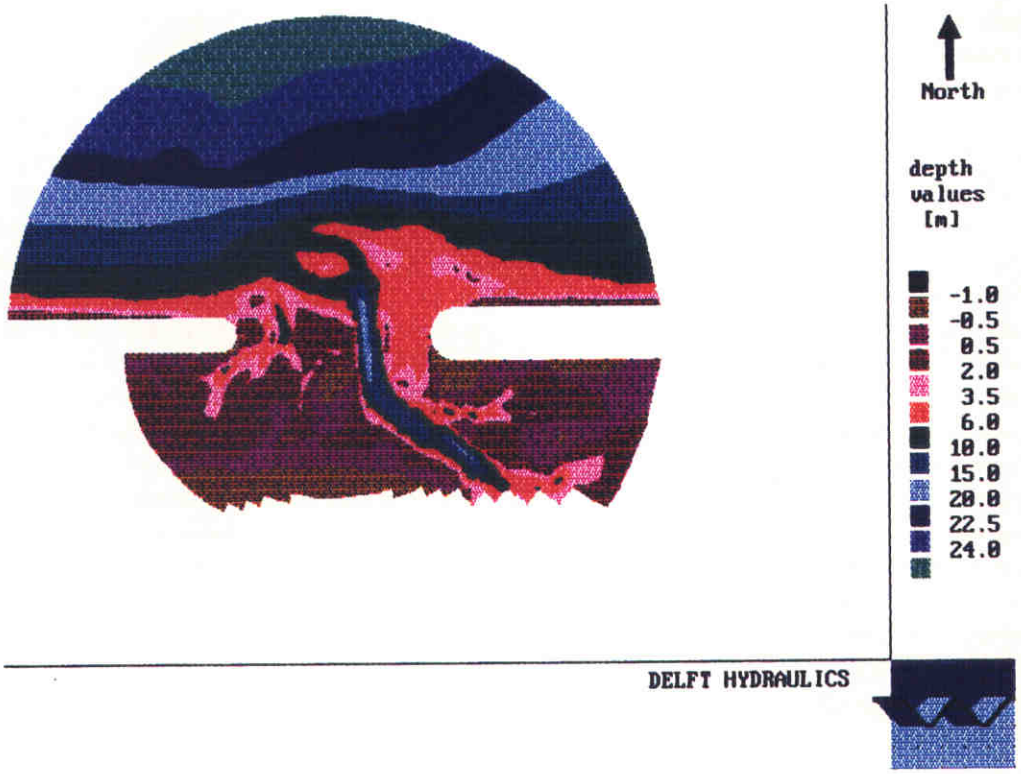

The realistic bathymetry
based on the measurements in 1970
shortly after the closure of the Lauwerszee

Kustgenese Project

DELFT HYDRAULICS

h840.50

Fig.3.2

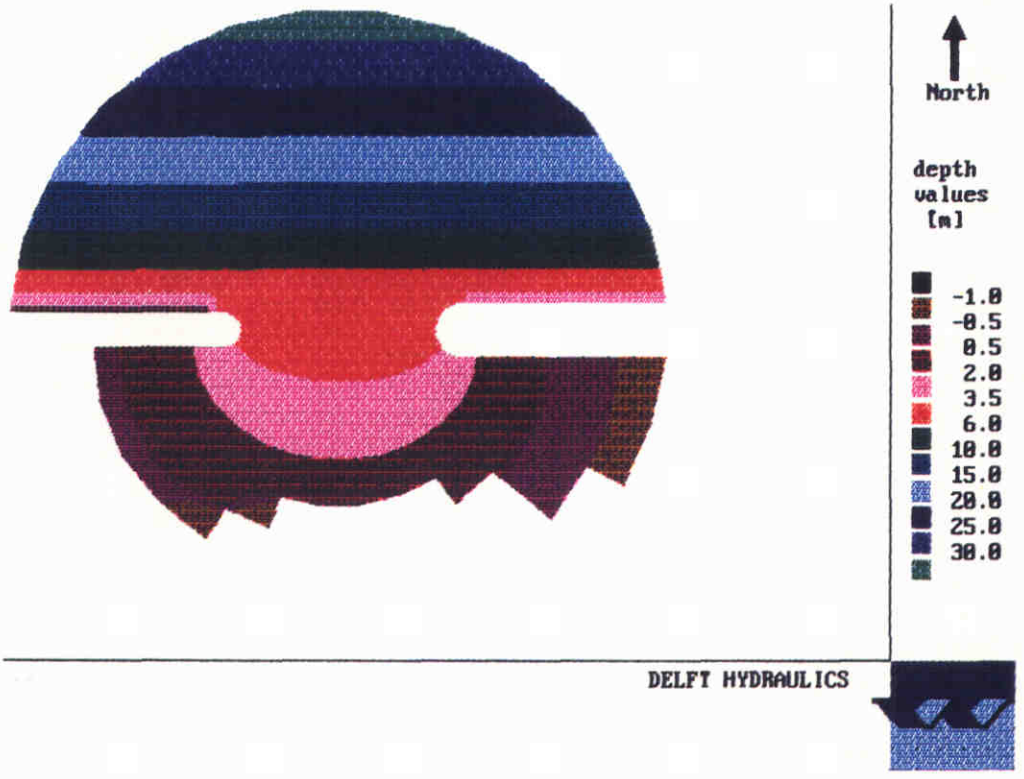

The schematised bathymetry

Kustgenese Project

DELFT HYDRAULICS | h840.50 | Fig.3.3

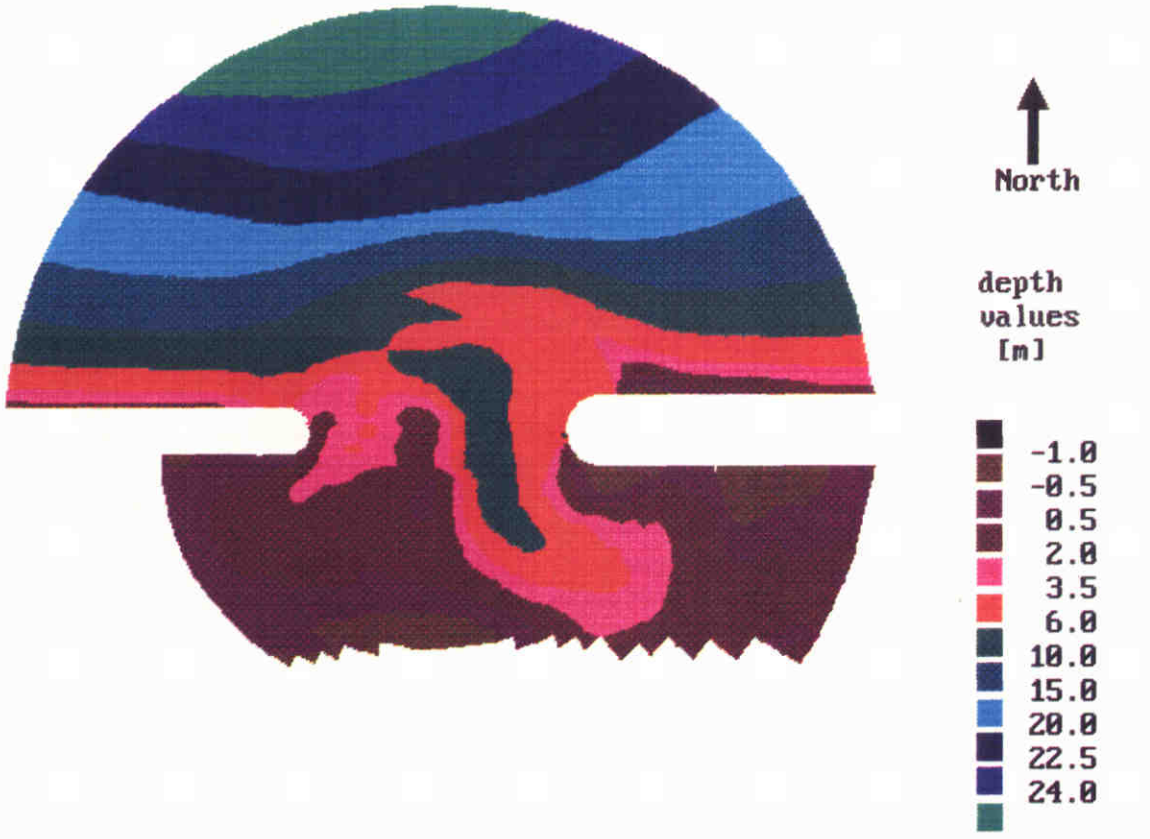

e03 DELFT HYDRAULICS

The schematised bathymetry
based on smoothing of the realistic bathymetry
in 1970 (fig.3.2)

Kustgenese Project

DELFT HYDRAULICS | h840.50 | Fig.3.4

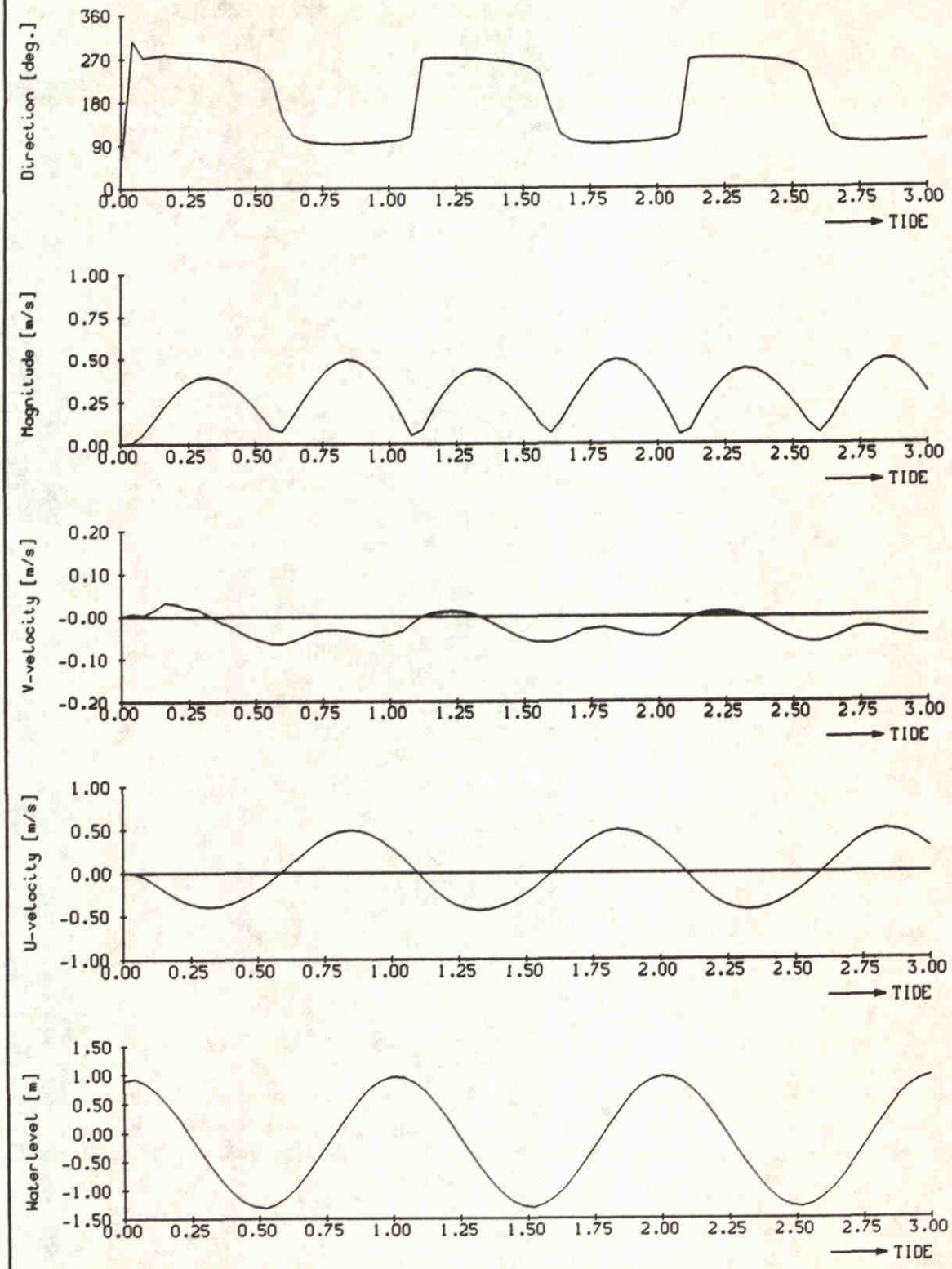

Waterlevel and velocities Station 1 tide, no wind, no wave	e32	
	Kustgenese	
DELFT HYDRAULICS	h840.50	Fig. 4.1

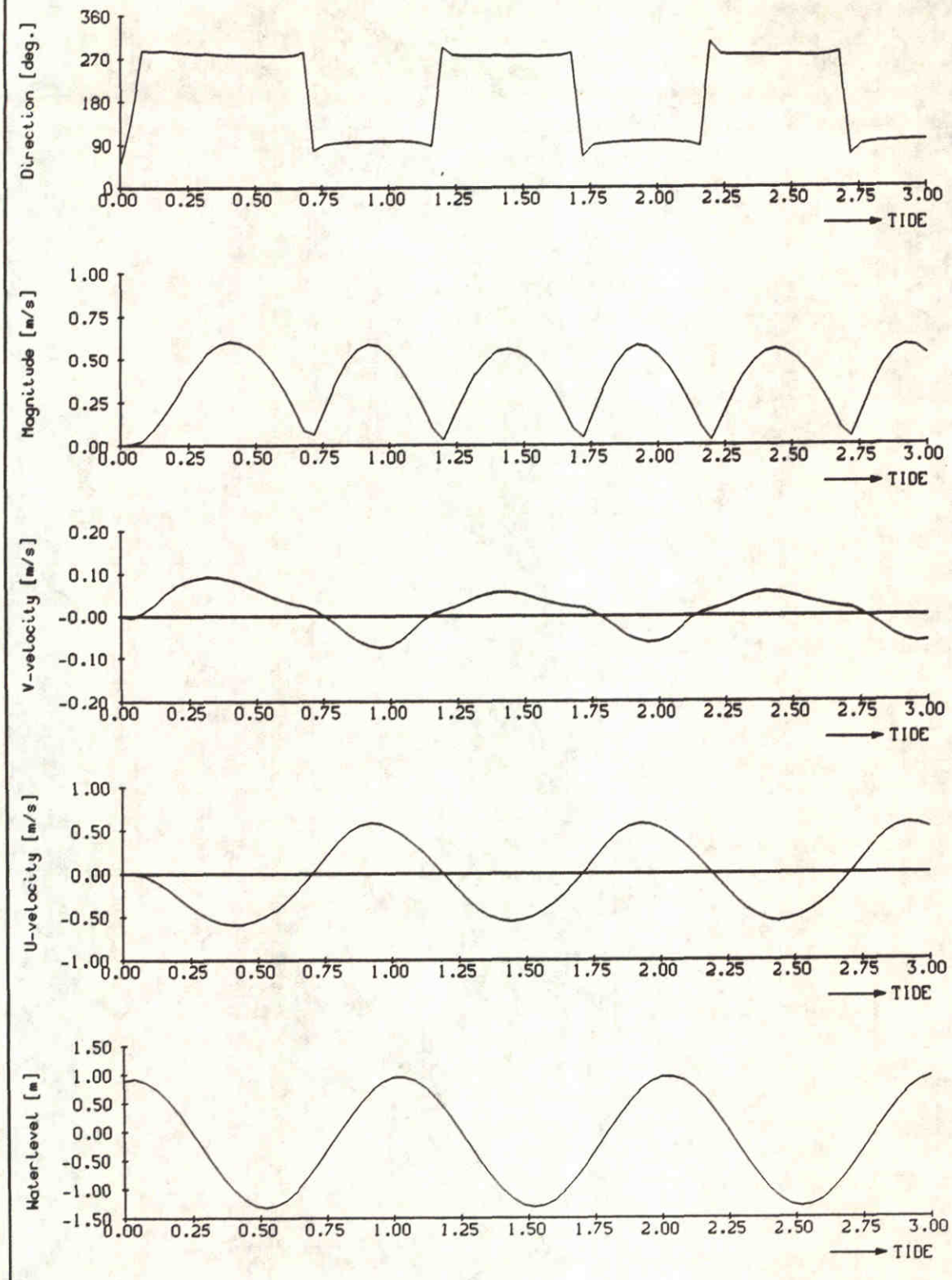

Waterlevel and velocities Station 2 tide, no wind, no wave	e32	
	Kustgenese	
DELFT HYDRAULICS	h840.50	Fig. 4.2

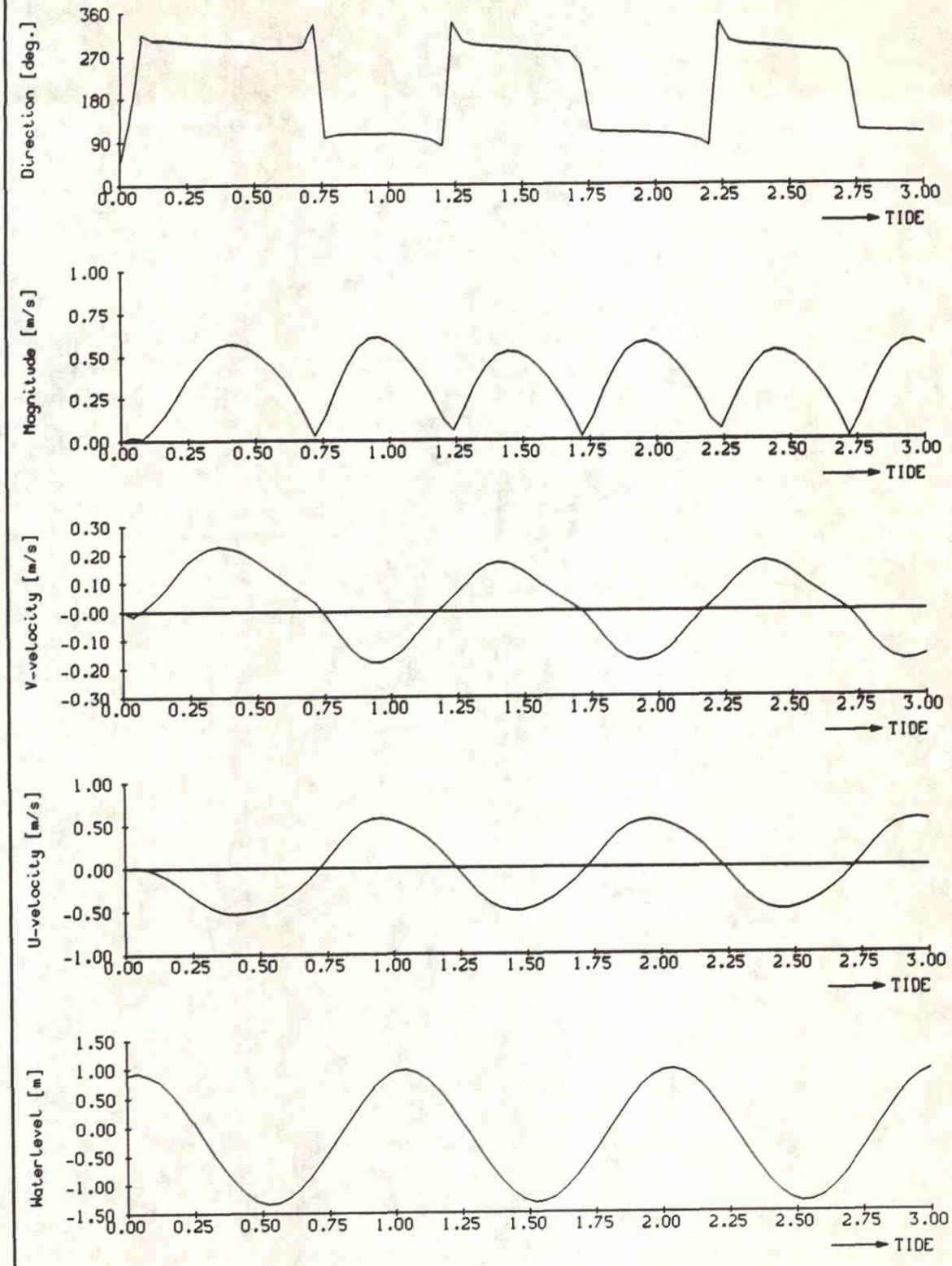

Waterlevel and velocities Station 3 tide, no wind, no wave	e32	
	Kustgenese	
DELFT HYDRAULICS	h840.50	Fig. 4.3

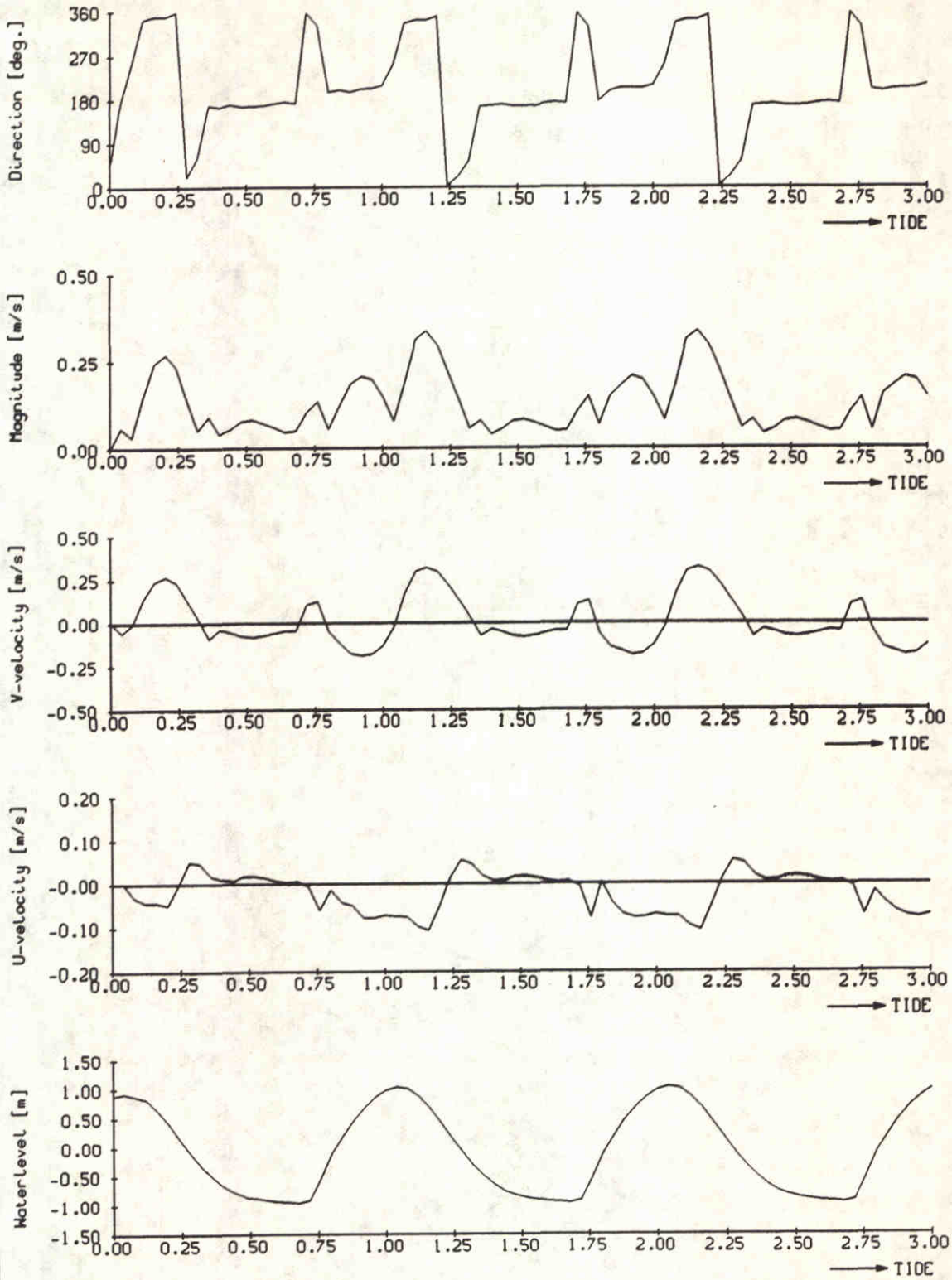

Waterlevel and velocities Station 4 tide, no wind, no wave	e32	
	Kustgenese	
DELFT HYDRAULICS	h840.50	Fig. 4.4

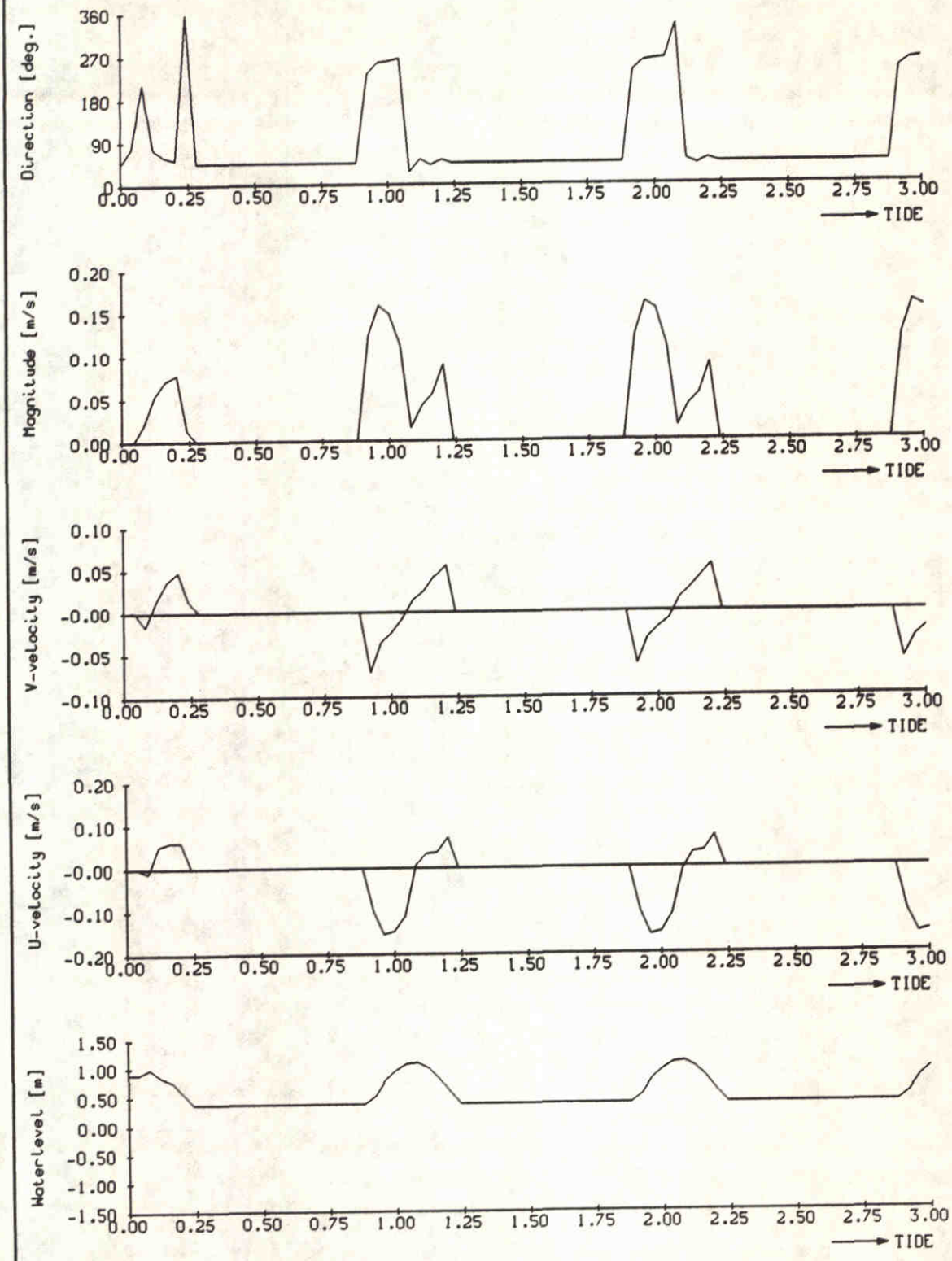

Waterlevel and velocities Station 5 tide, no wind, no wave	e32	
	Kustgenese	
DELFT HYDRAULICS	h840.50	Fig. 4.5

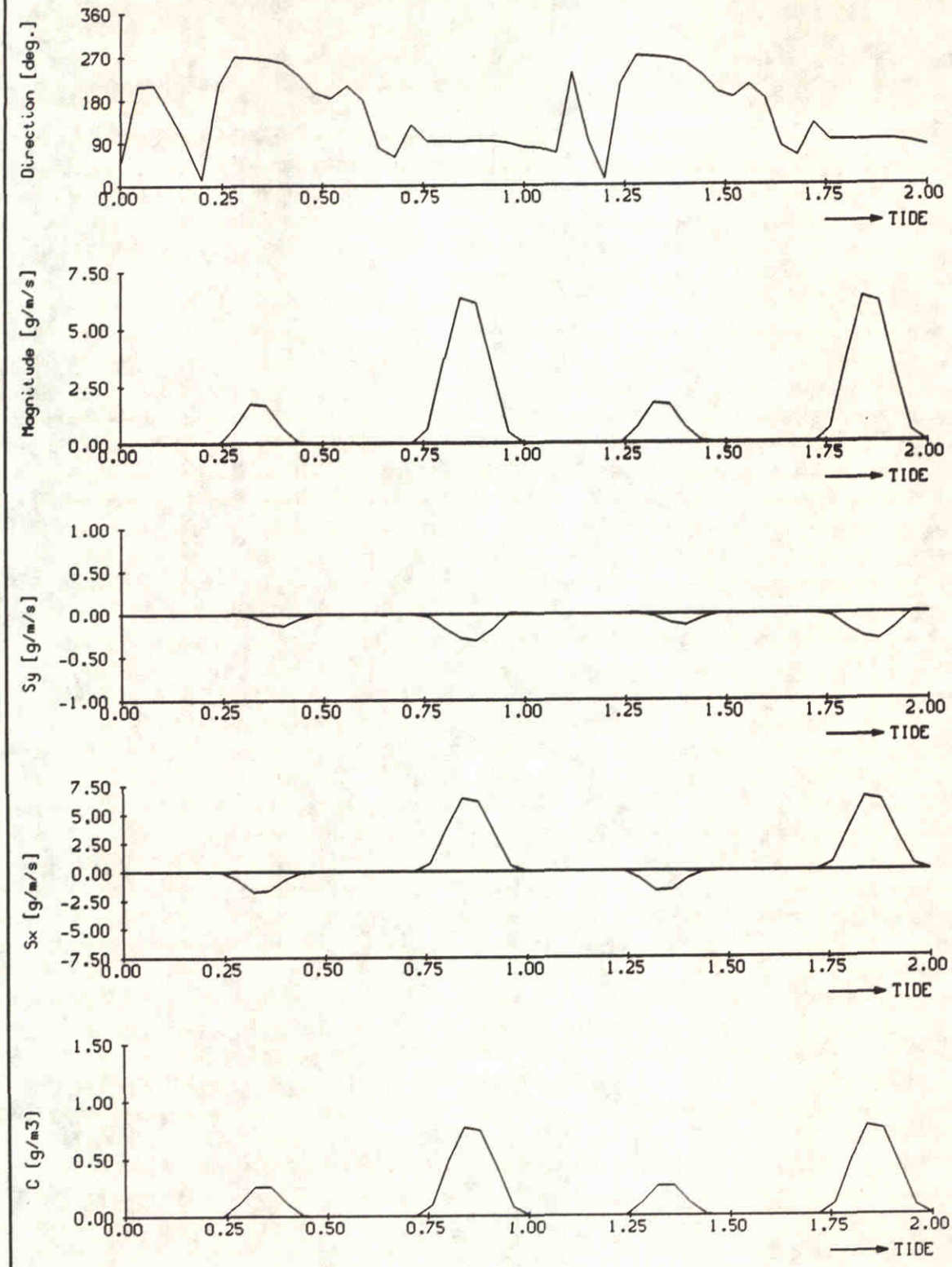

sediment concentration and transport	e32	
station 1	Kustgenese	
DELFT HYDRAULICS	h840.50	Fig. 4.6

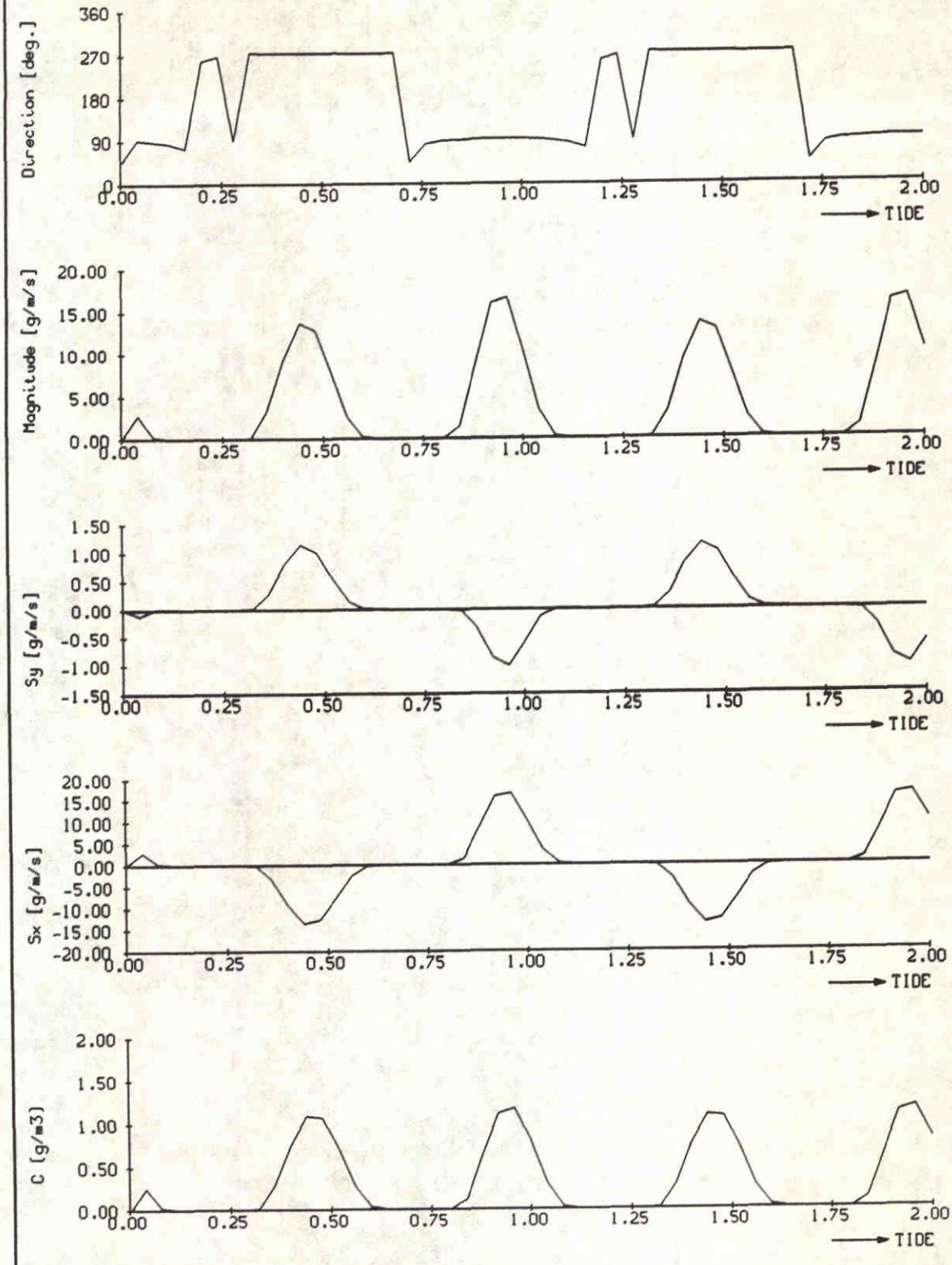

sediment concentration and transport station 2	e32	
	Kustgenese	
DELFT HYDRAULICS	h840.50	Fig. 4.7

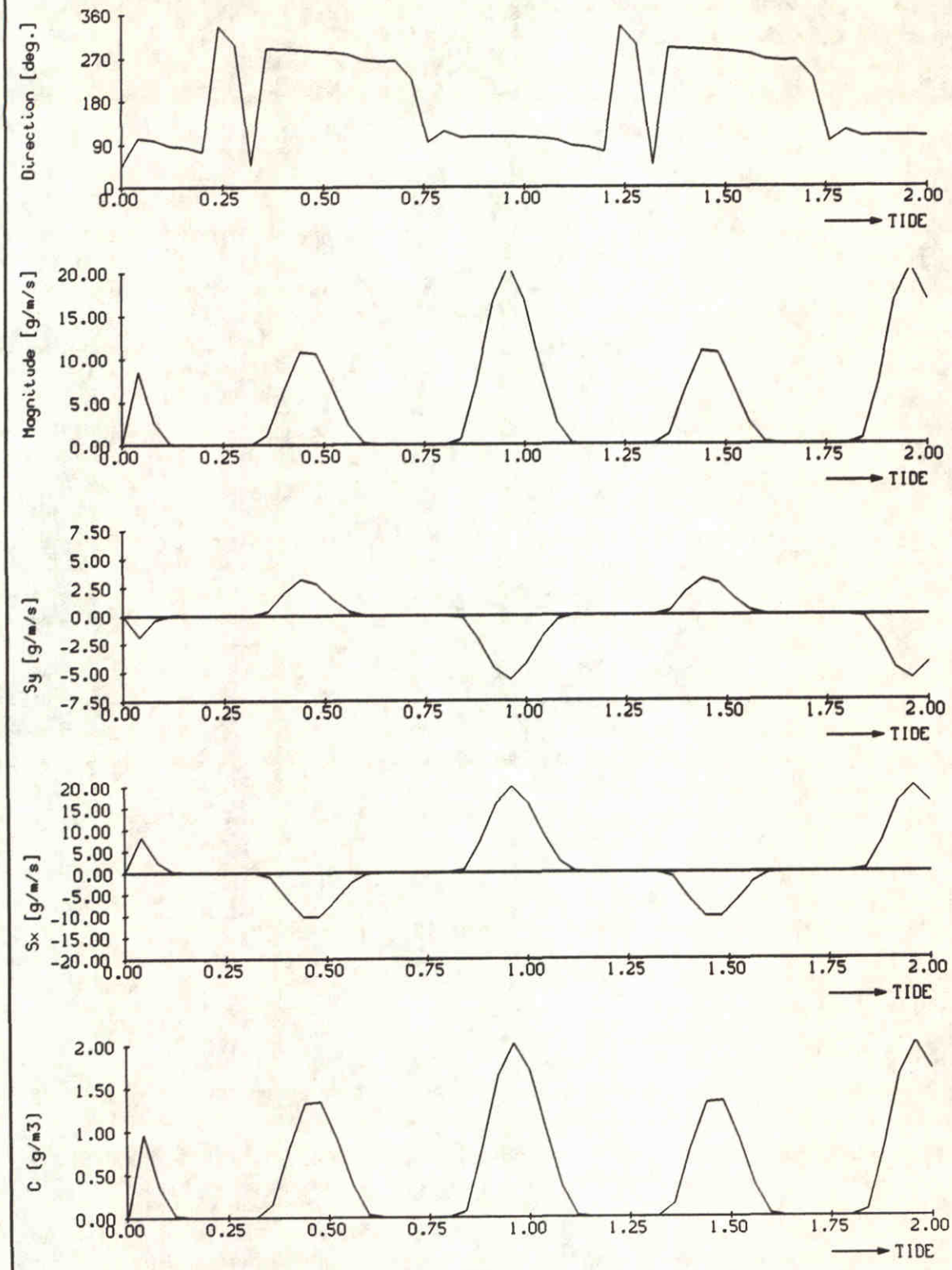

sediment concentration and transport station 3	e32	
	Kustgenese	
DELFT HYDRAULICS	h840.50	Fig. 4. 8

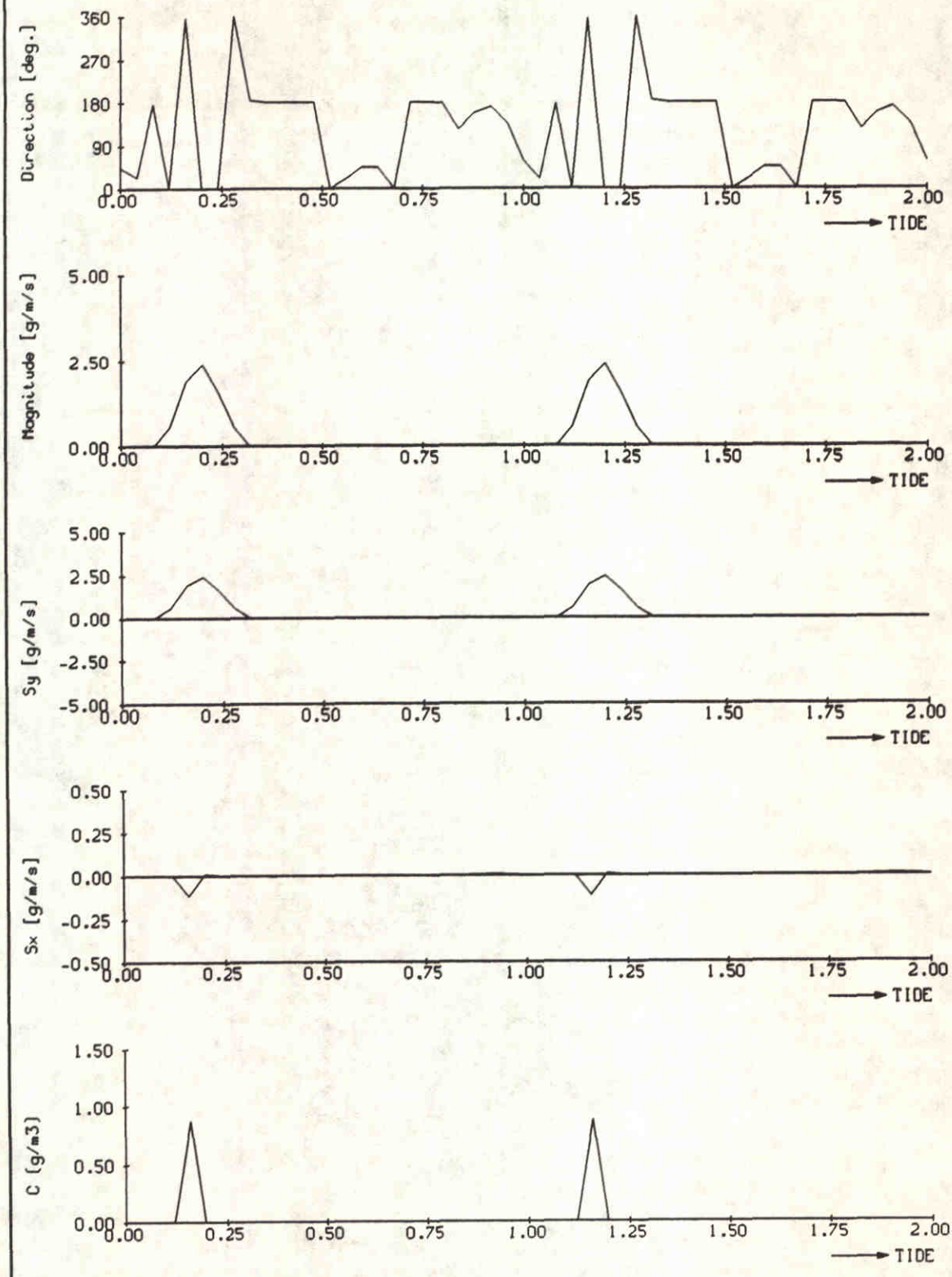

sediment concentration and transport station 4	e32	
	Kustgenese	
DELFT HYDRAULICS	h840.50	Fig.4.9

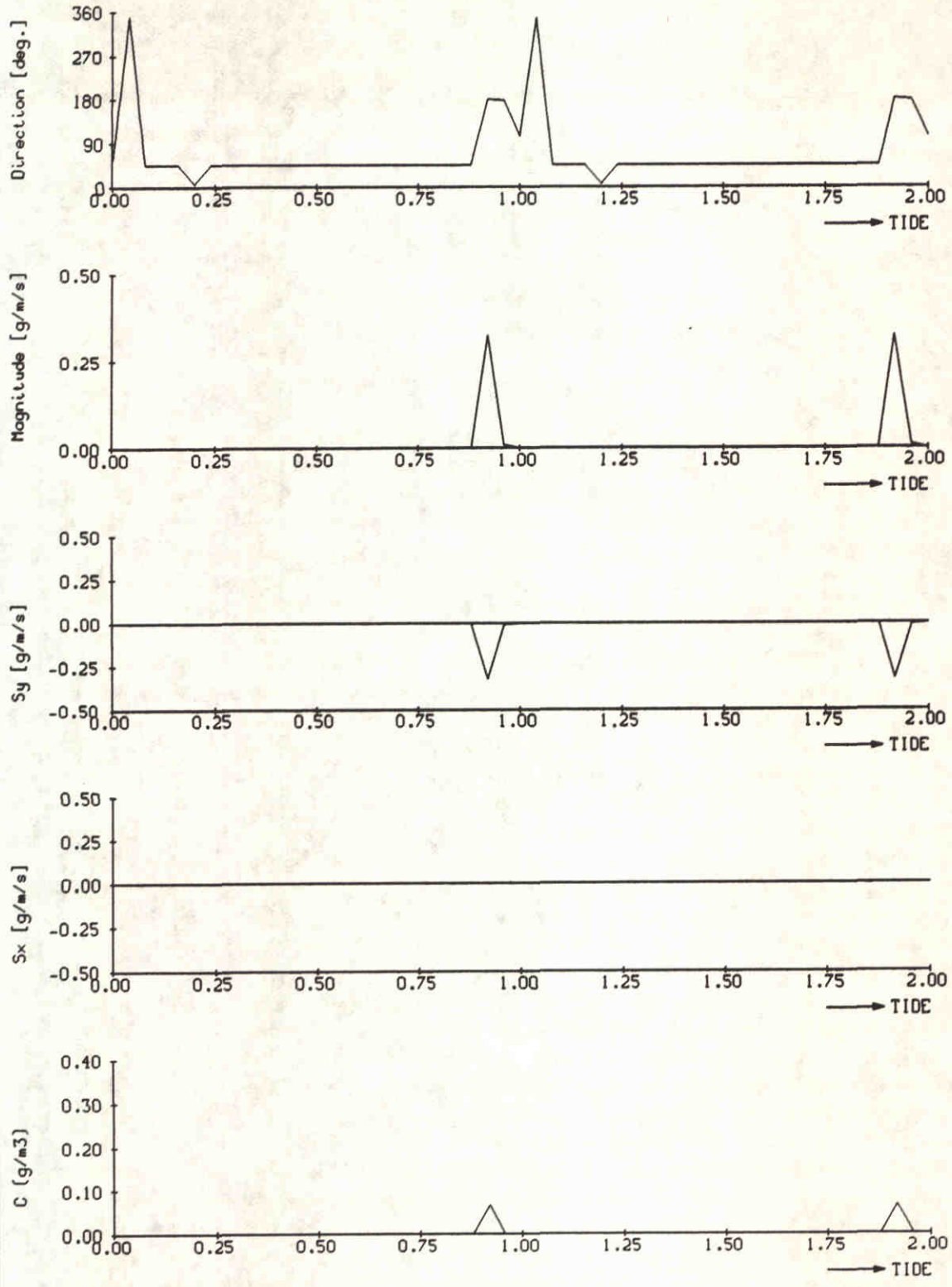

sediment concentration and transport station 5	e32	
	Kustgenese	
DELFT HYDRAULICS	h840.50	Fig. 4.10

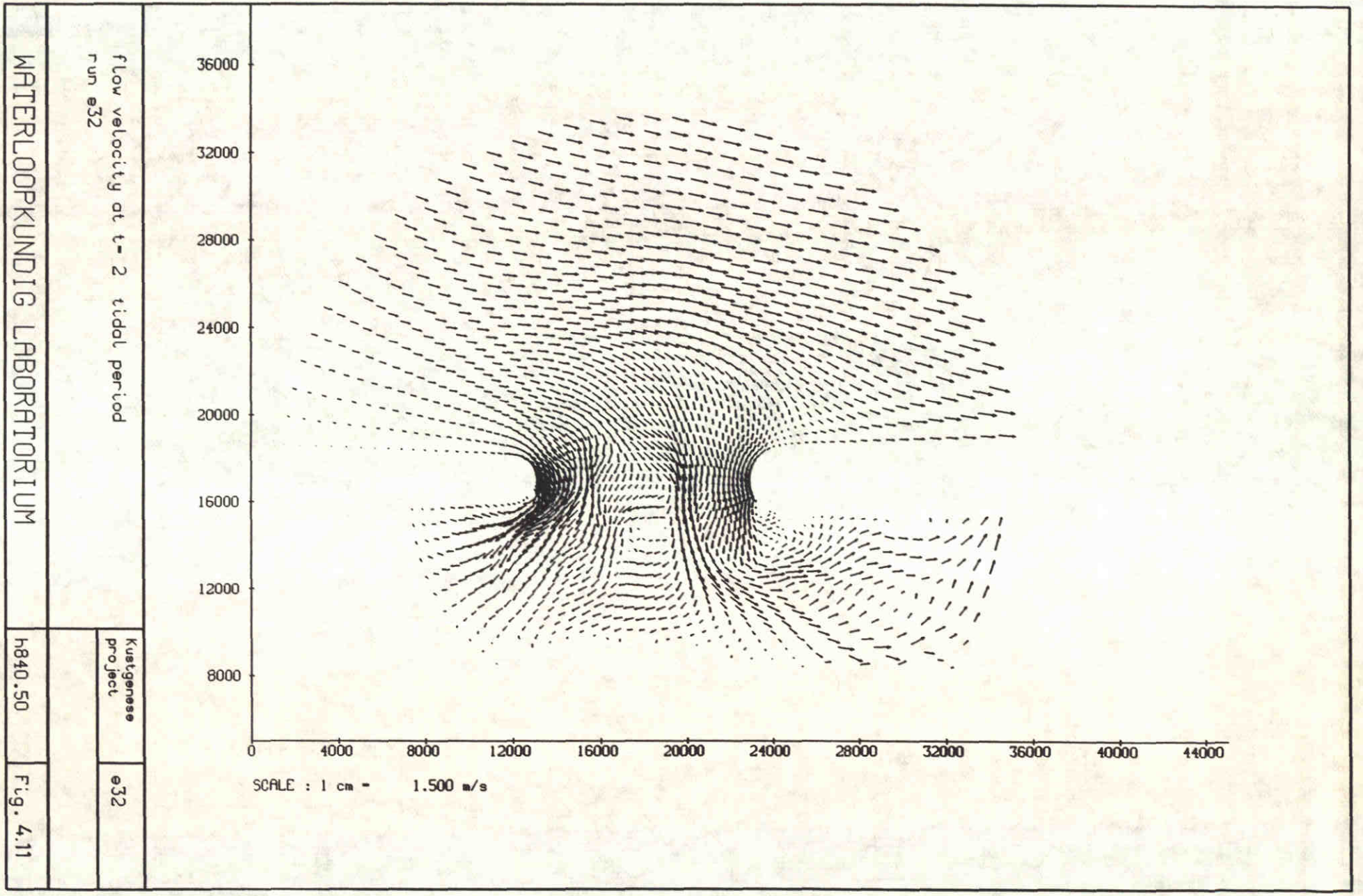

flow velocity at t= 2 tidal period
run e32

Kustgenese project

e32

h840.50

Fig. 4.11

WATERLOOPKUNDIG LABORATORIUM

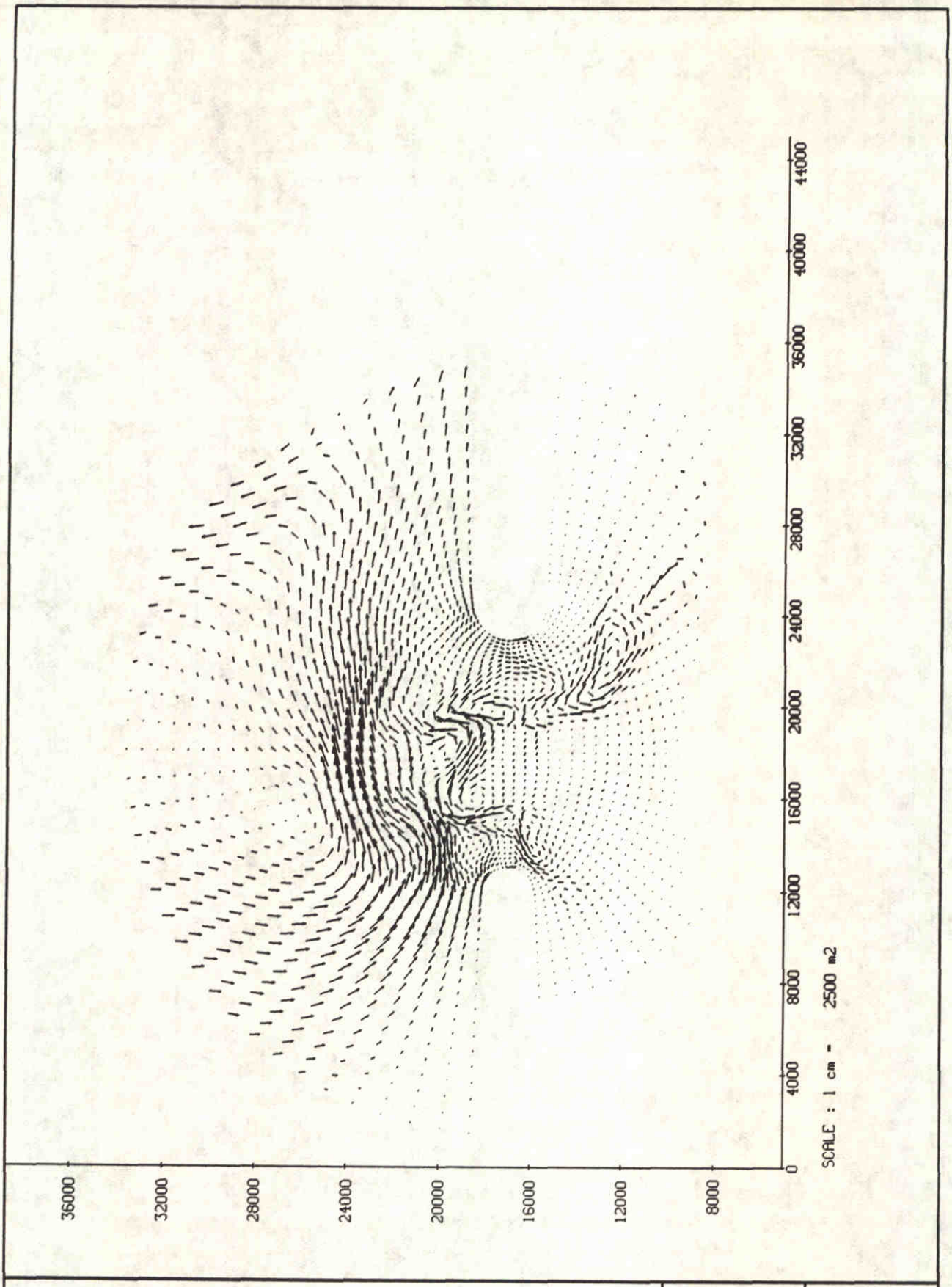

residual flow field

bathymetry from 1970

project
Kustgenese

WATERLOOPKUNDIG LABORATORIUM

H840.50

Fig. 4.12

net sediment transport
run e32
bathymetry from 1970

project Kustgenese	e32
H840.50	Fig. 4.13

WATERLOOPKUNDIG LABORATORIUM

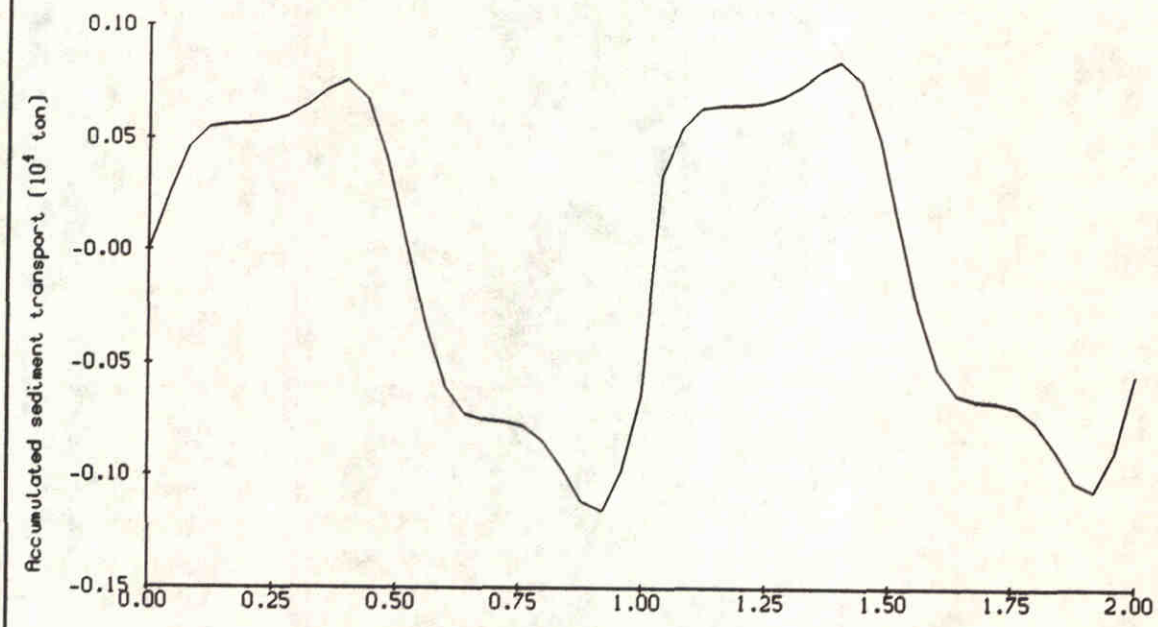

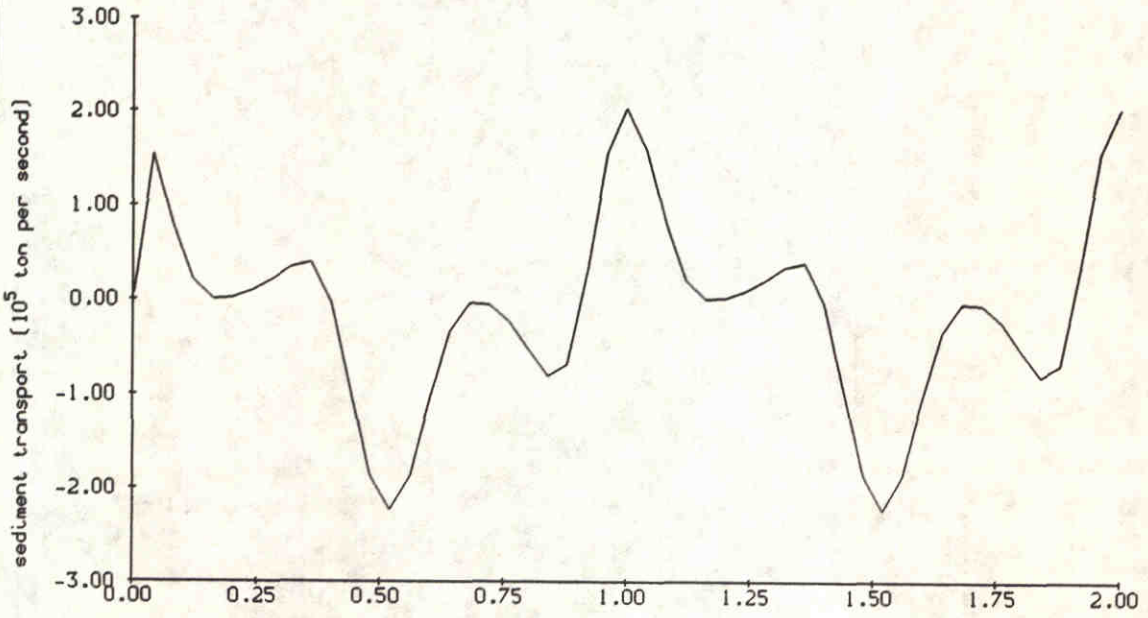

DELFT HYDRAULICS

sediment flux through cross section V03	e32	test run
tide, no wind, no wave	Kustgenese	
DELFT HYDRAULICS	h840.50	Fig. 4.14

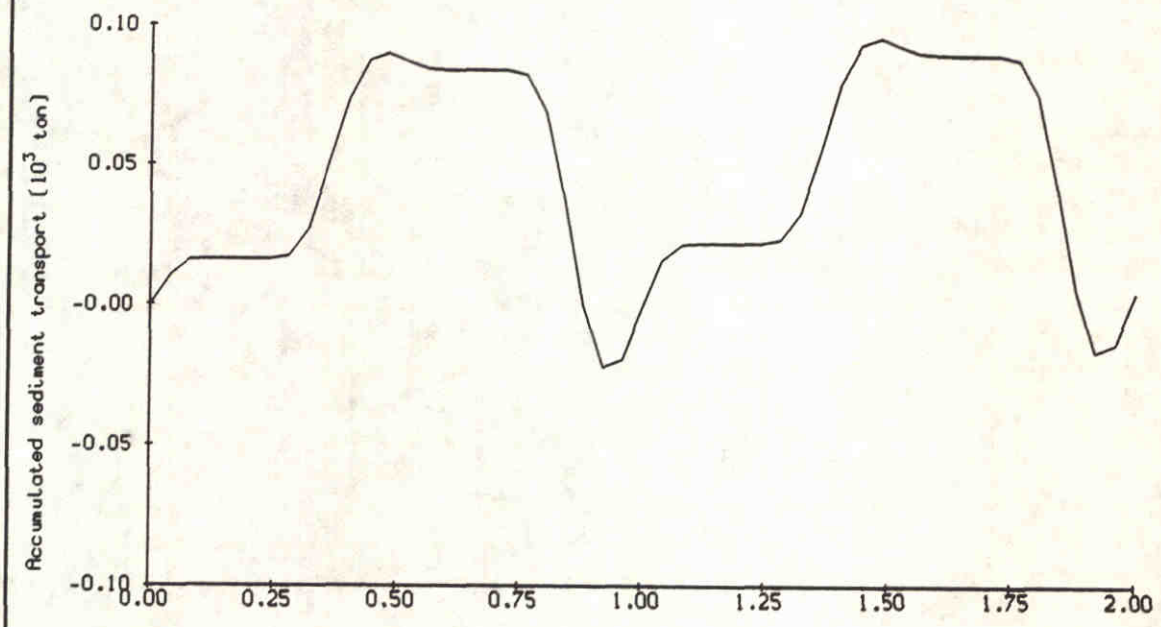

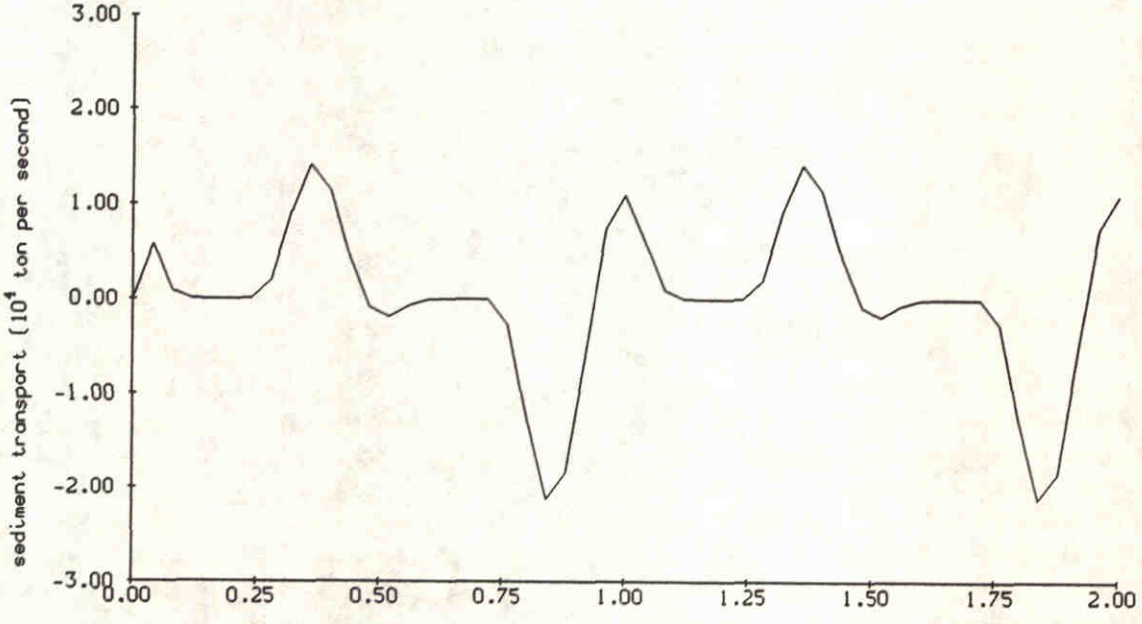

DELFT HYDRAULICS

sediment flux through cross section V06	e32	test run
tide, no wind, no wave	Kustgenese	
DELFT HYDRAULICS	h840.50	Fig. 4.15

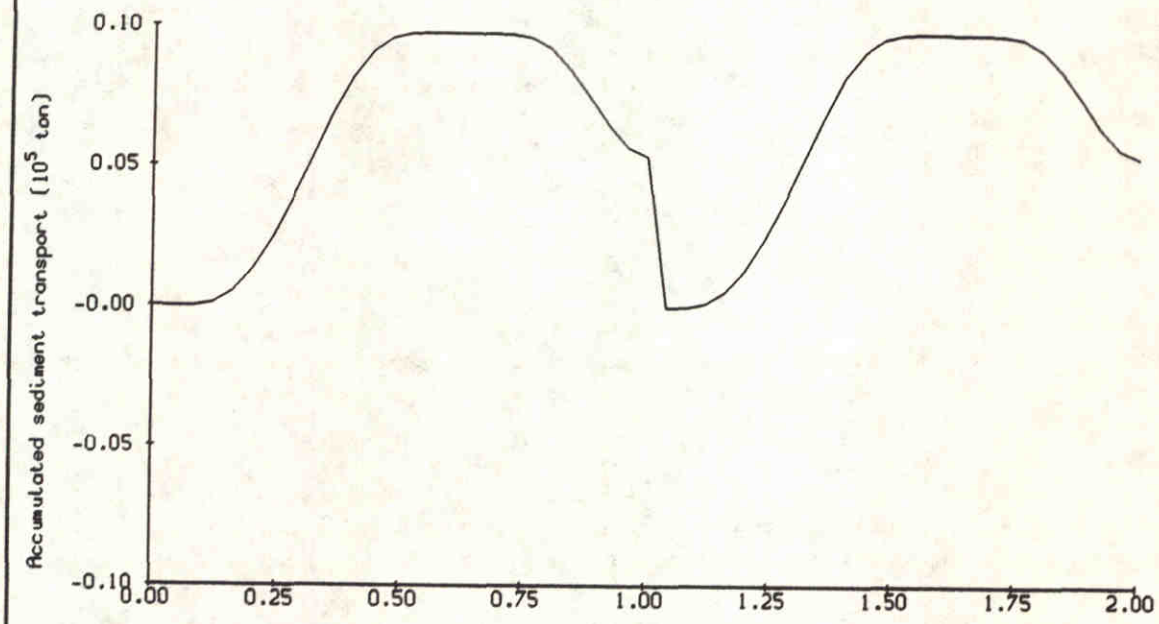

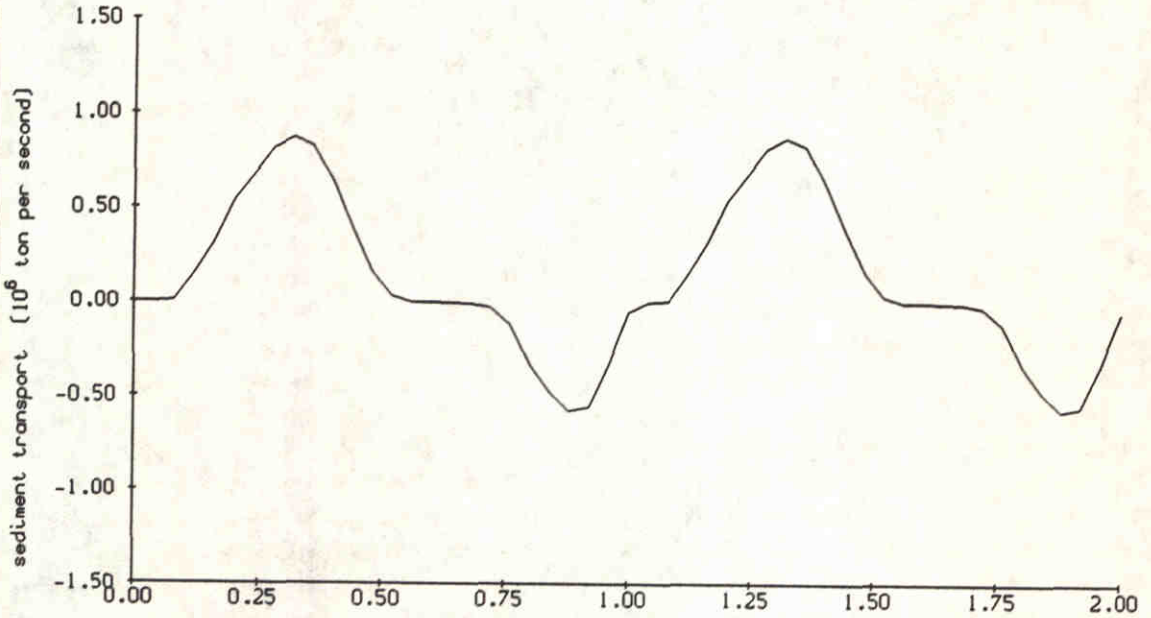

DELFT HYDRAULICS

sediment flux through cross section V09 tide, no wind, no wave	e32	test run
	Kustgenese	
DELFT HYDRAULICS	h840.50	Fig. 4.16

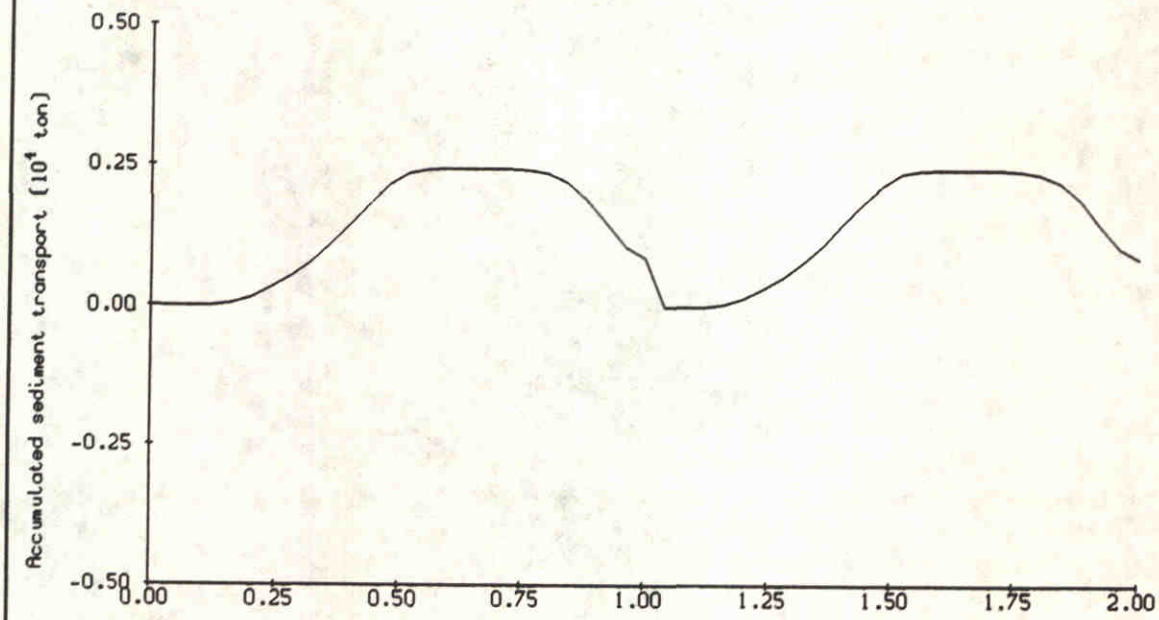

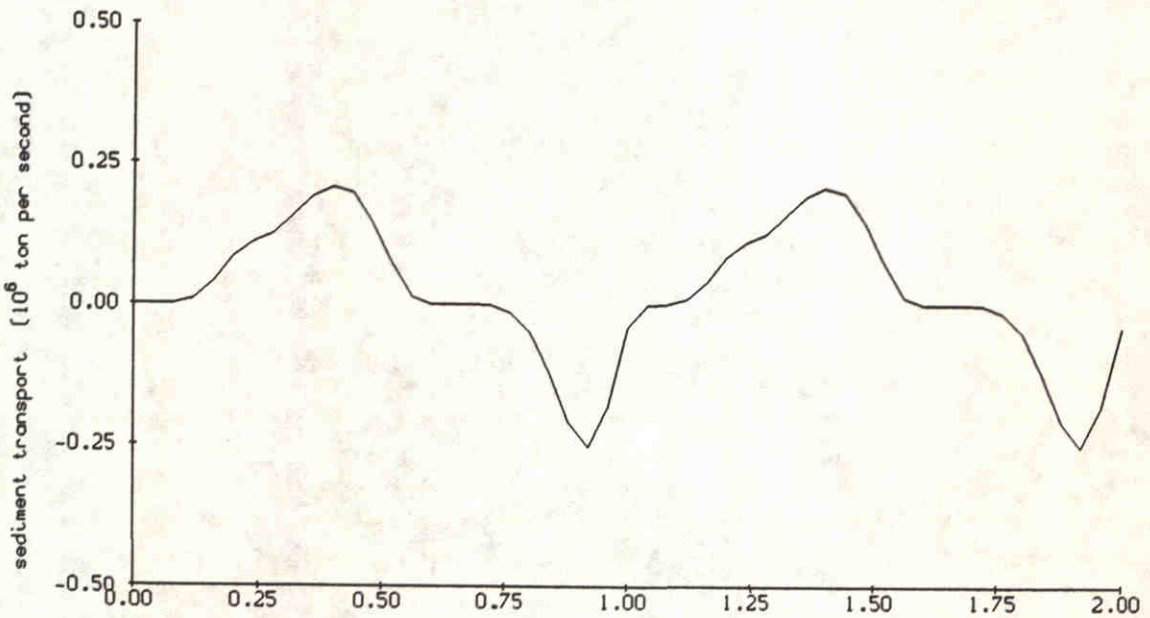

sediment flux through cross section V12 tide, no wind, no wave	e32	test run
	Kustgenese	
DELFT HYDRAULICS	h840.50	Fig. 4.17

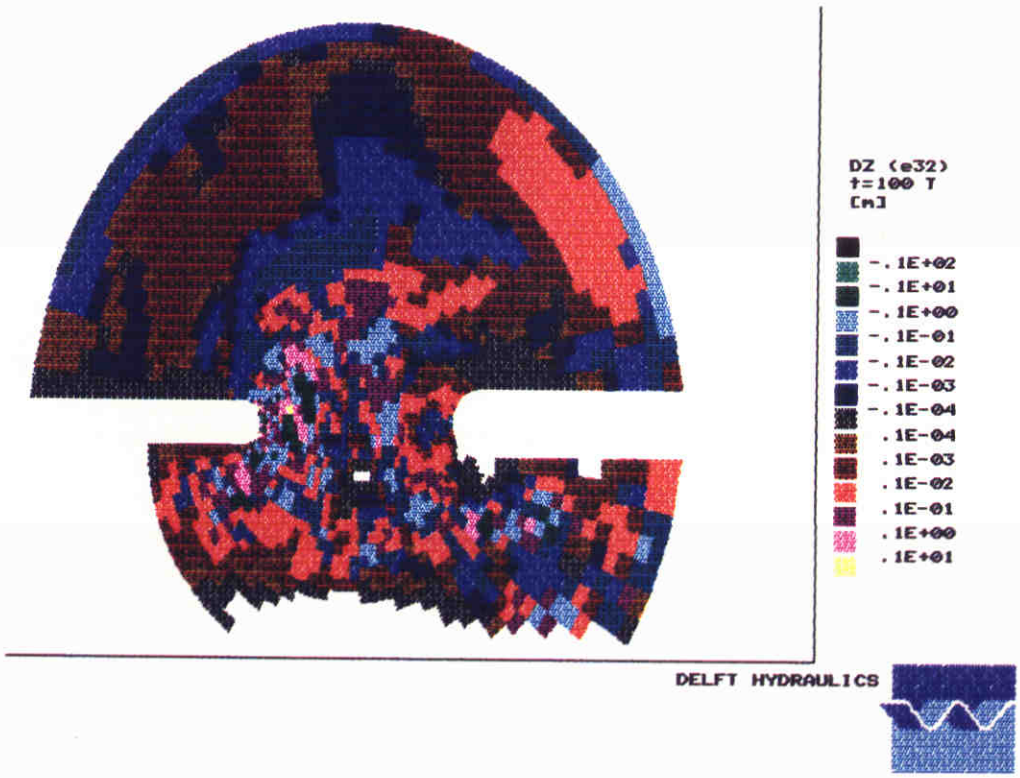

The sedimentation-erosion pattern
Run E32
(negative=erosion, positive=sedimentation)

Kustgenese Project

DELFT HYDRAULICS

h840.50

Fig.4.18

residual flow field
run e40
bathymetry from 1970

project Kustgenese	e40

WATERLOOPKUNDIG LABORATORIUM | H840.50 | Fig. 4.19

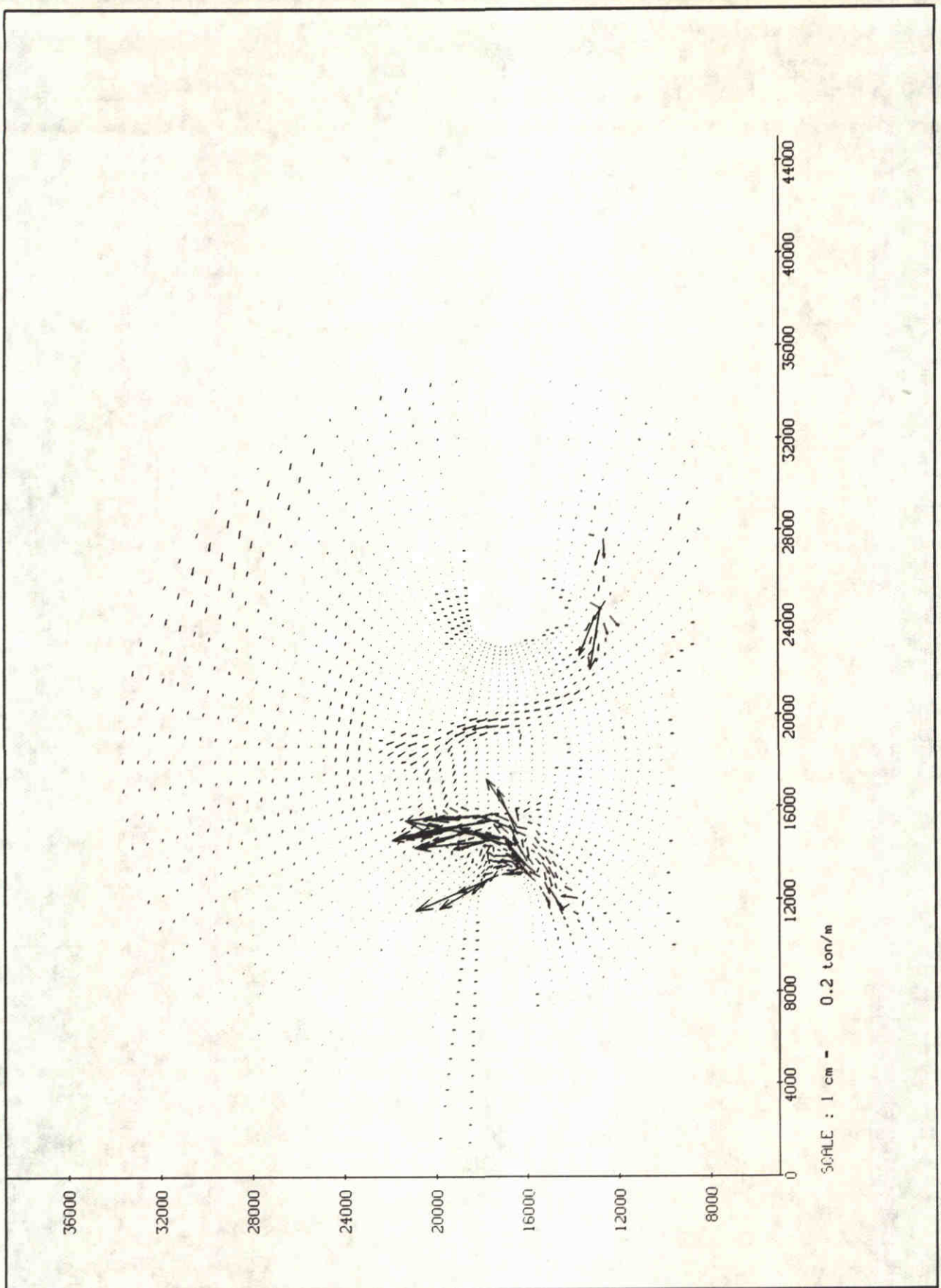

net sediment transport
run e40
bathymetry from 1970

project Kustgenese	e40
H840.50	Fig. 4.20

WATERLOOPKUNDIG LABORATORIUM

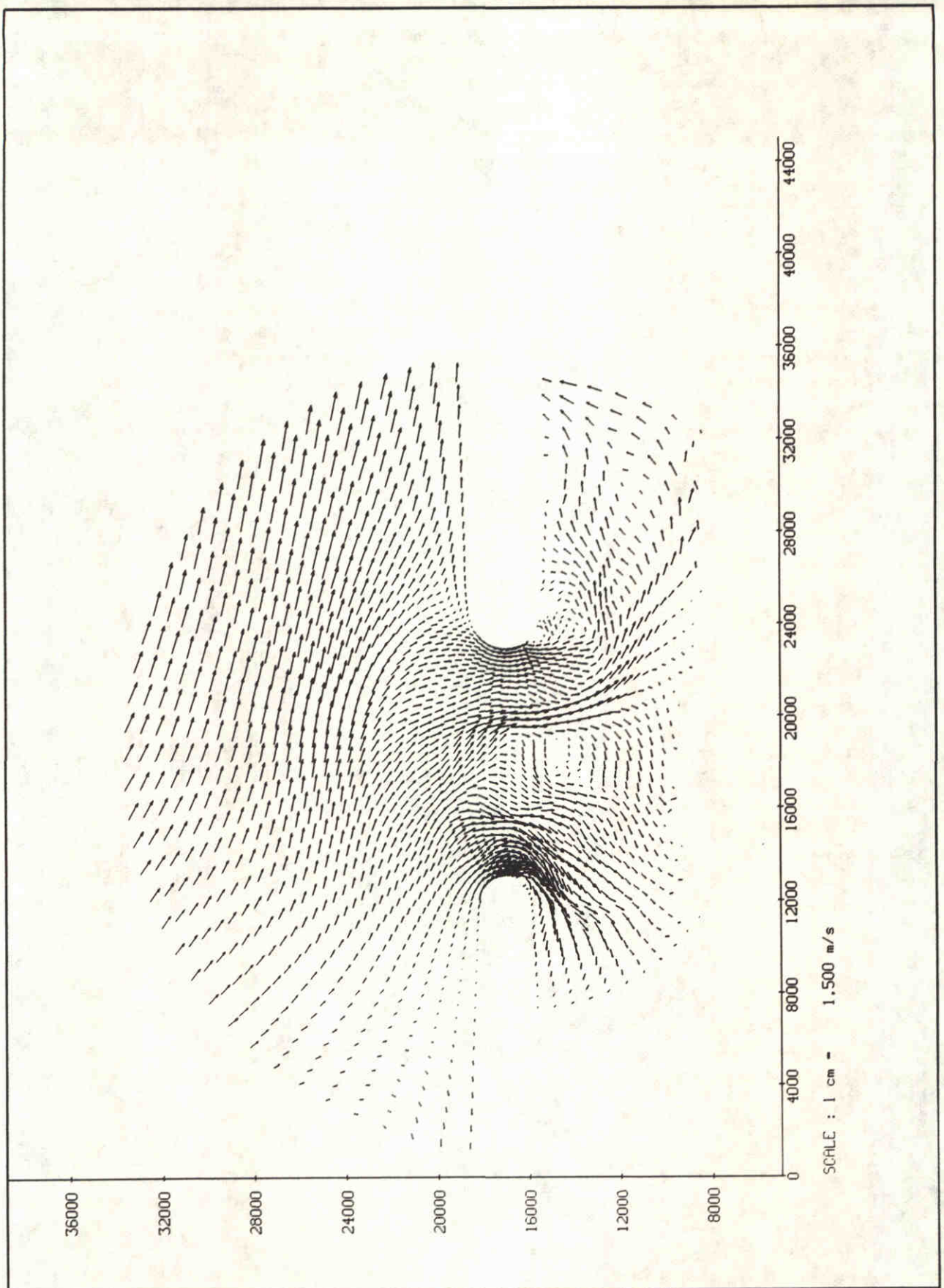

flow velocity at t= 1500 min.
run e40

Kustgenese project	e40
h840.50	Fig. 4.21

WATERLOOPKUNDIG LABORATORIUM

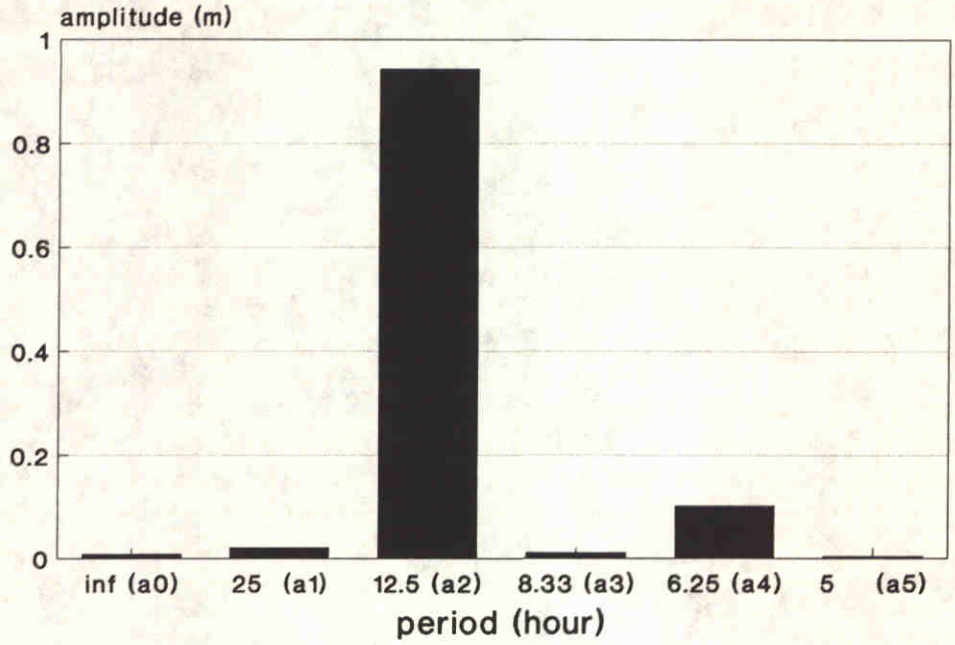

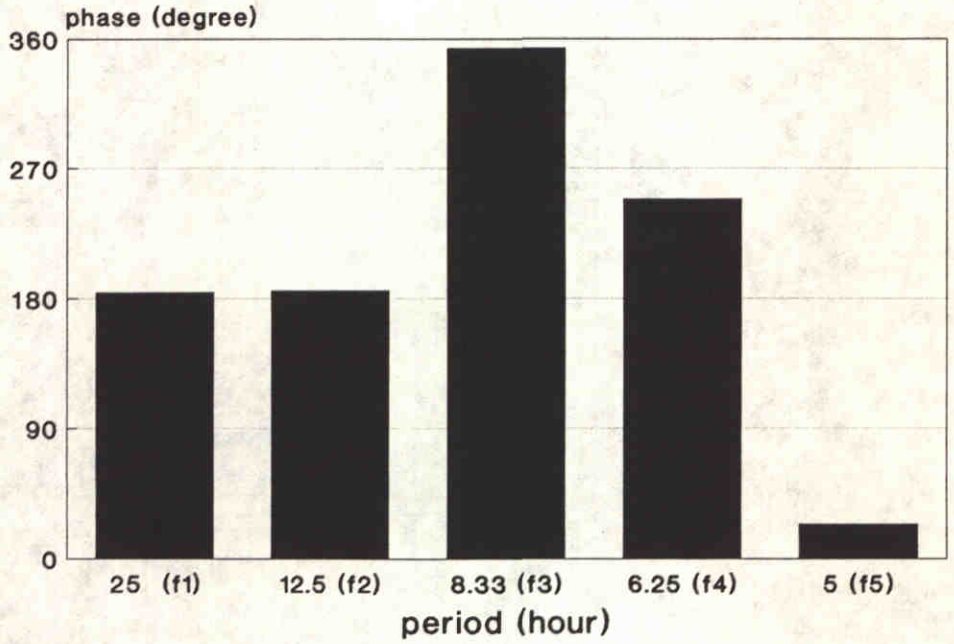

The Fourier components
at the grid point (M-2, N-62)
the western end of the open sea boundary

Kustgenese Project

DELFT HYDRAULICS | h840.50 | Fig.4.22

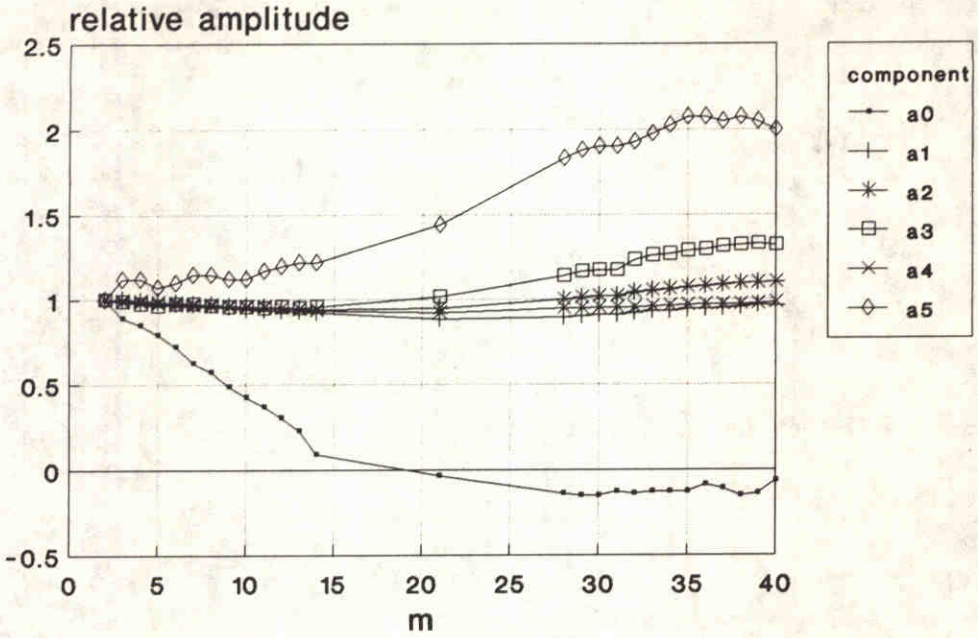

relative amplitude =
local amplitude/amplitude at m=2

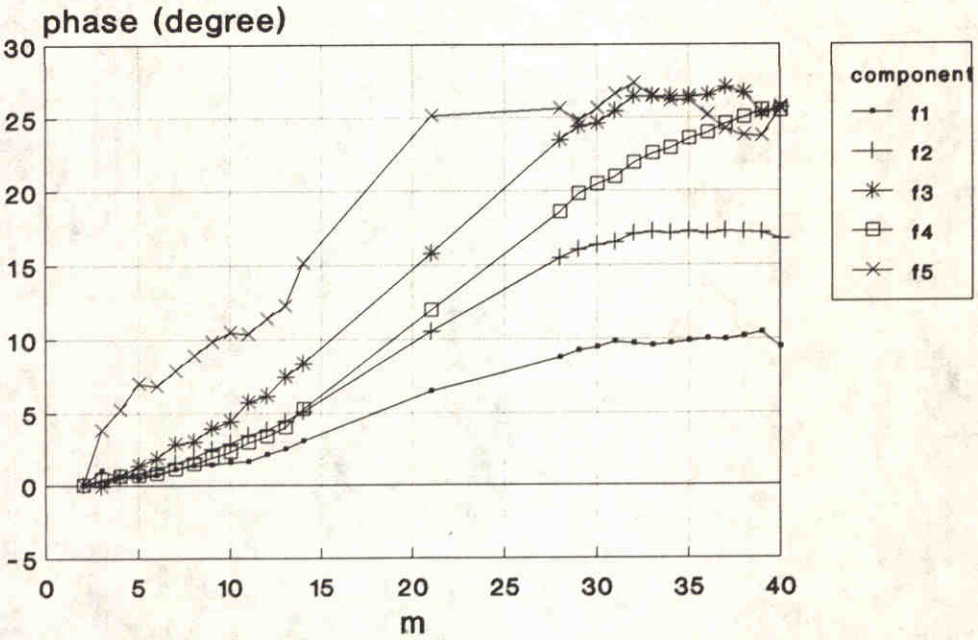

phase lag with respect to m=2
western end of the boundary

The Fourier components varying along the boundary from west to east (m=grid number)		
	Kustgenese Project	
DELFT HYDRAULICS	h840.50	Fig.4.23

residual flow
run E03
bathymetry from 1970

project
Kustgenese

E03

DELFT HYDRAULICS

H0840.50

Fig. 4.24

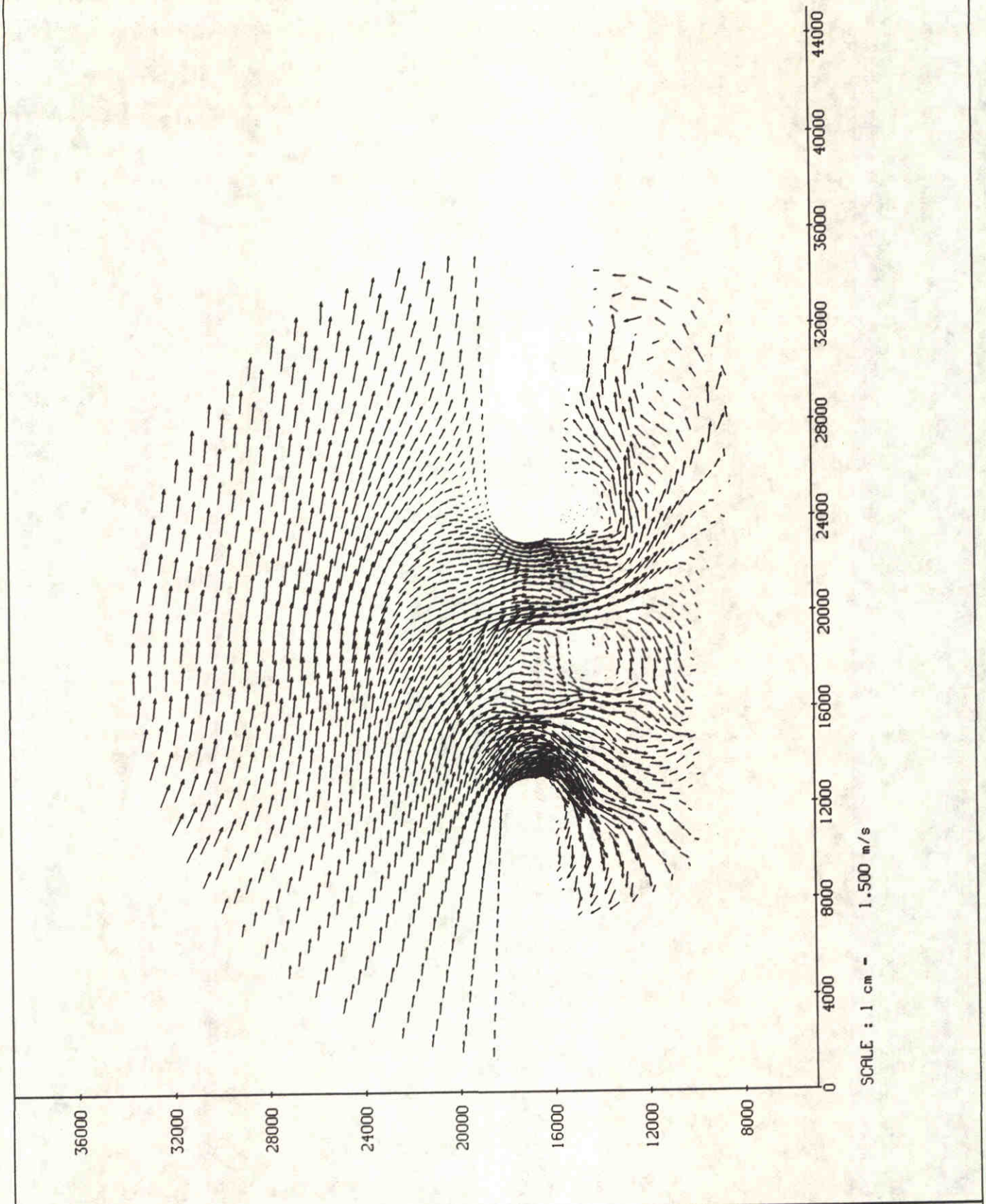

flow velocity at t= 1800 min.
run e03

Kustgenese project	e03
h840.50	Fig. 4.25

WATERLOOPKUNDIG LABORATORIUM

flow velocity at t= 2850 min.

E03 | 02-04-91

Kustgenese

WATERLOOPKUNDIG LABORATORIUM | H0840.50 | Fig. 4.26

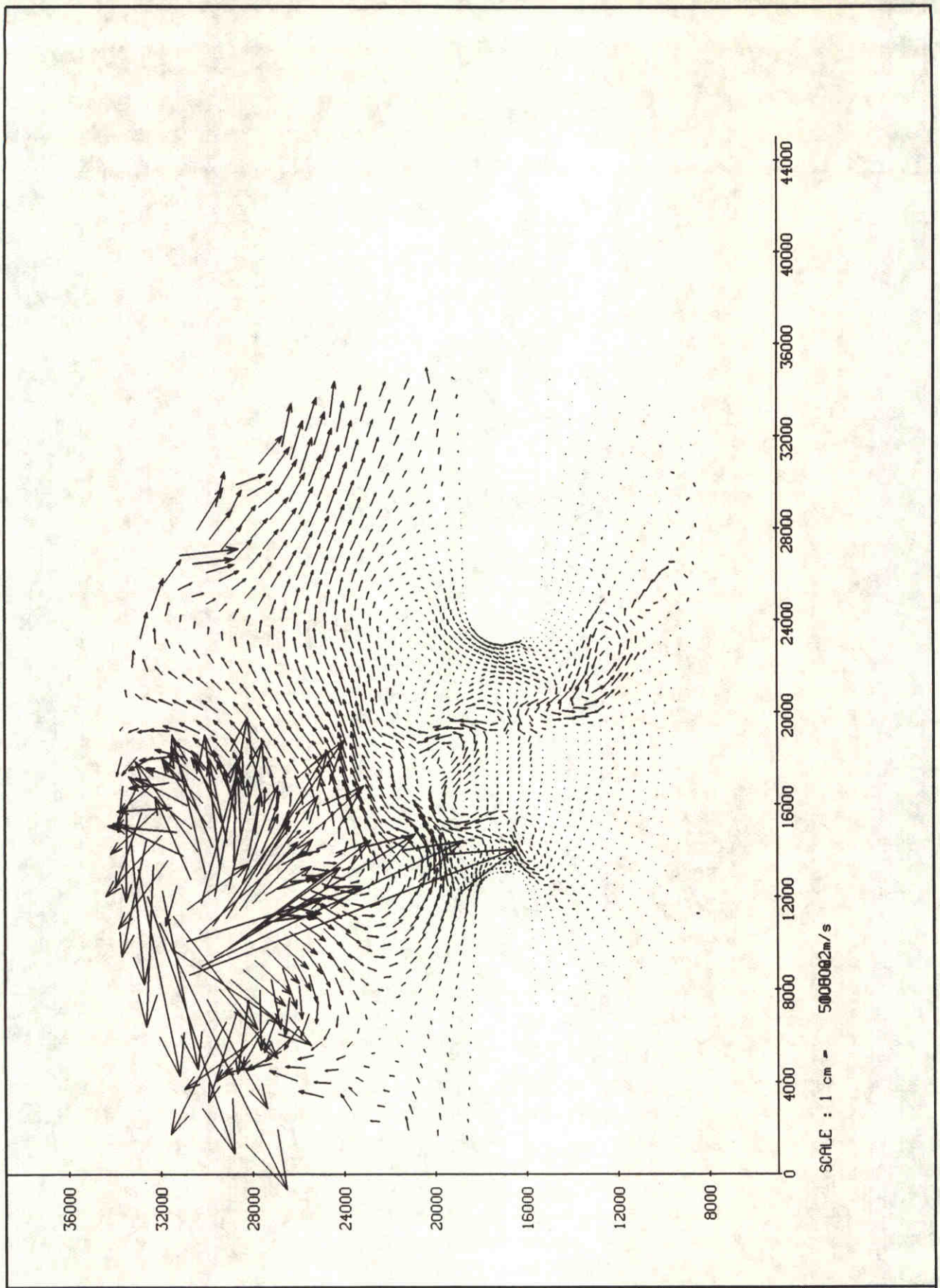

residual flow	E04	03-04-91
bathymetry from 1970	Kustgenese	
WATERLOOPKUNDIG LABORATORIUM	H0840.50	Fig. 4.27

residual sediment transport run e03 step - 1	e03 91-08-26	mapinf.e07
WATERLOOPKUNDIG LABORATORIUM	H840.50	Fig. 4.28

The sedimentation-erosion pattern
Run E03
(negative=erosion, positive=sedimentation)

Kustgenese Project

DELFT HYDRAULICS

h840.50

Fig.4.29

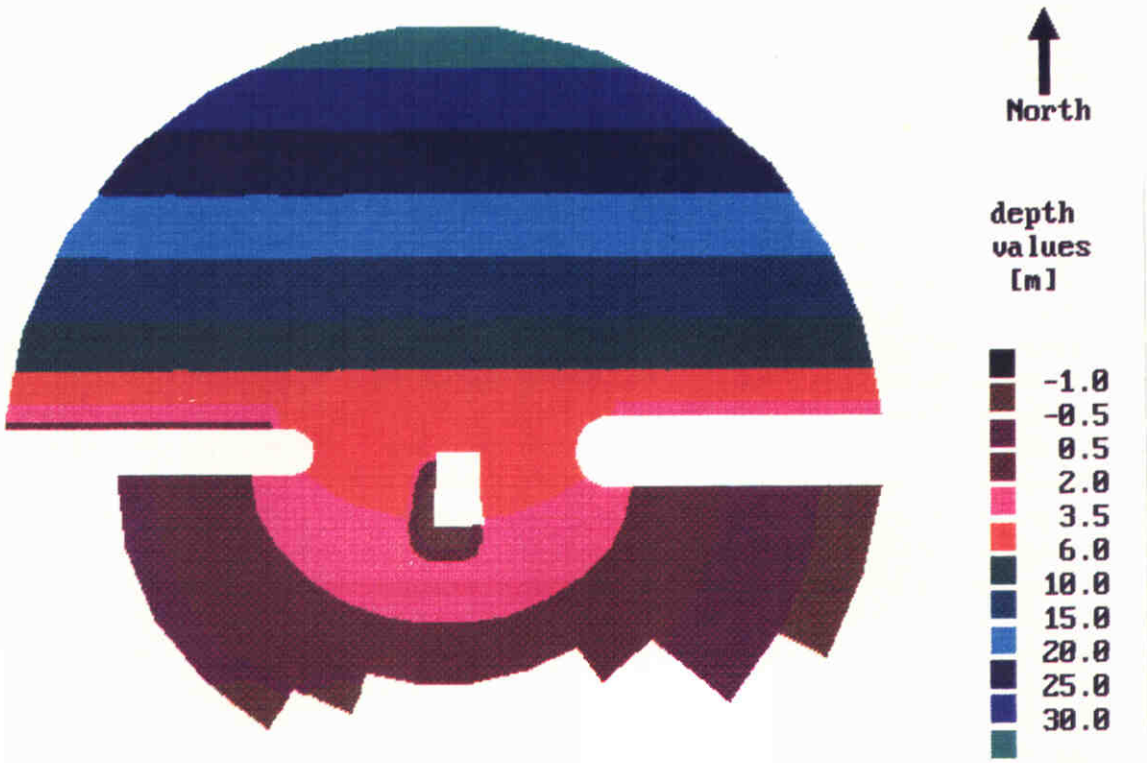

w40 DELFT HYDRAULICS

Initial bathymetry of run W40

Kustgenese Project

DELFT HYDRAULICS | h840.50 | Fig.5.1

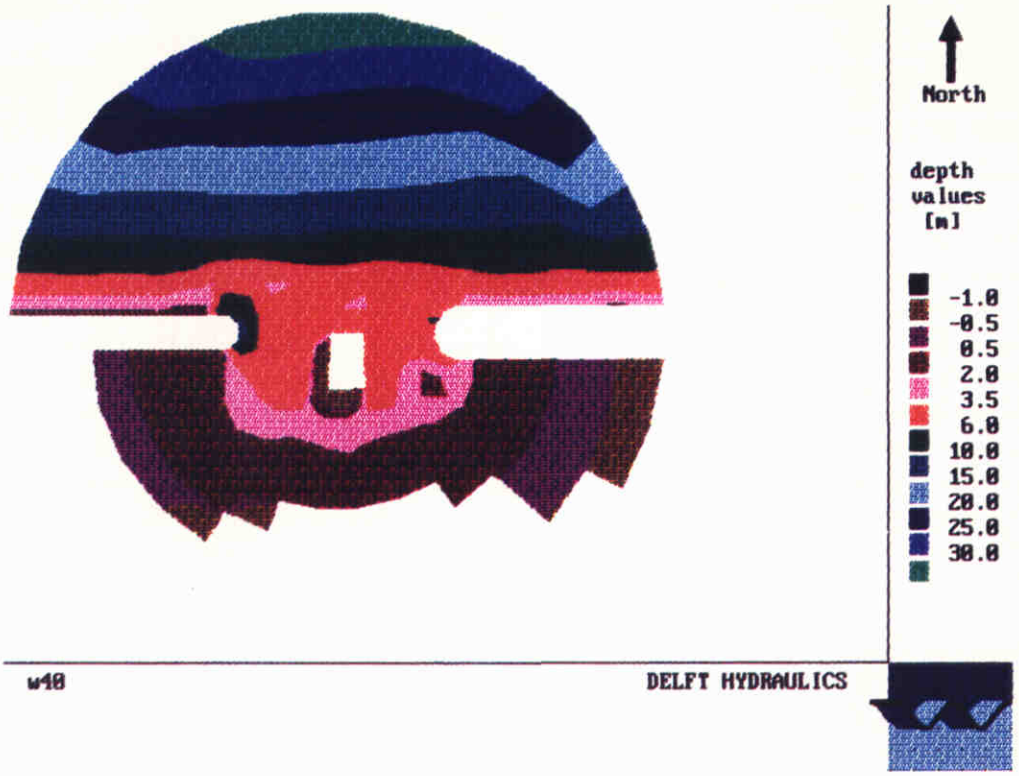

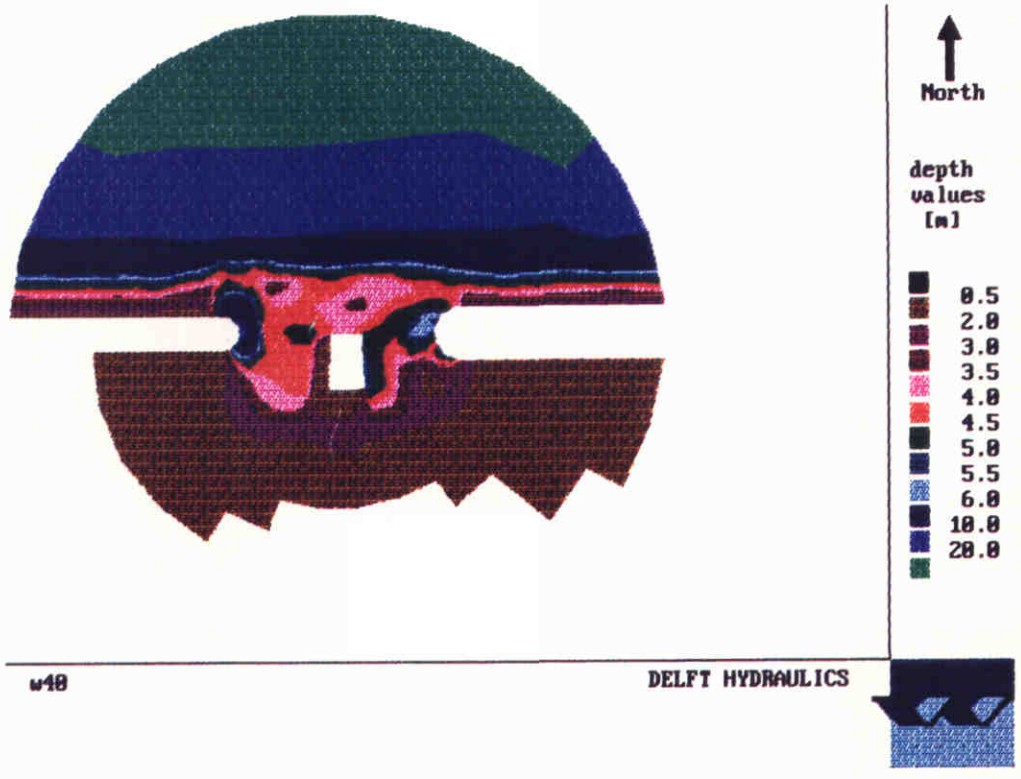

Computed bathymetry after 17 steps (run W40)
Top: overal picture
Bottom: detail around the gorge

Kustgenese Project

DELFT HYDRAULICS | h840.50 | Fig.5.2

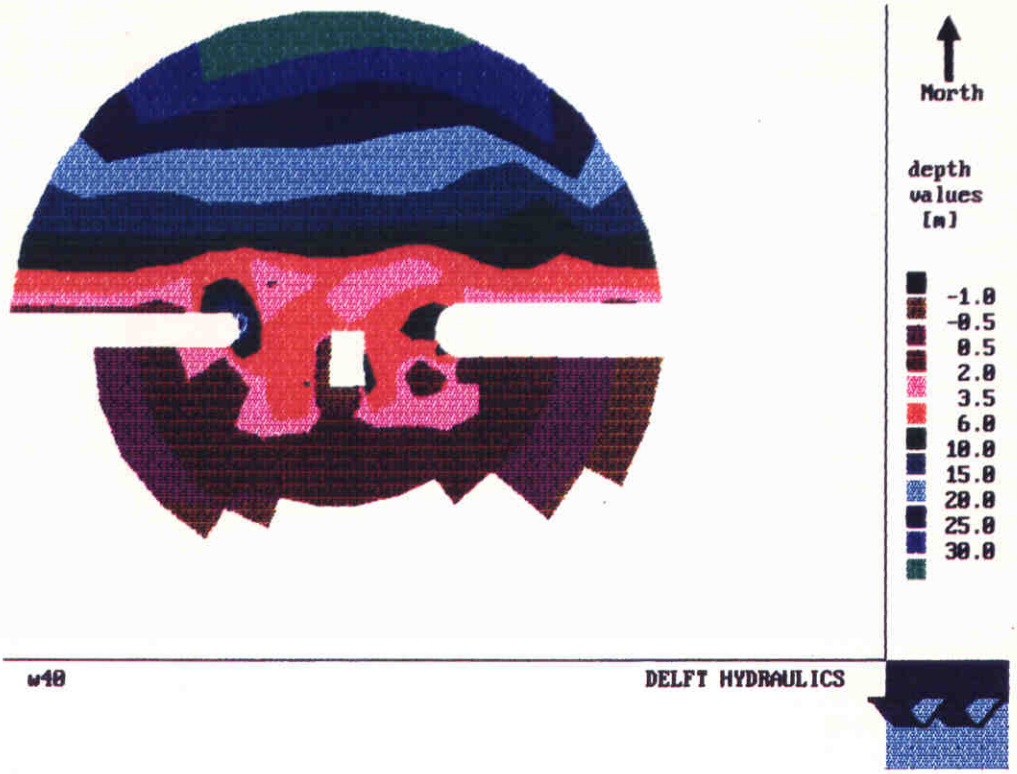

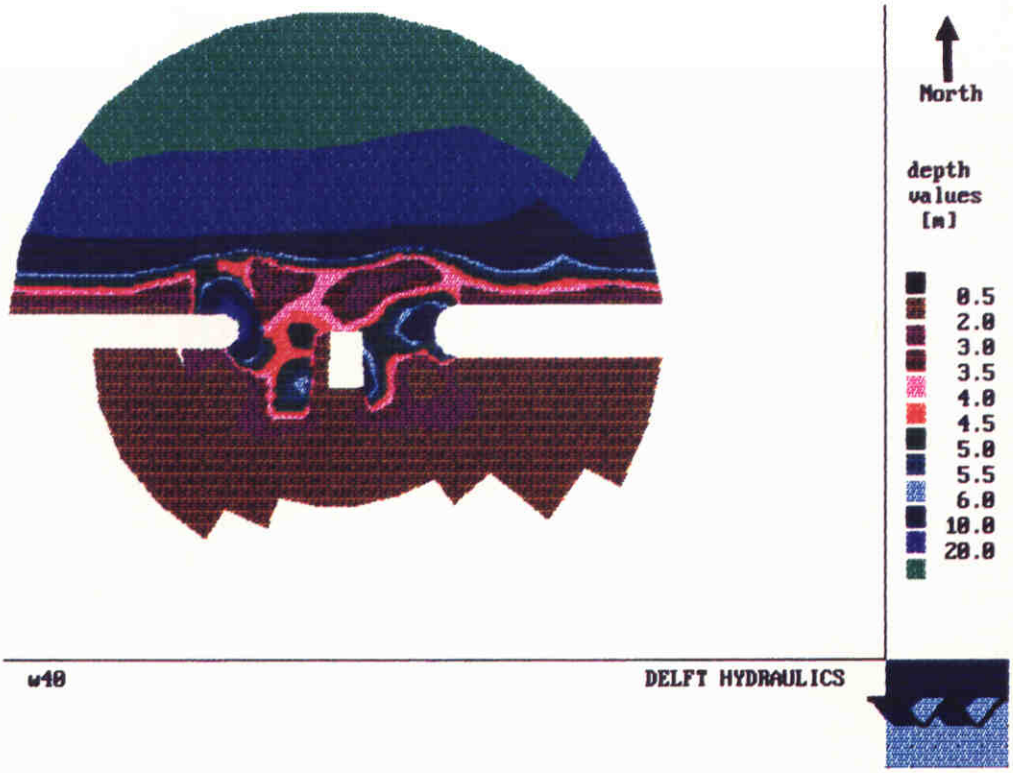

Computed bathymetry after 41 steps (run W40)
Top: overal picture
Bottom: detail around the gorge

Kustgenese Project

DELFT HYDRAULICS | h840.50 | Fig.5.3

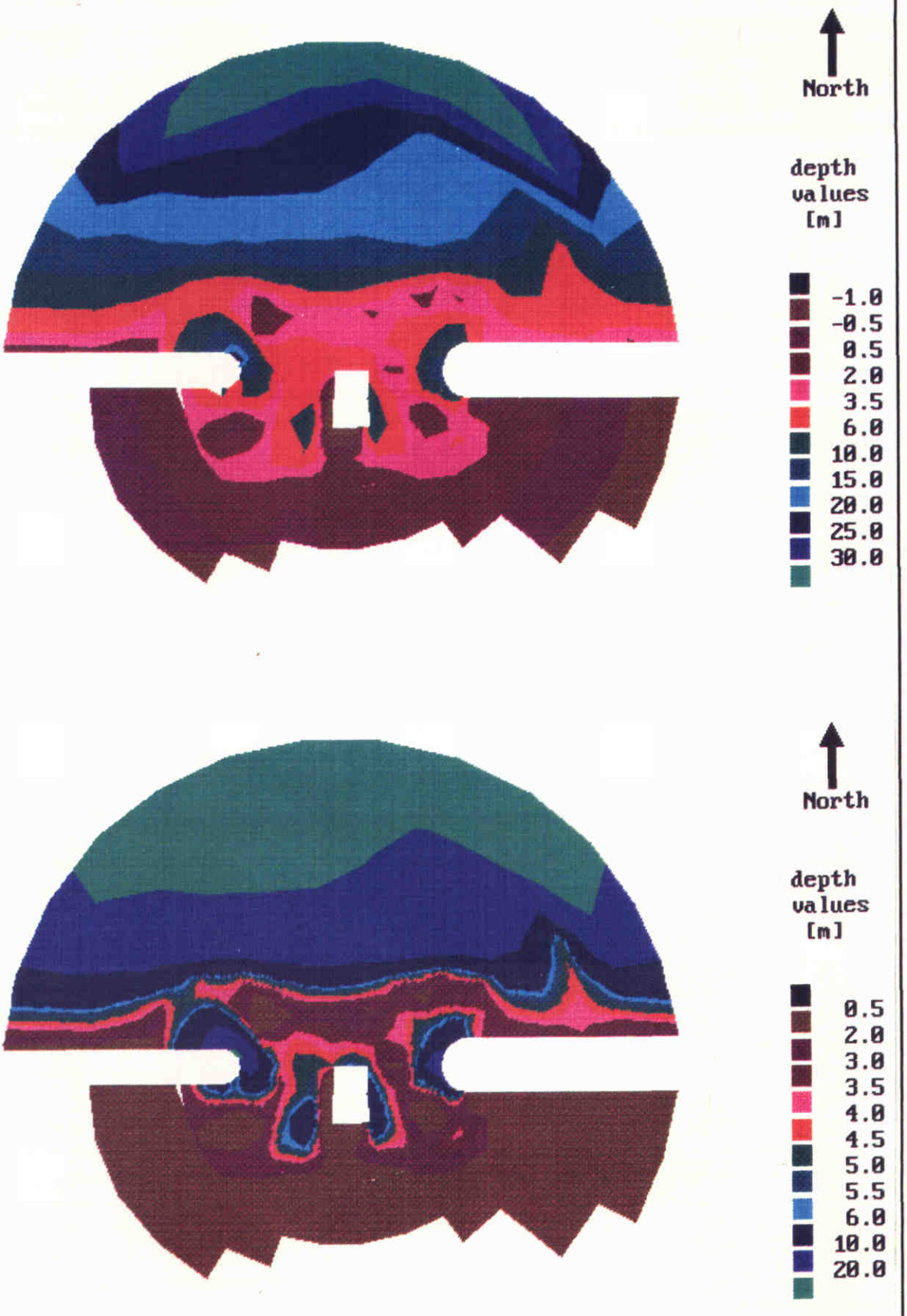

Computed bathymetry after 81 steps (run W40)
Top: overal picture
Bottom: detail around the gorge

Kustgenese Project

DELFT HYDRAULICS | h840.50 | Fig.5.4

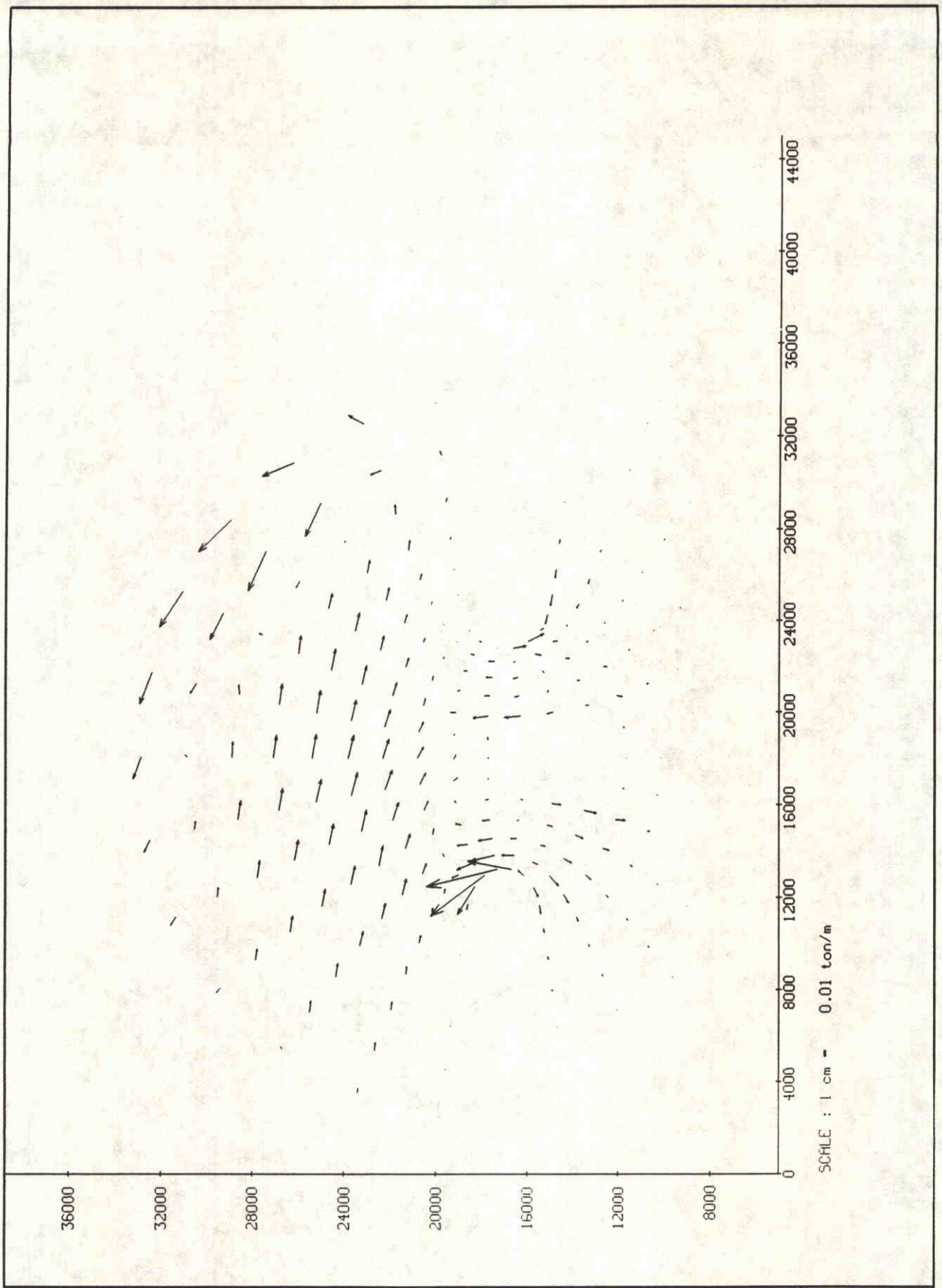

net sediment transport
run w40
Tm=0.

project Kustgenese	w40

WATERLOOPKUNDIG LABORATORIUM | H840.50 | Fig. 5.5

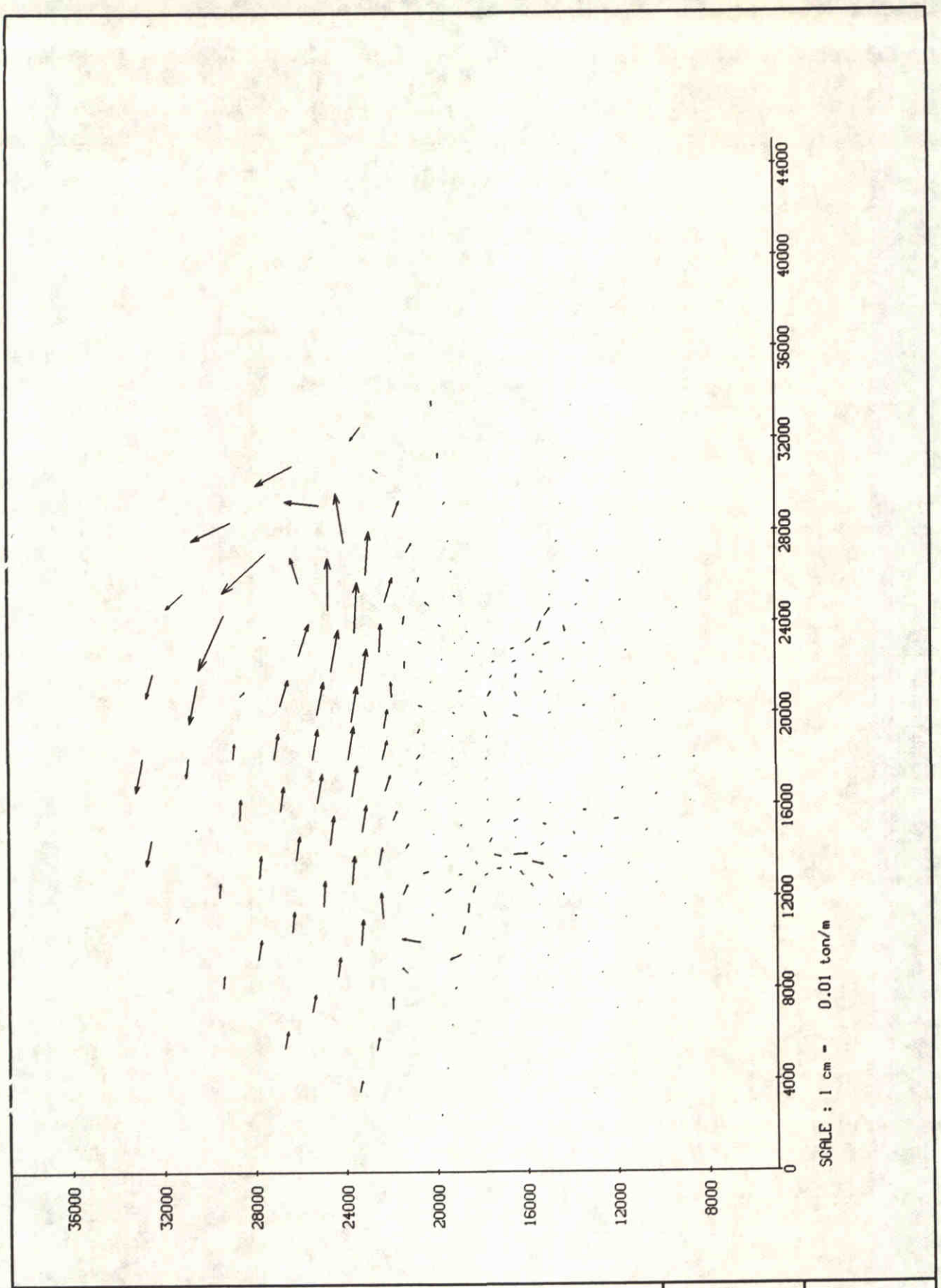

net sediment transport
run w40
Tm=81 year

	project Kustgenese	w40
WATERLOOPKUNDIG LABORATORIUM	H840.50	Fig. 5.6

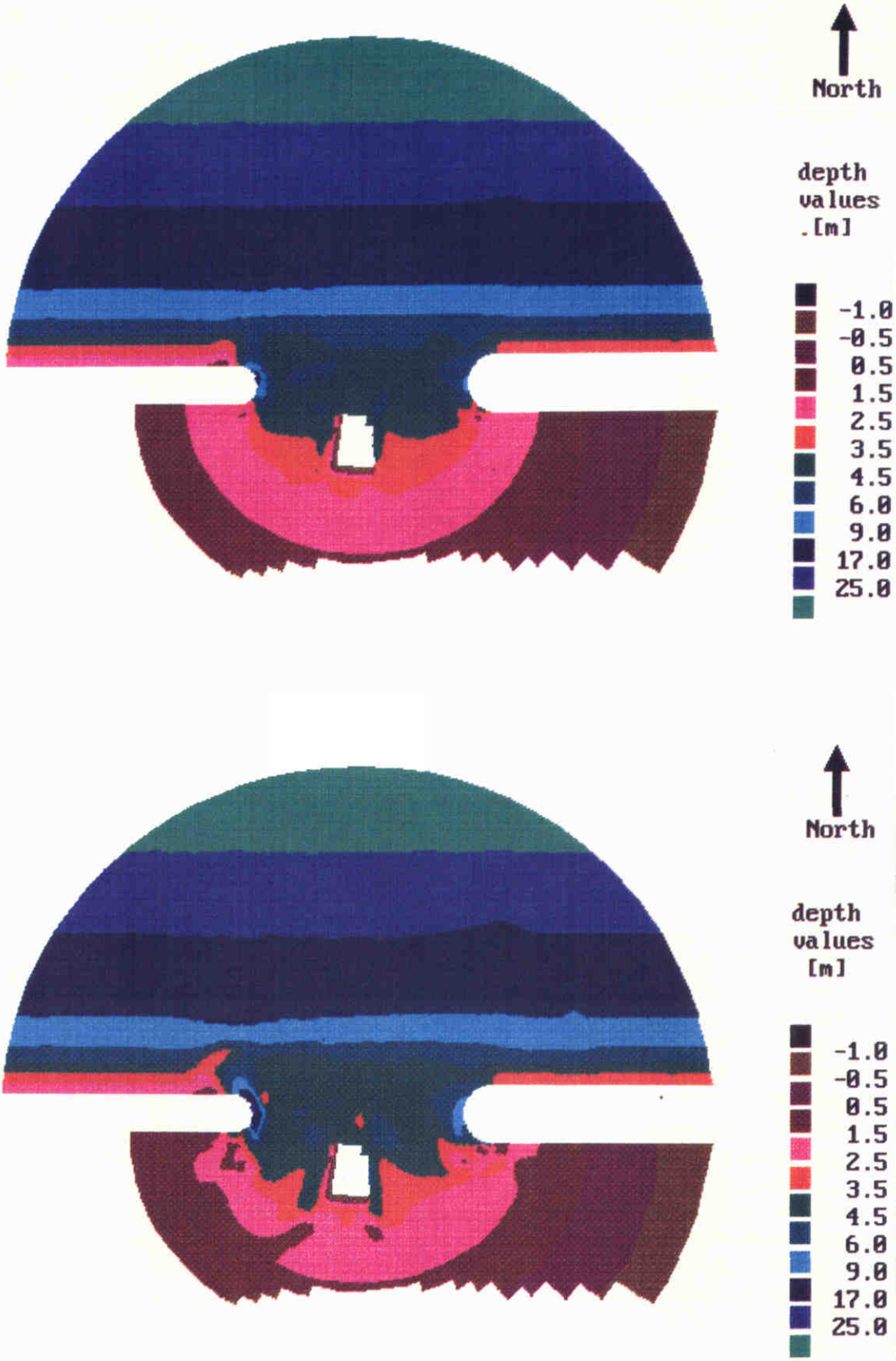

Computed bathymetry from run WS6
Top: after 21 steps
Bottom: after 42 steps

Kustgenese Project

DELFT HYDRAULICS

h840.50

Fig.5.7

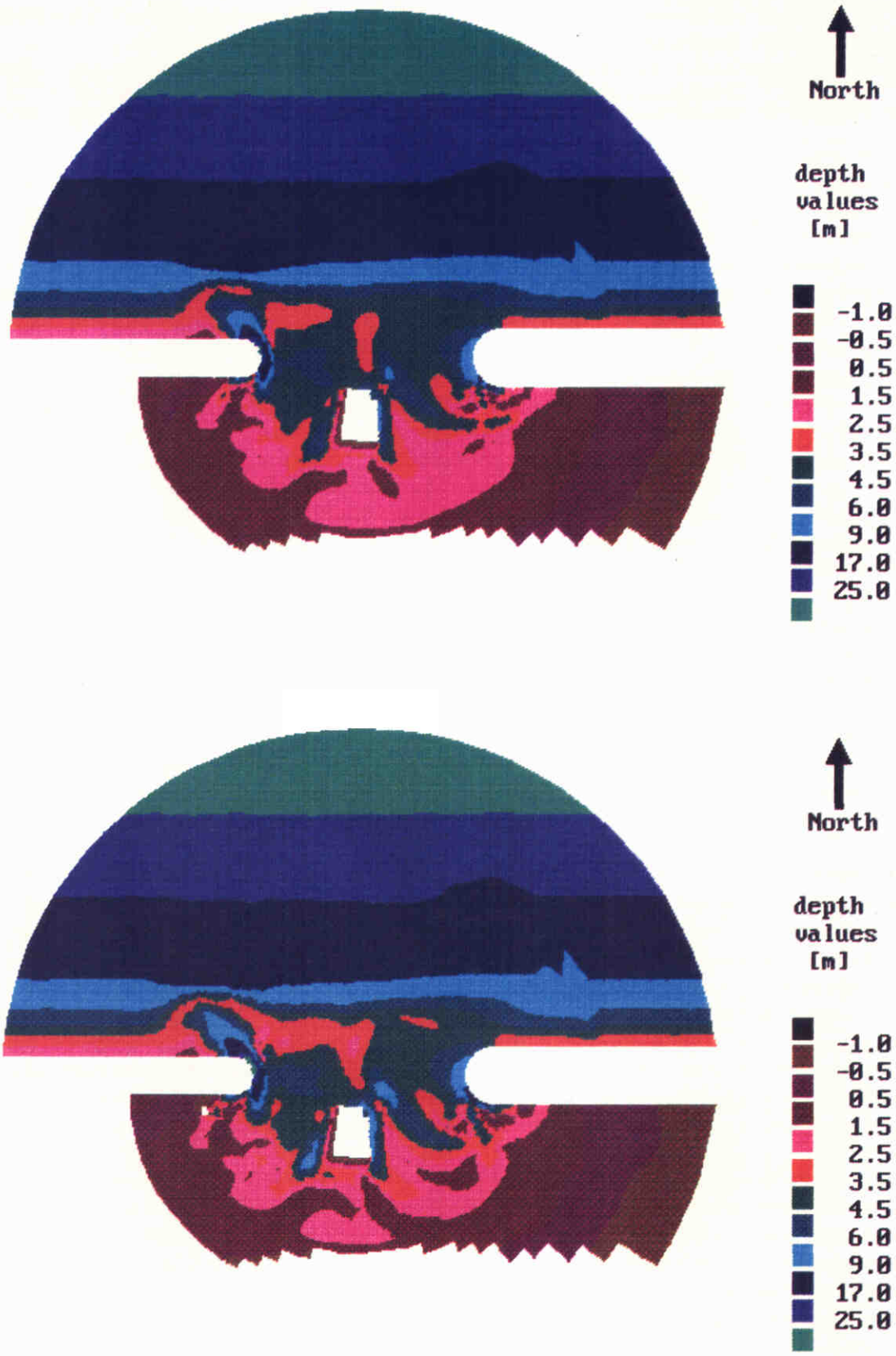

Computed bathymetry from run WS6
Top: after 63 steps
Bottom: after 84 steps

Kustgenese Project

DELFT HYDRAULICS

h840.50

Fig.5.8

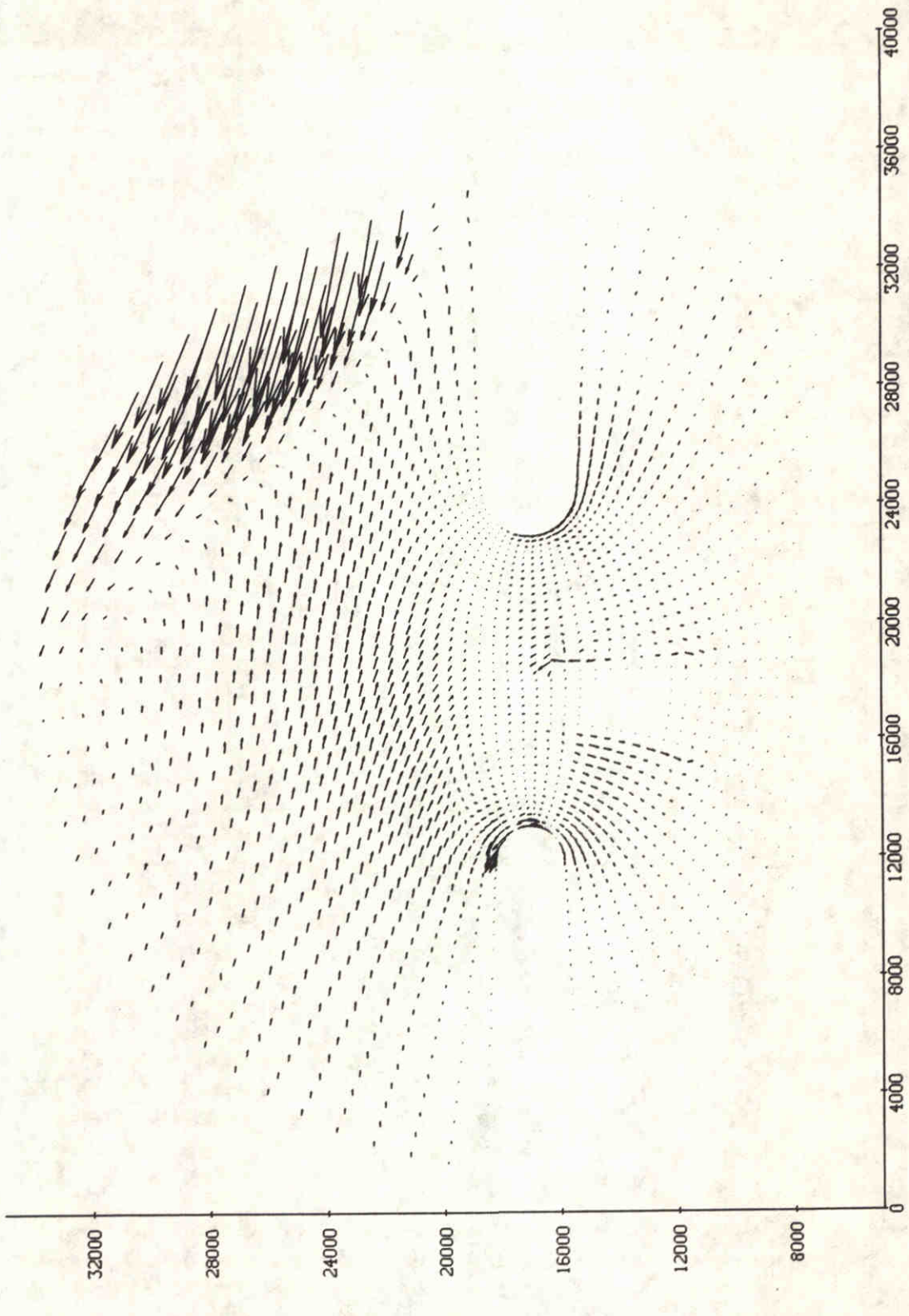

Net Sediment transport at Tm=1	91-06-28	mapinf.
WATERLOOPKUNDIG LABORATORIUM	H840.50	Fig.5.9

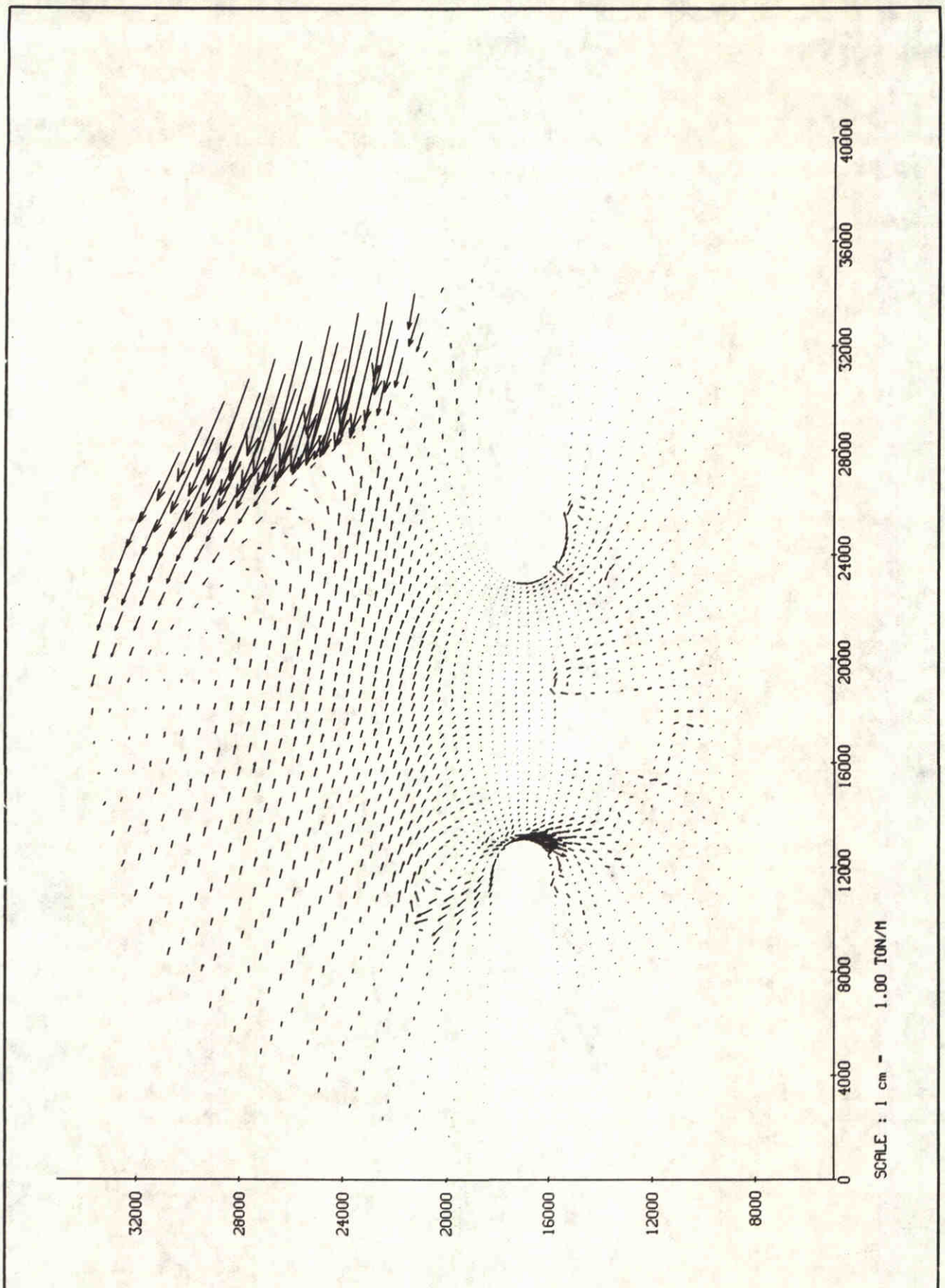

NET SEDIMENT TRANSPORT	91-09-20	mopinf
at Tm=84 steps		
DELFT HYDRAULICS	H840.50	Fig. 5.10

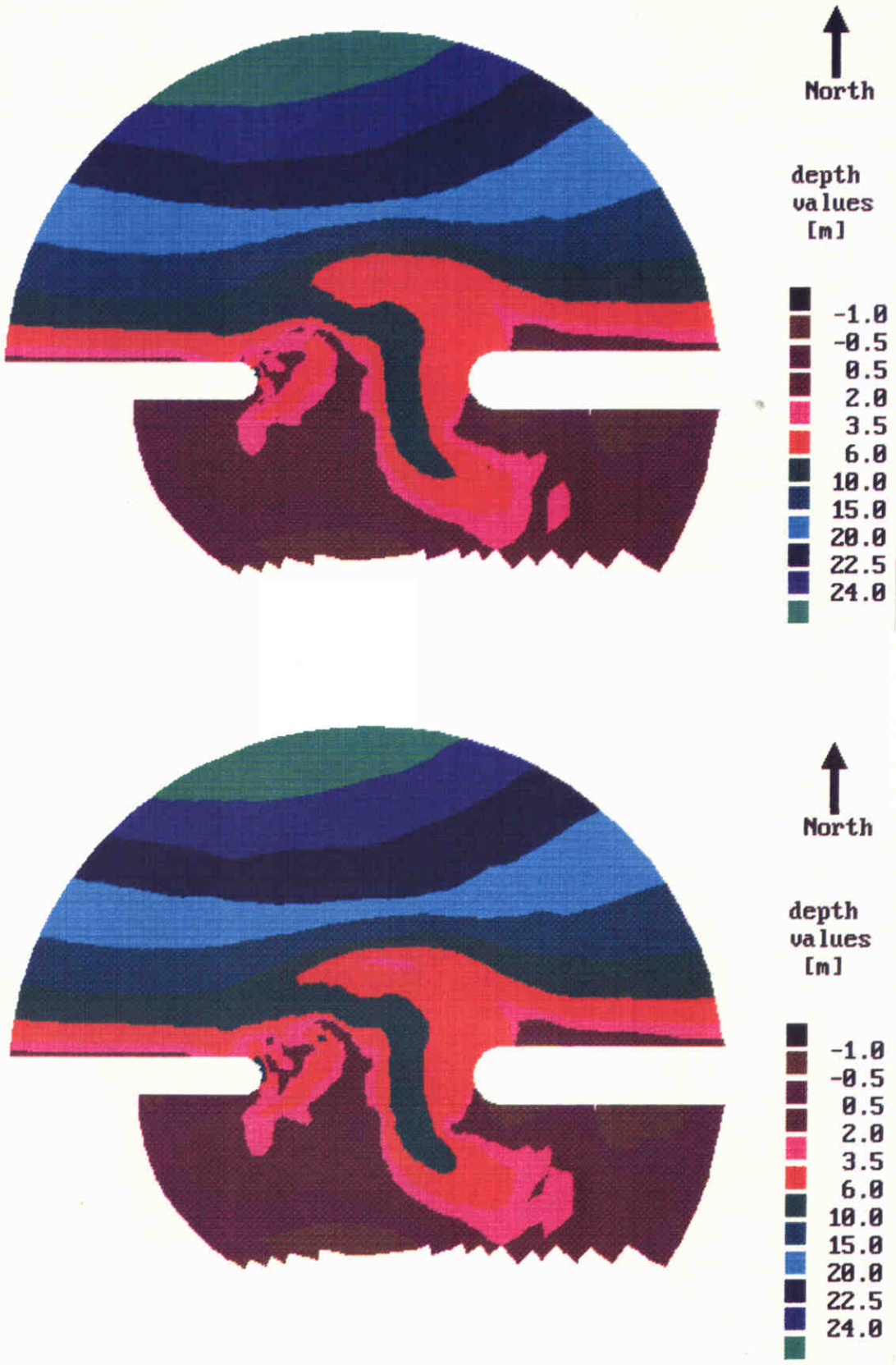

Computed bathymetry from run SM4
Top: after 41 steps
Bottom: after 66 steps

Kustgenese Project

DELFT HYDRAULICS | h840.50 | Fig.5.11

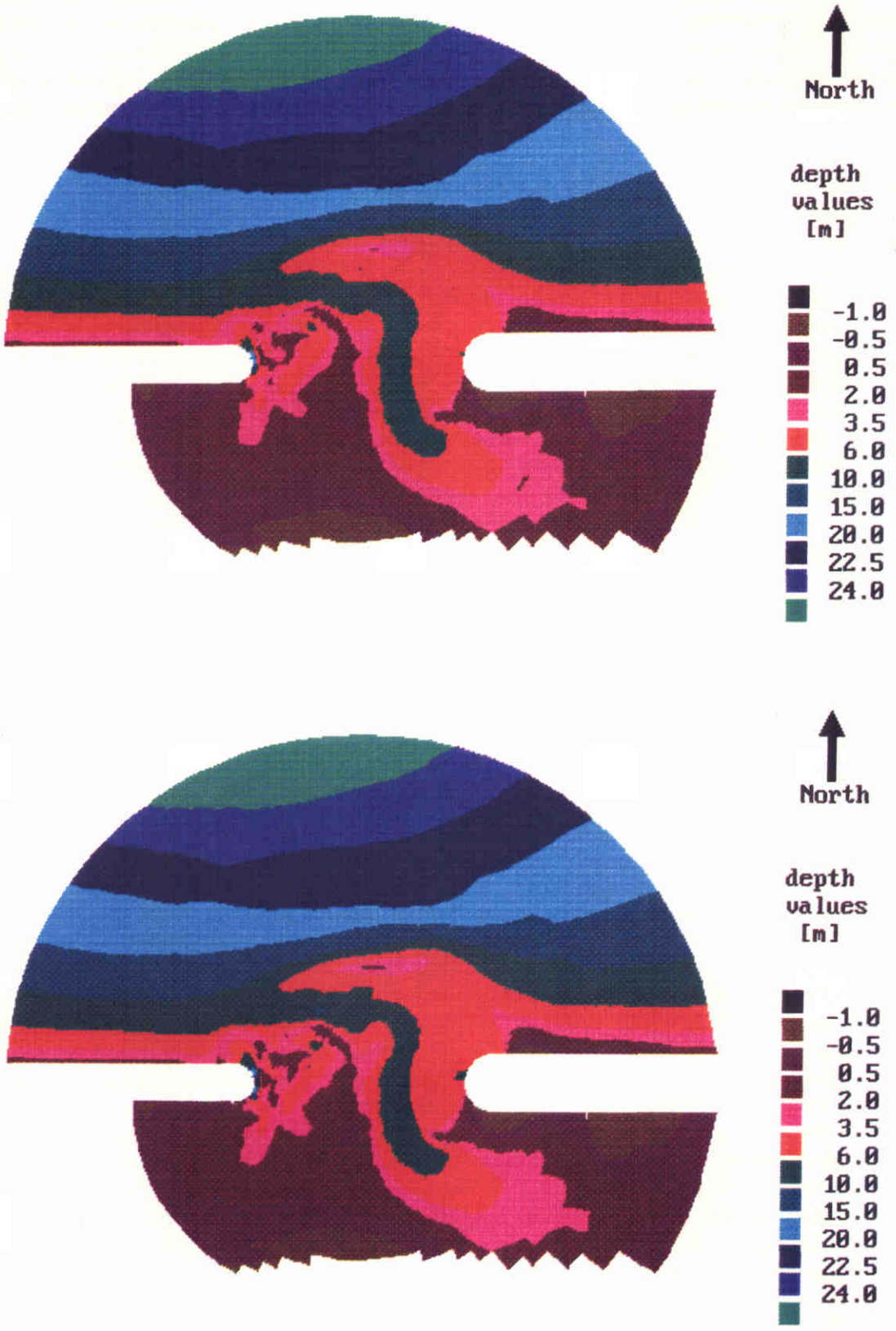

Computed bathymetry from run SM4
Top: after 91 steps
Bottom: after 116 steps

Kustgenese Project

DELFT HYDRAULICS

h840.50

Fig.5.12

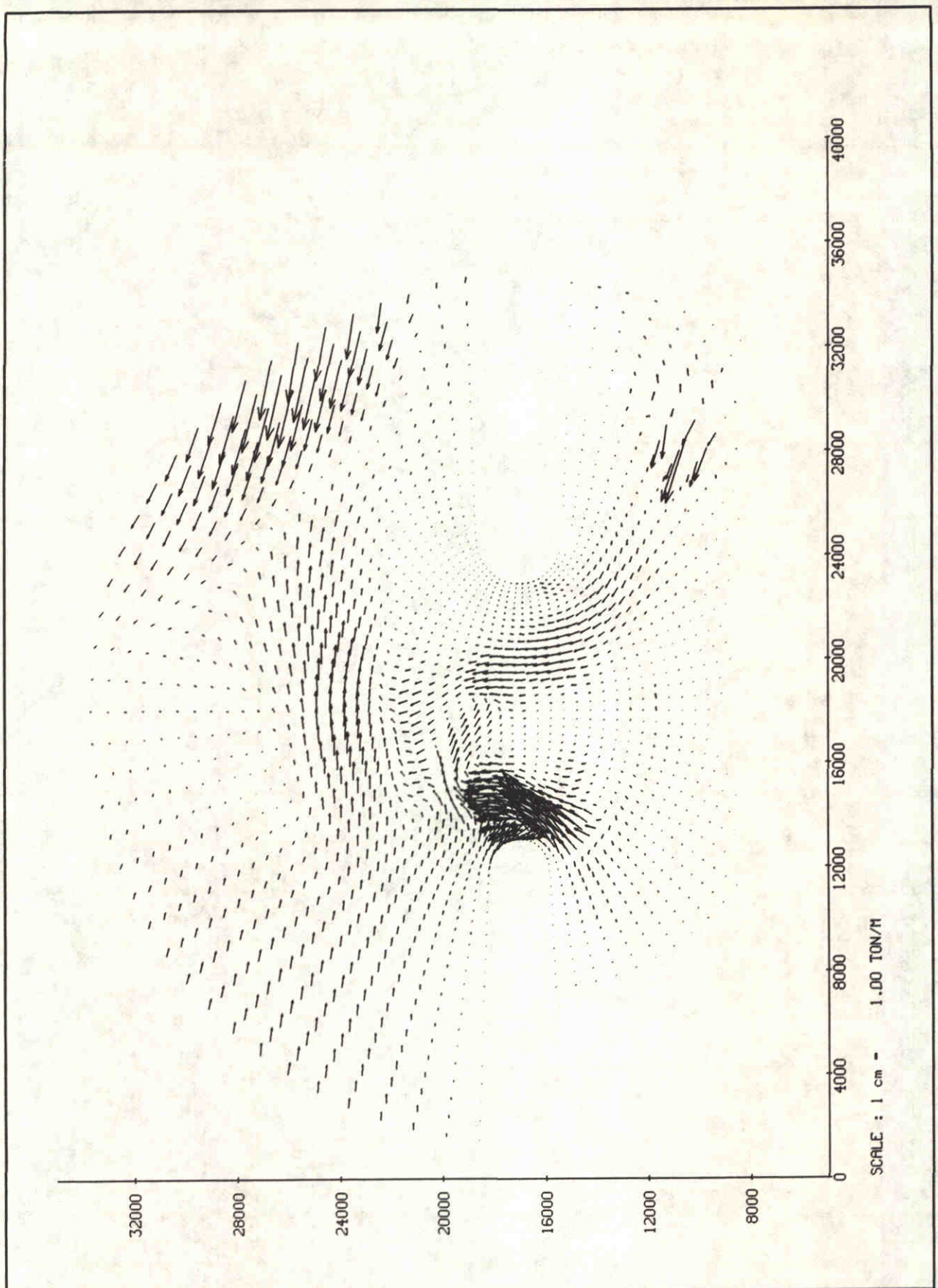

NET SEDIMENT TRANSPORT run sm4 at Tm=0.	sm 4 91-06-20	mopinf.sm4
DELFT HYDRAULICS	H840.50	Fig. 5.13

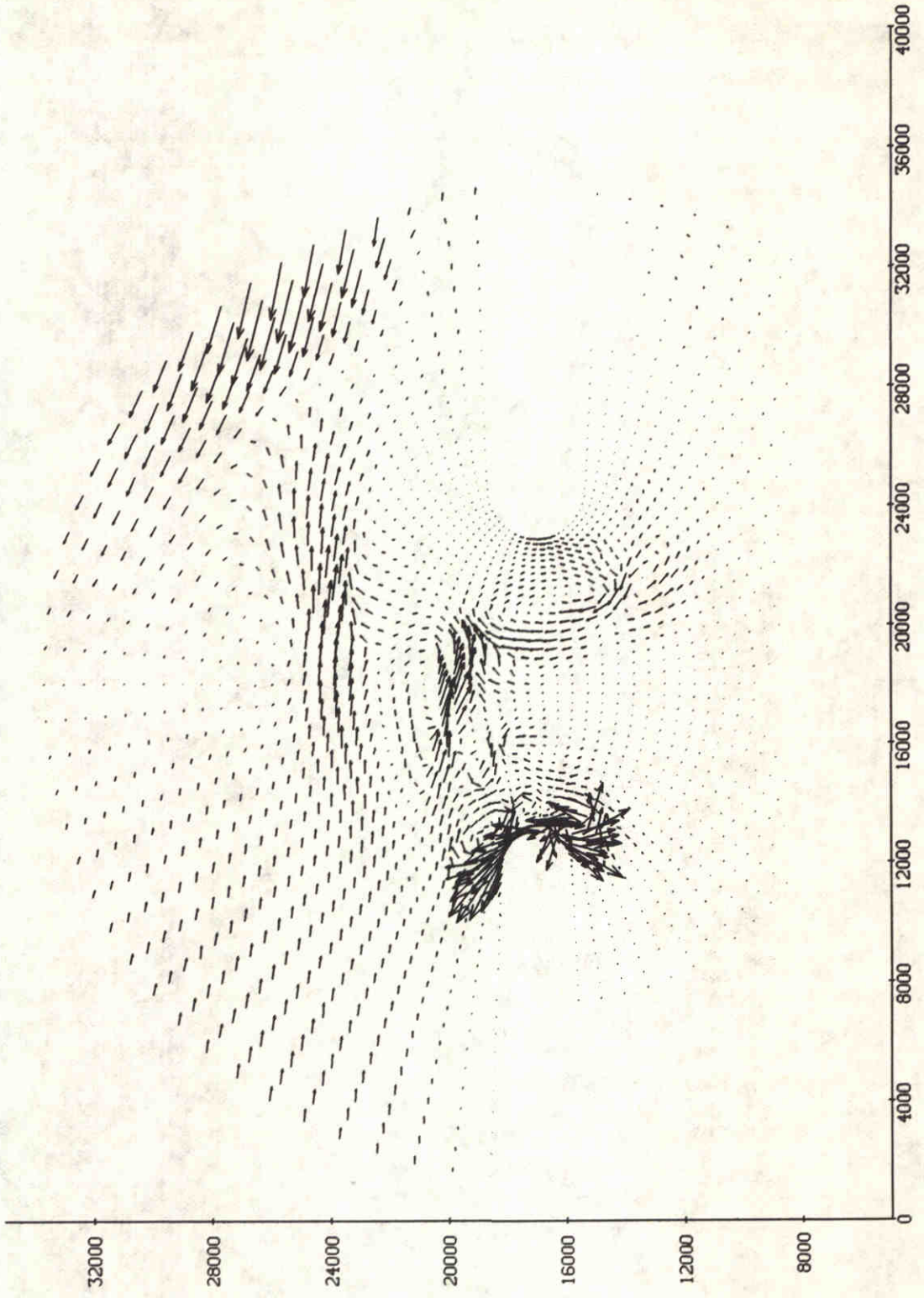

NET SEDIMENT TRANSPORT run sm7 at Tm=116 steps	sm7 91-09-20	mopinf.sm7
DELFT HYDRAULICS	H840.50	Fig. 5.14

cross sections
before and after smoothing

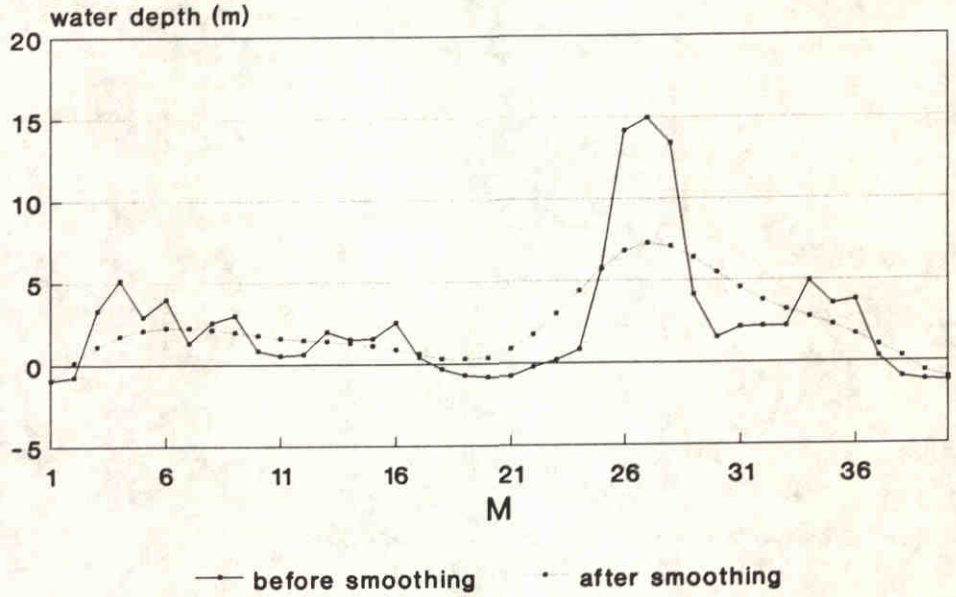

cross sections
initial and after 100 steps

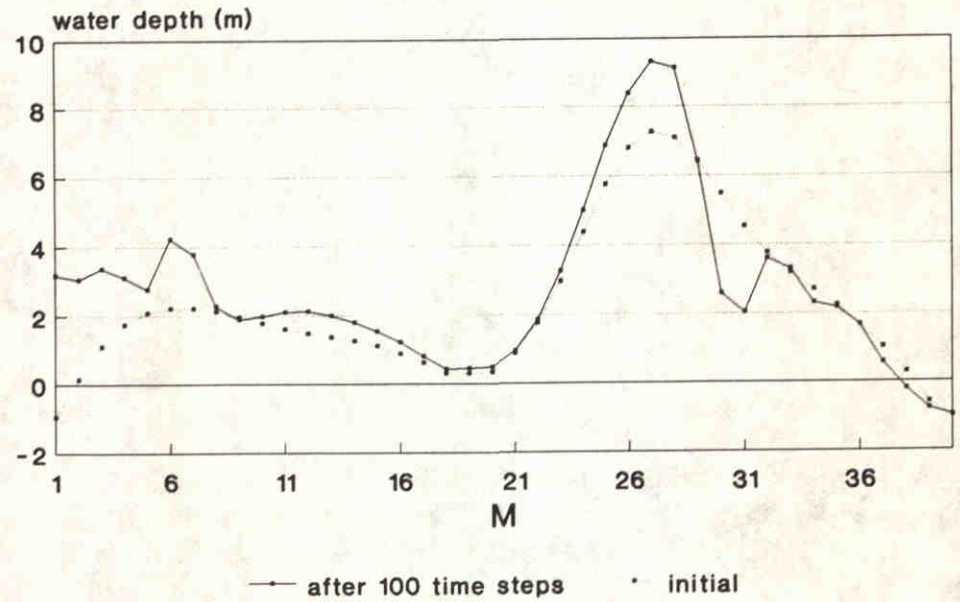

Water depth change along cross section N-25 Top: original and smoothed depth Bottom: inintial (smoothed) and computed depth		
	Kustgenese Project	
DELFT HYDRAULICS	h840.50	Fig.5.15

cross sections
before and after smoothing

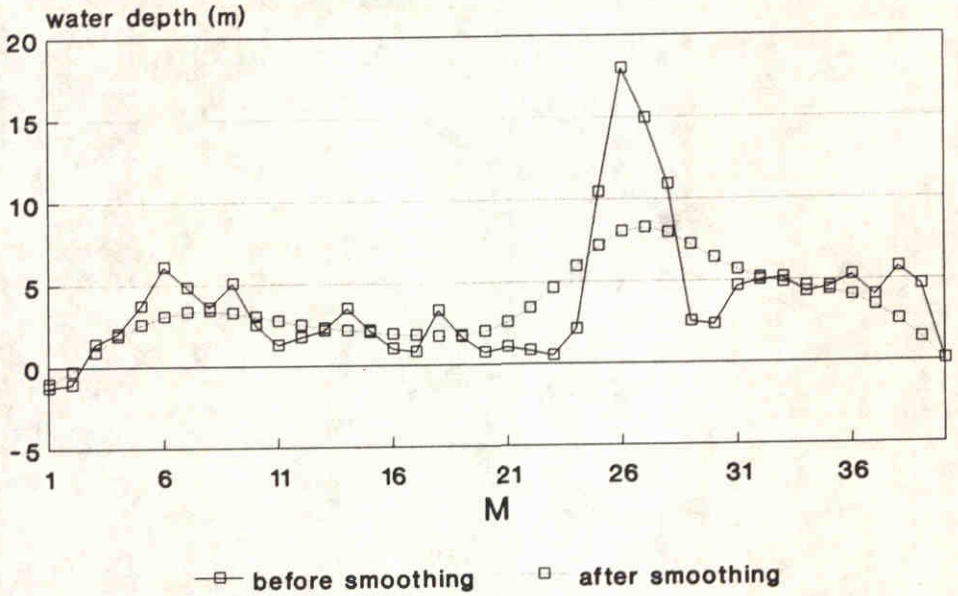

cross sections
initial and after 100 steps

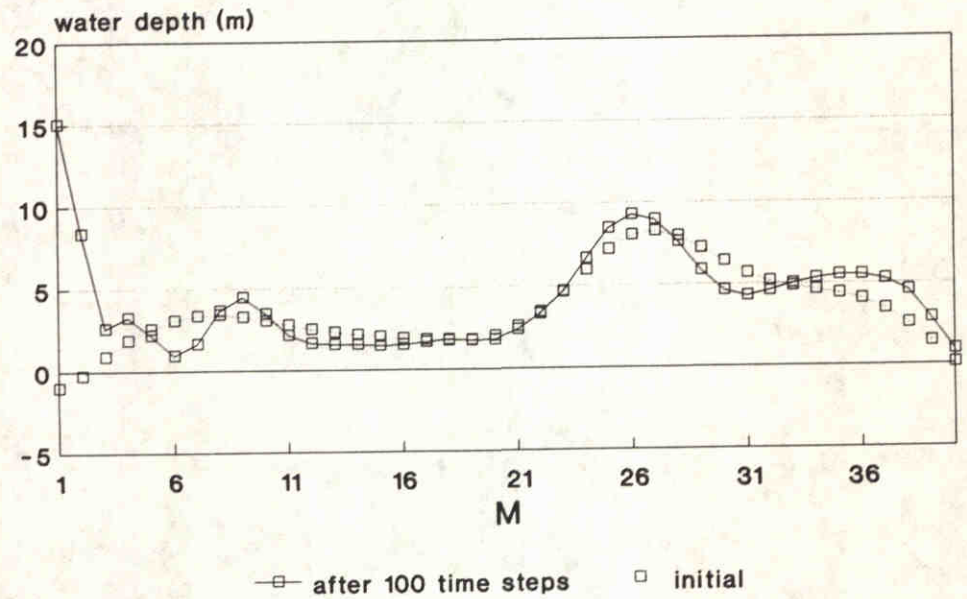

Water depth change along cross section N-28
Top: original and smoothed depth
Bottom: inintial (smoothed) and computed depth

Kustgenese Project

DELFT HYDRAULICS | h840.50 | Fig.5.16

cross sections
before and after smoothing

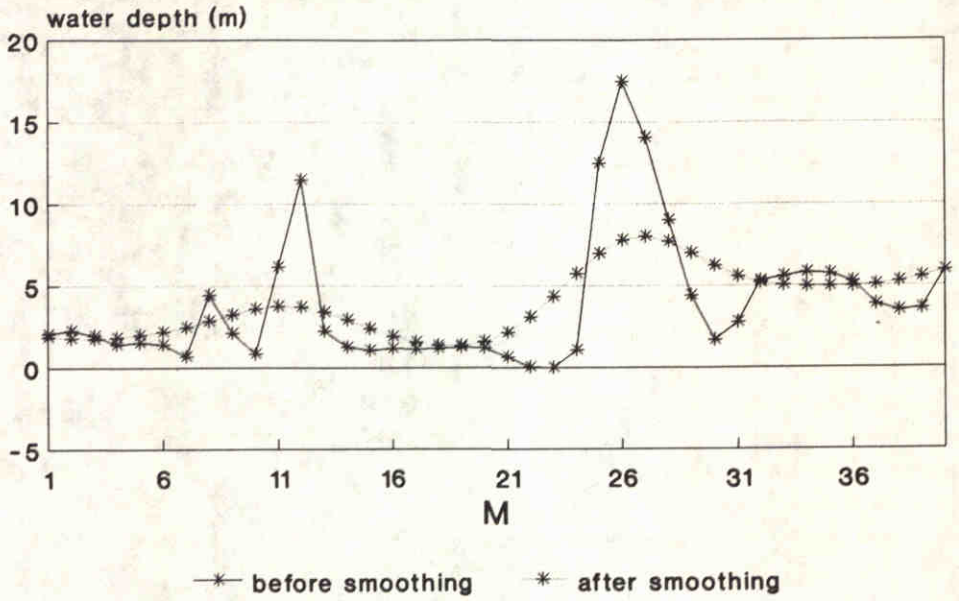

cross sections
initial and after 100 steps

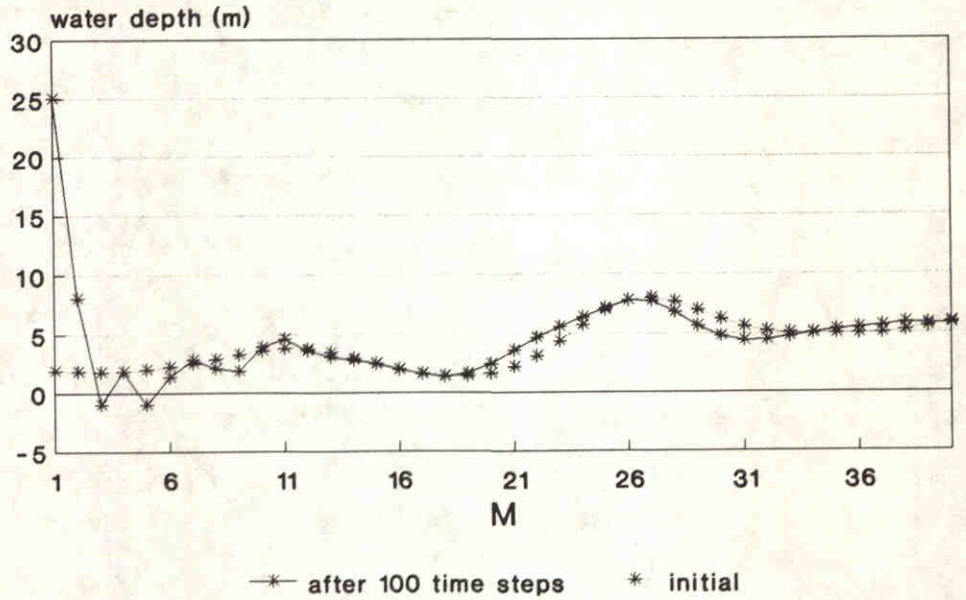

Water depth change along cross section N-31 Top: original and smoothed depth Bottom: inintial (smoothed) and computed depth		
	Kustgenese Project	
DELFT HYDRAULICS	h840.50	Fig.5.17

cross sections
before and after smoothing

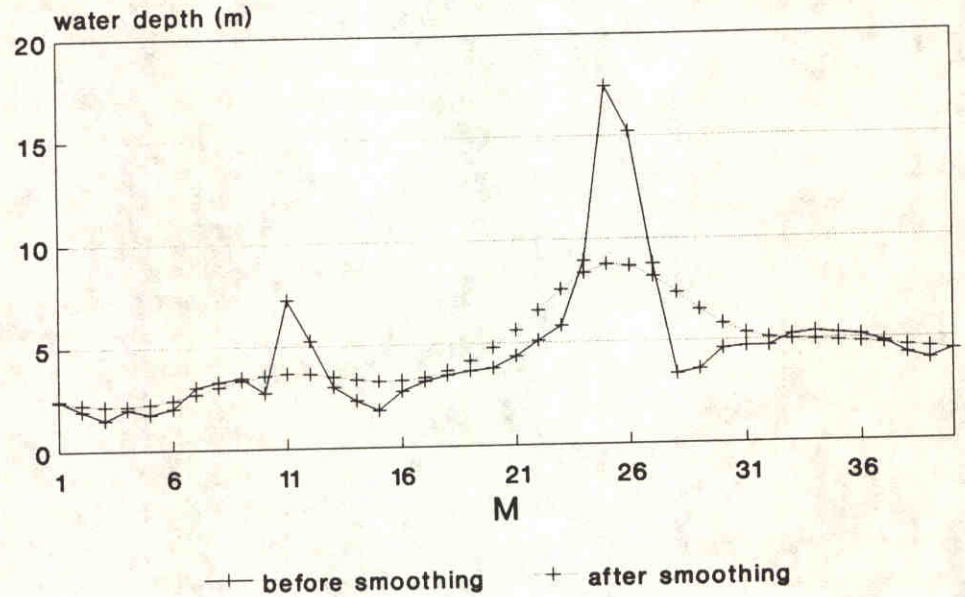

cross sections
initial and after 100 steps

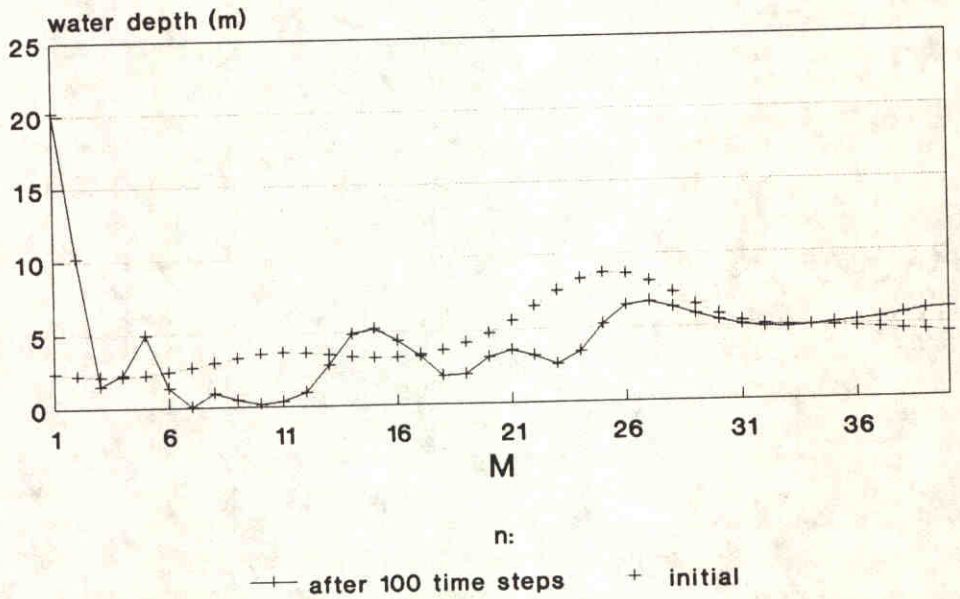

Water depth change along cross section N-34
Top: original and smoothed depth
Bottom: inintiol (smoothed) and computed depth

Kustgenese Project

DELFT HYDRAULICS | h840.50 | Fig.5.18

longitudinal profiles
before and after smoothing

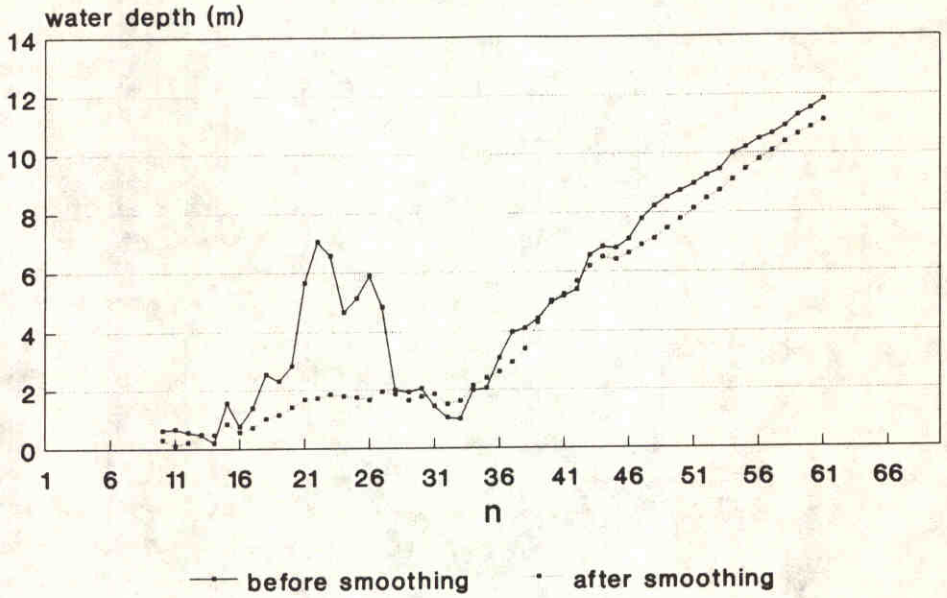

longitudinal profiles (run sm6)
after 100 time steps

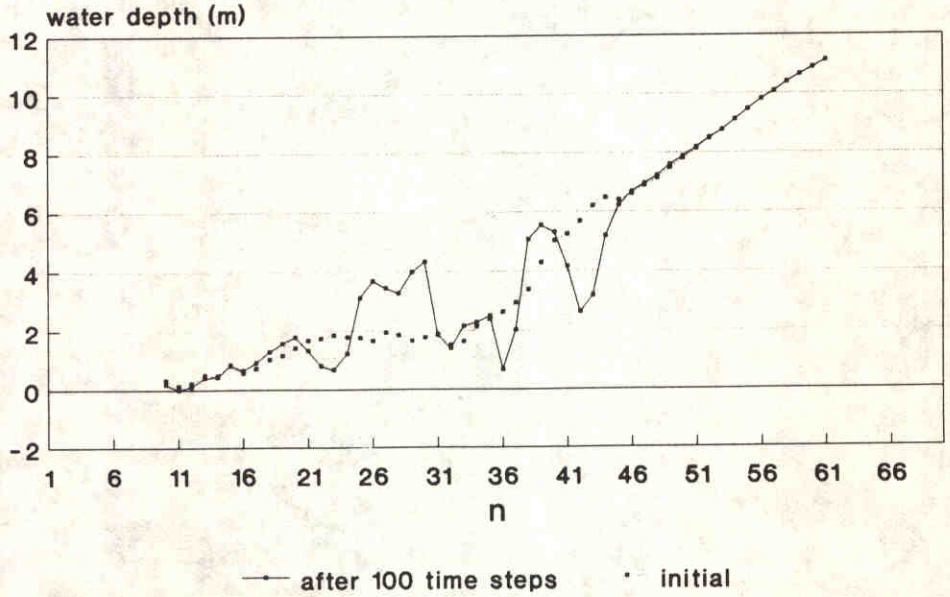

Water depth change along longitudinal profile M-4
Top: inintial (smoothed) and computed depth
Bottom: original and smoothed depth

Kustgenese Project

DELFT HYDRAULICS | h840.50 | Fig.5.19

longitudinal profiles
before and after smoothing

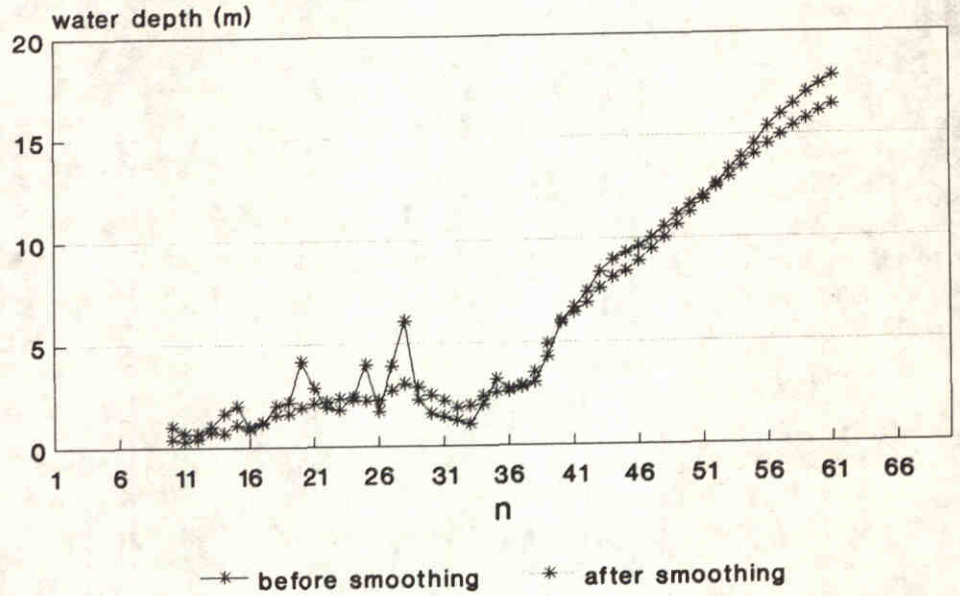

longitudinal profiles (run sm6)
after 100 time steps

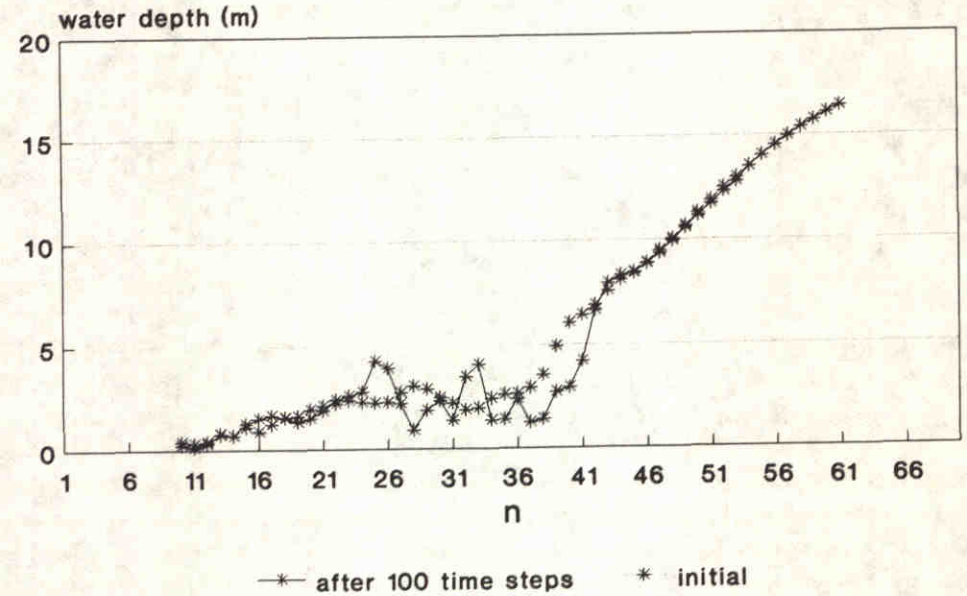

Water depth change along longitudinal profile M-6
Top: inintial (smoothed) and computed depth
Bottom: original and smoothed depth

Kustgenese Project

DELFT HYDRAULICS | h840.50 | Fig.5.20

longitudinal profiles
before and after smoothing

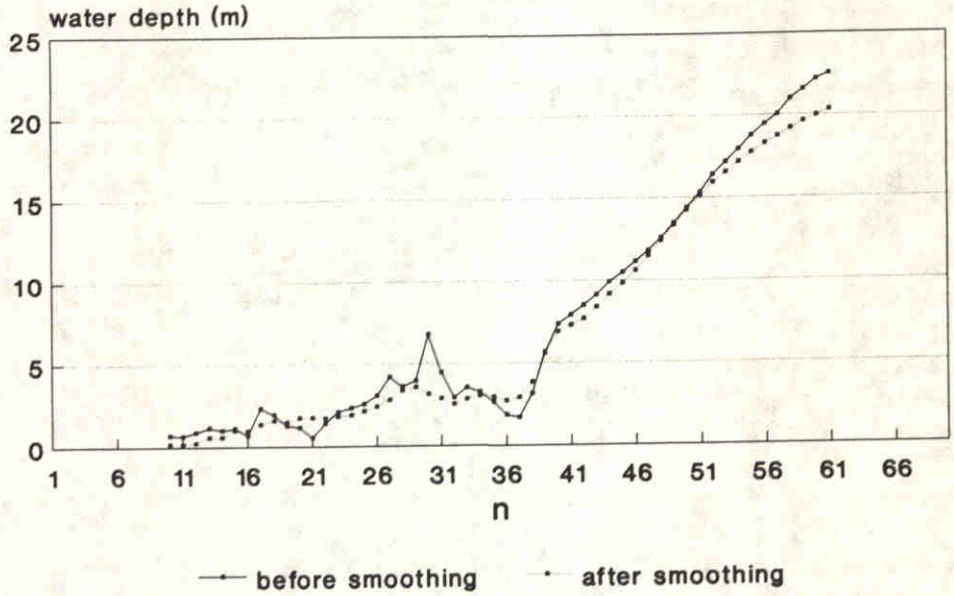

longitudinal profiles (run sm6)
after 100 time steps

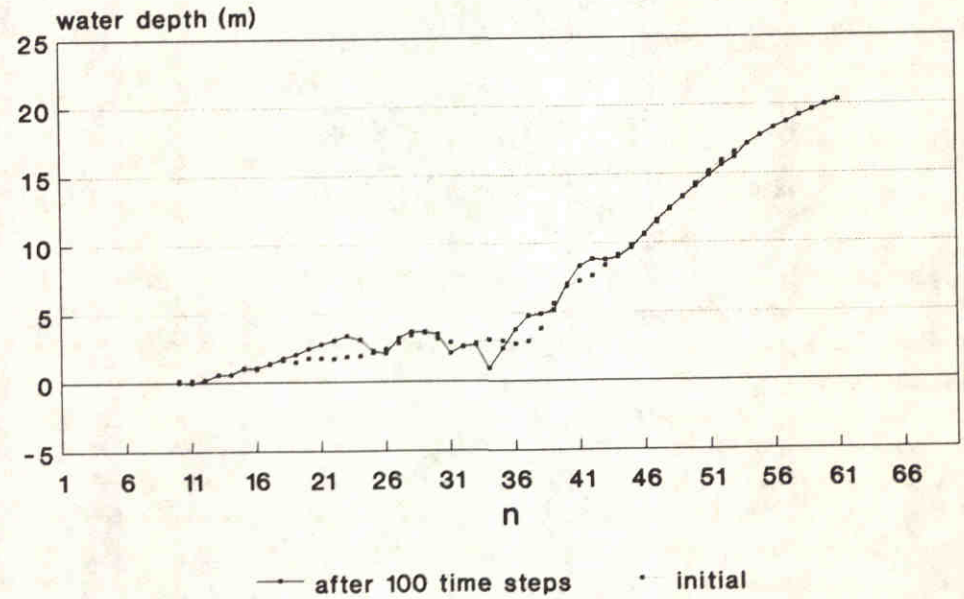

Water depth change along longitudinal profile M-8 Top: inintial (smoothed) and computed depth Bottom: original and smoothed depth		
	Kustgenese Project	
DELFT HYDRAULICS	h840.50	Fig.5.21

longitudinal profiles
before and after smoothing

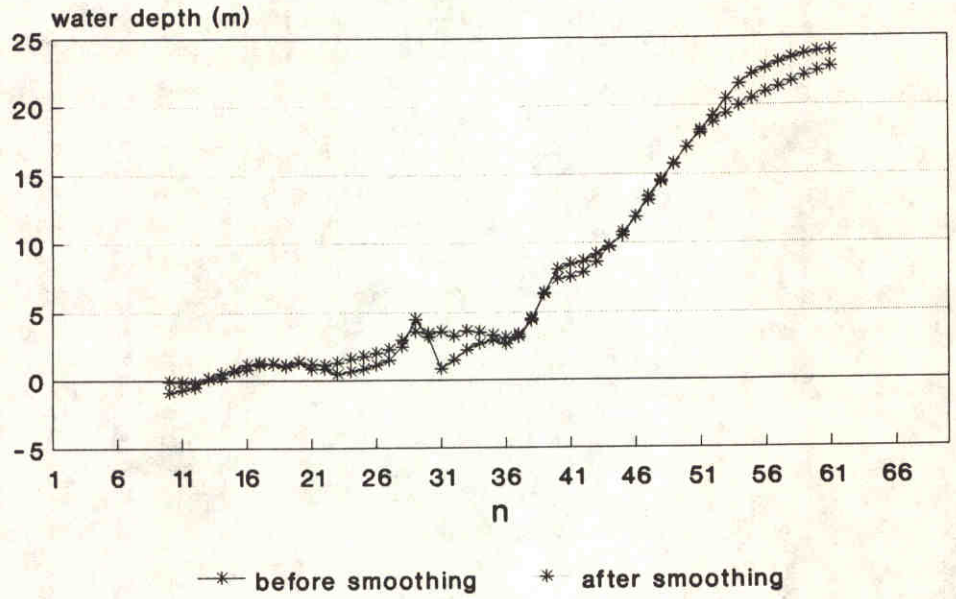

longitudinal profiles (run sm6)
after 100 time steps

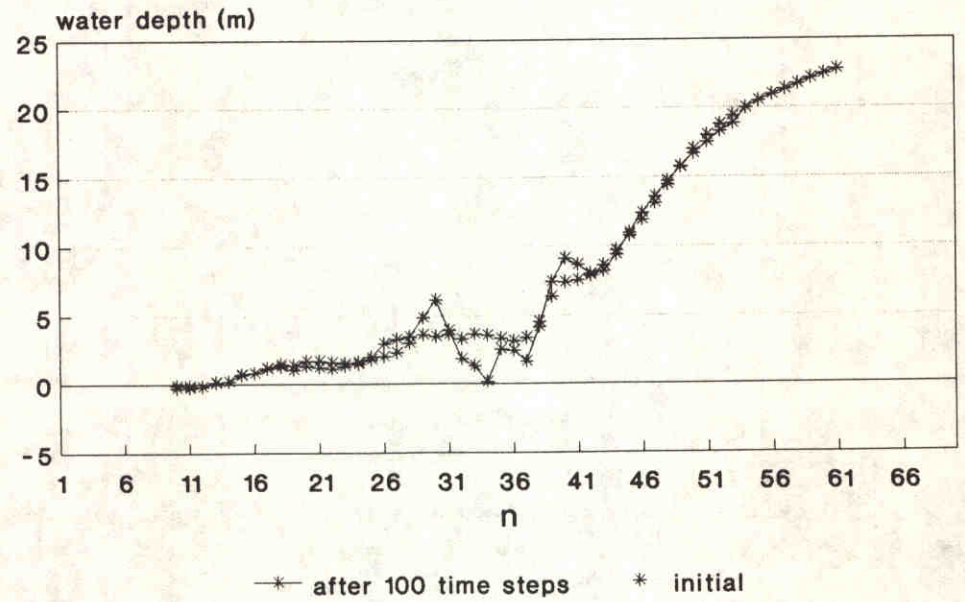

Water depth change along longitudinal profile M-10 Top: inintial (smoothed) and computed depth Bottom: original and smoothed depth		
	Kustgenese Project	
DELFT HYDRAULICS	h840.50	Fig.5.22

longitudinal profiles
before and after smoothing

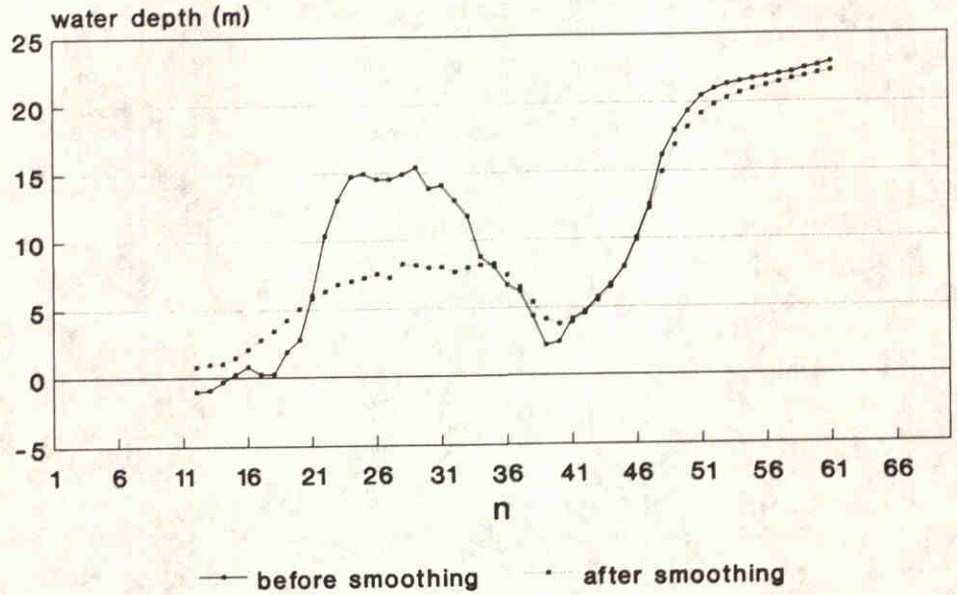

longitudinal profiles (run sm6)
after 100 time steps

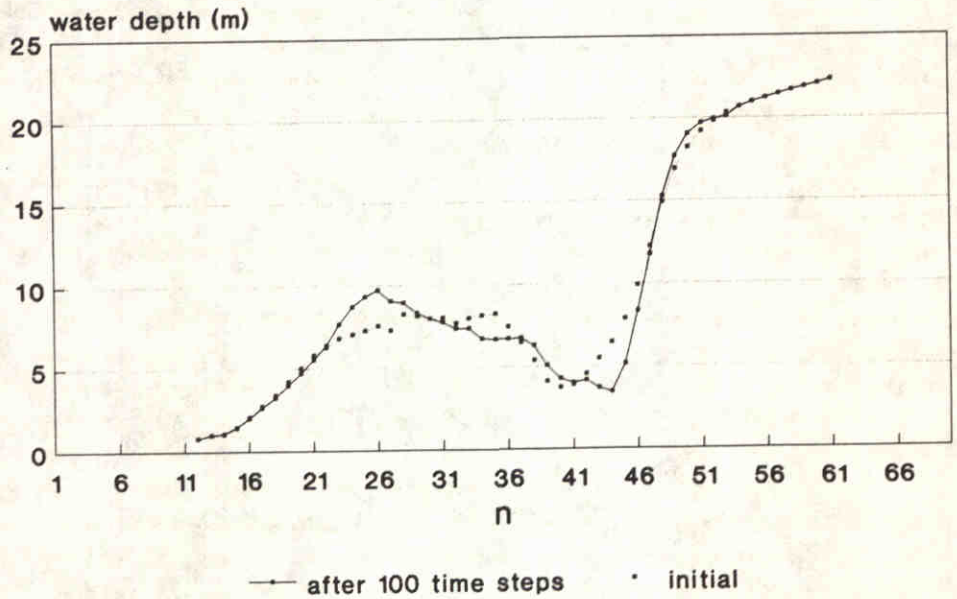

Water depth change along longitudinal profile M-27
Top: inintial (smoothed) and computed depth
Bottom: original and smoothed depth

Kustgenese Project

DELFT HYDRAULICS | h840.50 | Fig.5.23

longitudinal profiles
before and after smoothing

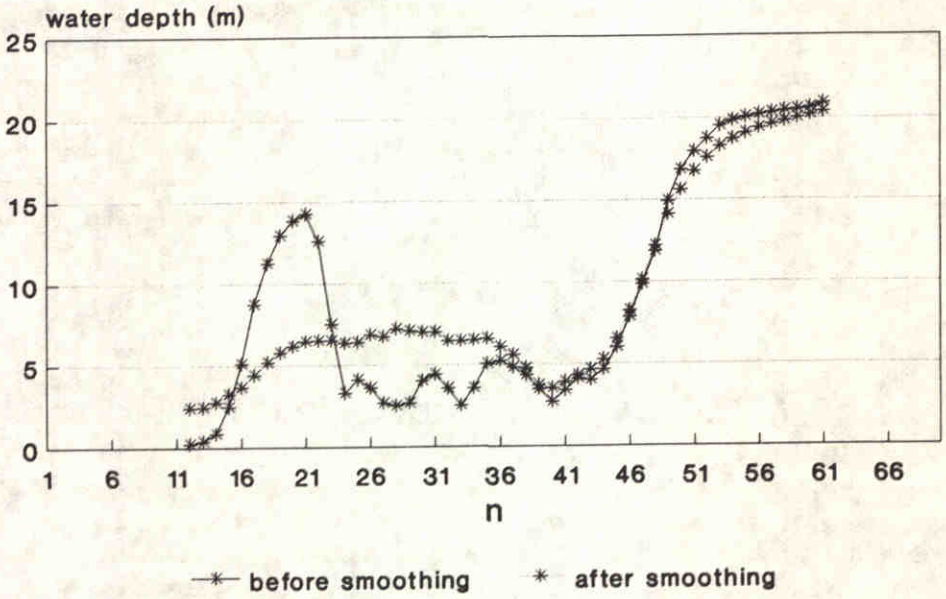

longitudinal profiles (run sm6)
after 100 time steps

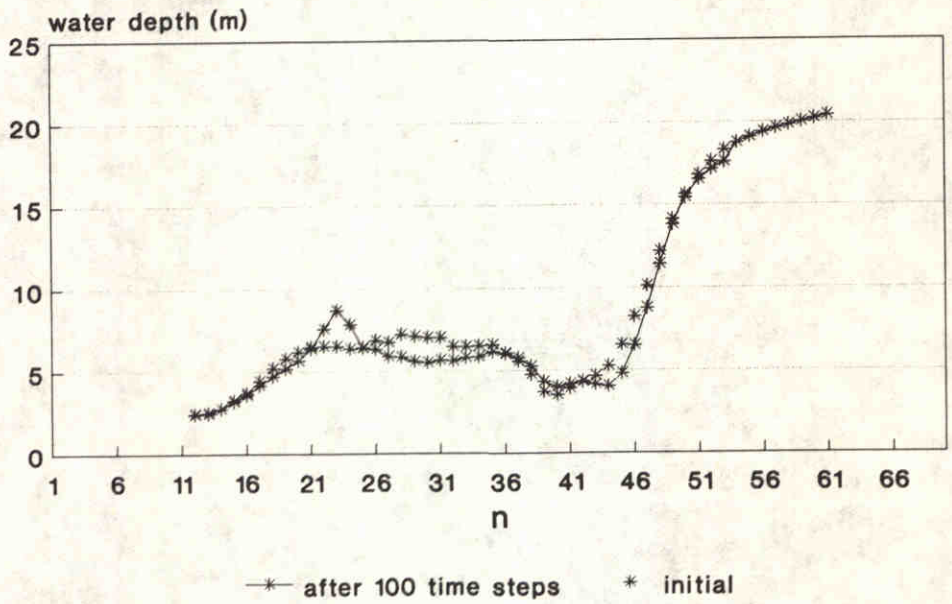

Water depth change along longitudinal profile M-29 Top: inintial (smoothed) and computed depth Bottom: original and smoothed depth		
	Kustgenese Project	
DELFT HYDRAULICS	h840.50	Fig.5.24

longitudinal profiles
before and after smoothing

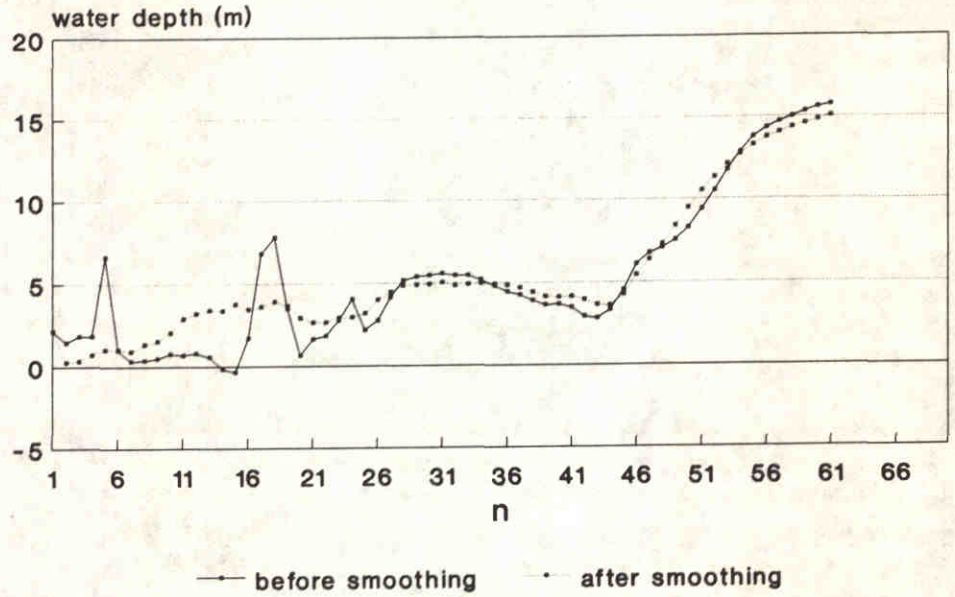

longitudinal profiles (run sm6)
after 100 time steps

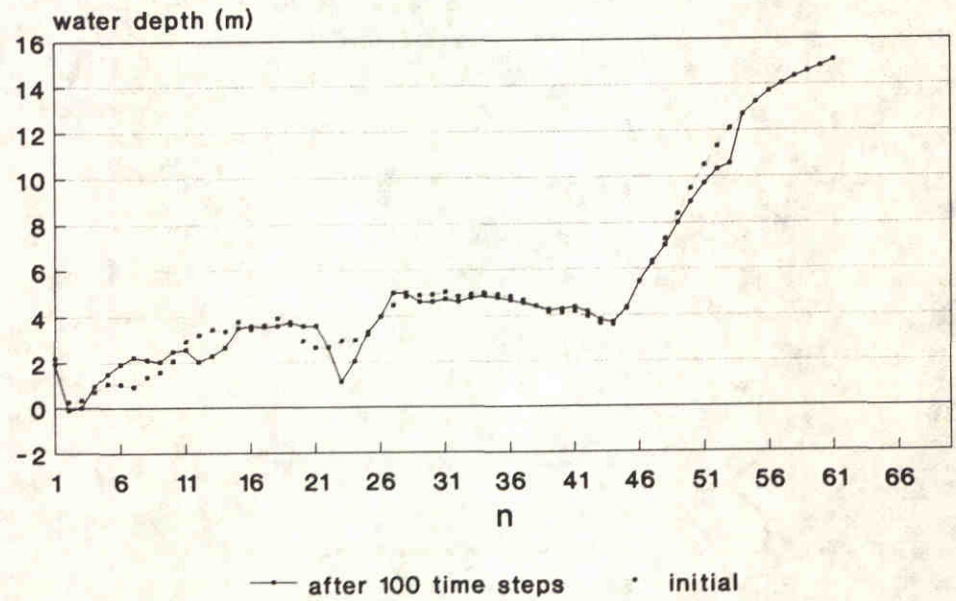

Water depth change along longitudinal profile M-33
Top: inintial (smoothed) and computed depth
Bottom: original and smoothed depth

Kustgenese Project

DELFT HYDRAULICS | h840.50 | Fig.5.25

longitudinal profiles
before and after smoothing

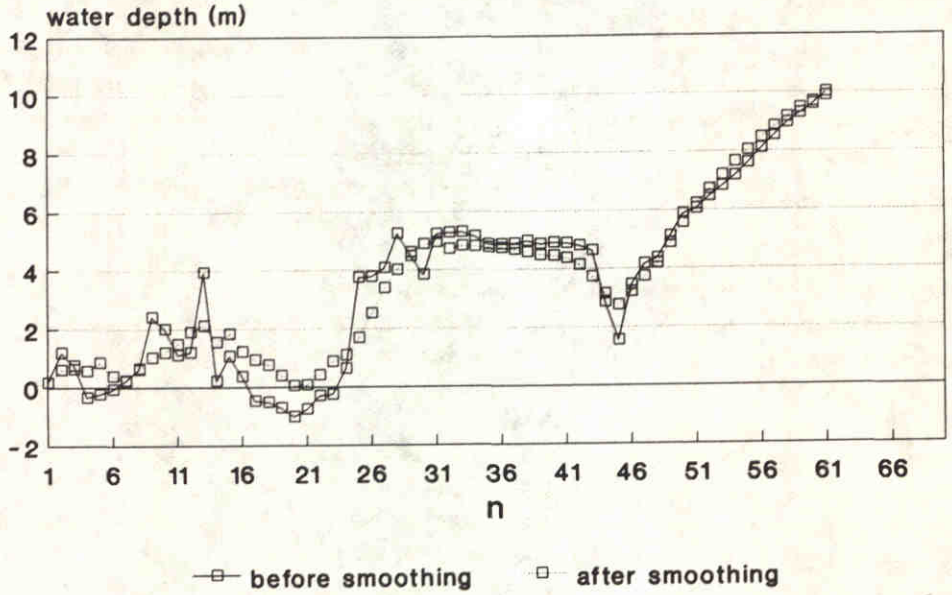

longitudinal profiles (run sm6)
after 100 time steps

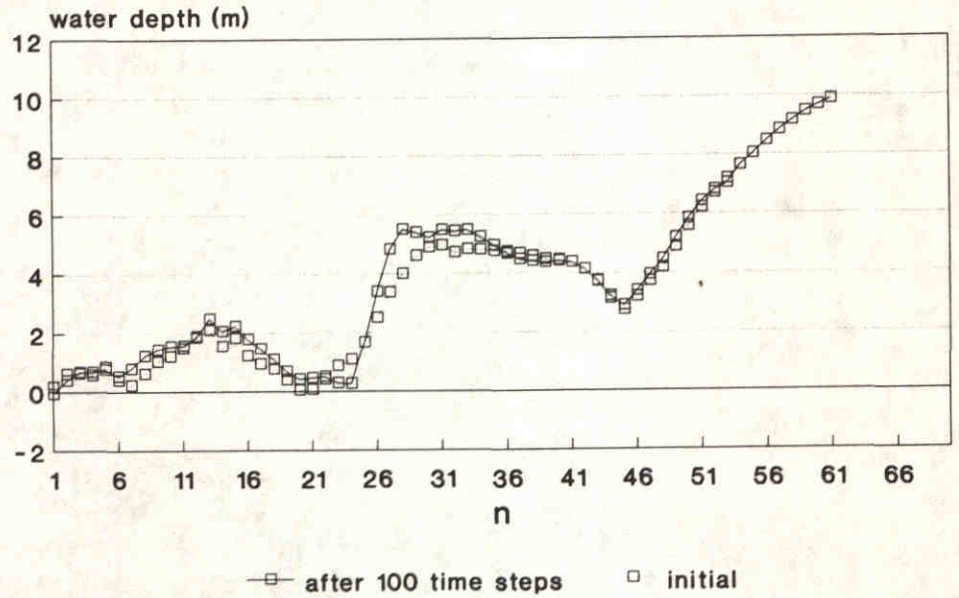

Water depth change along longitudinal profile M-36 Top: inintial (smoothed) and computed depth Bottom: original and smoothed depth		
	Kustgenese Project	
DELFT HYDRAULICS	h840.50	Fig.5.26

Schematised geometry and bathymetry before the closure of the Lauwerszee in 1969

Kustgenese Project

DELFT HYDRAULICS | h840.50 | Fig.5.27

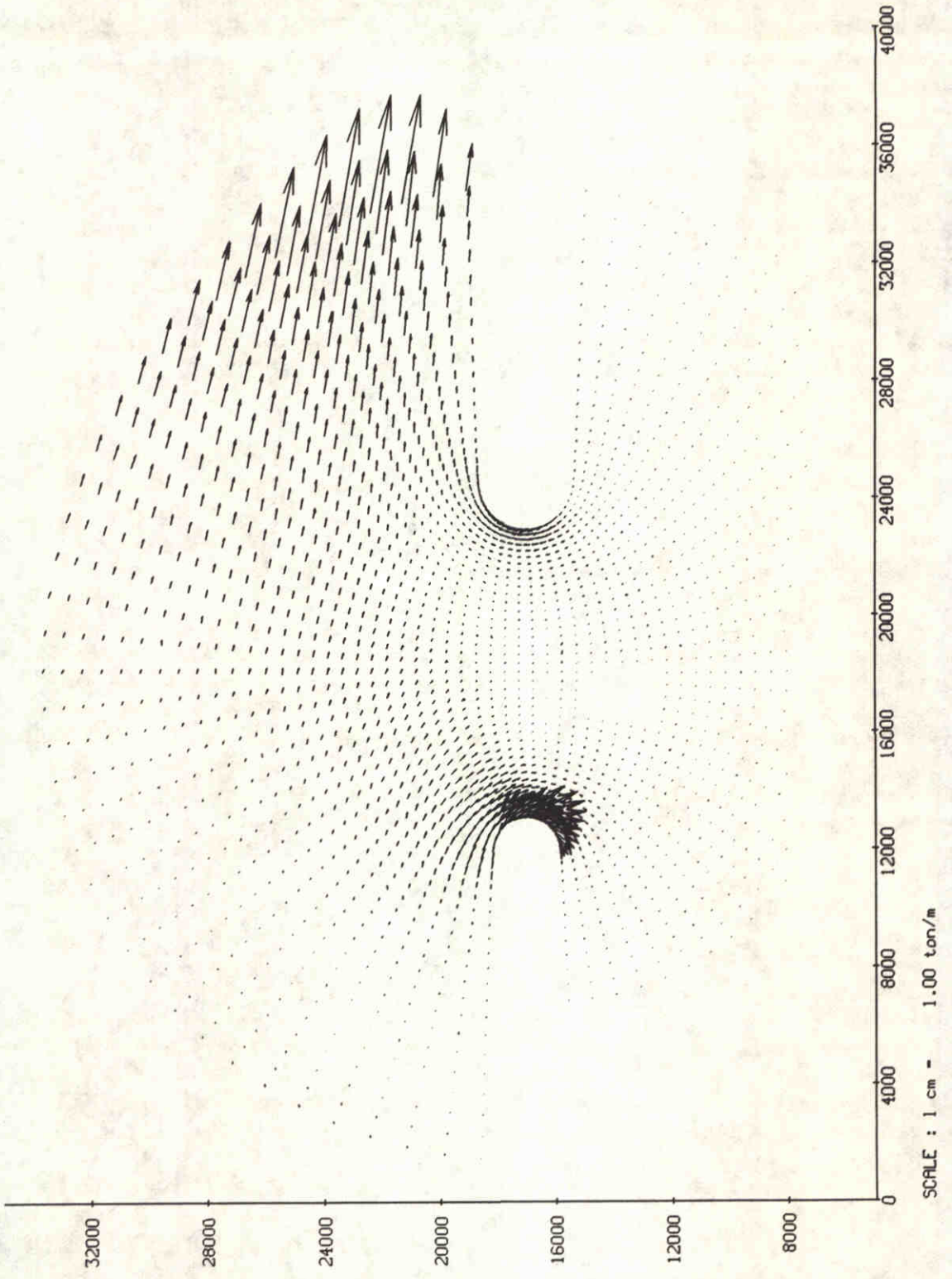

residual sediment transport run stm step = 1	stm 91-08-26	mapinf.
WATERLOOPKUNDIG LABORATORIUM	H840.50	Fig. 6.1

NET SEDIMENT TRANSPORT run sm3 at Tm=0.	sm3 91-06-20	mapinf.sm3
DELFT HYDRAULICS	H840.50	Fig. 6.2

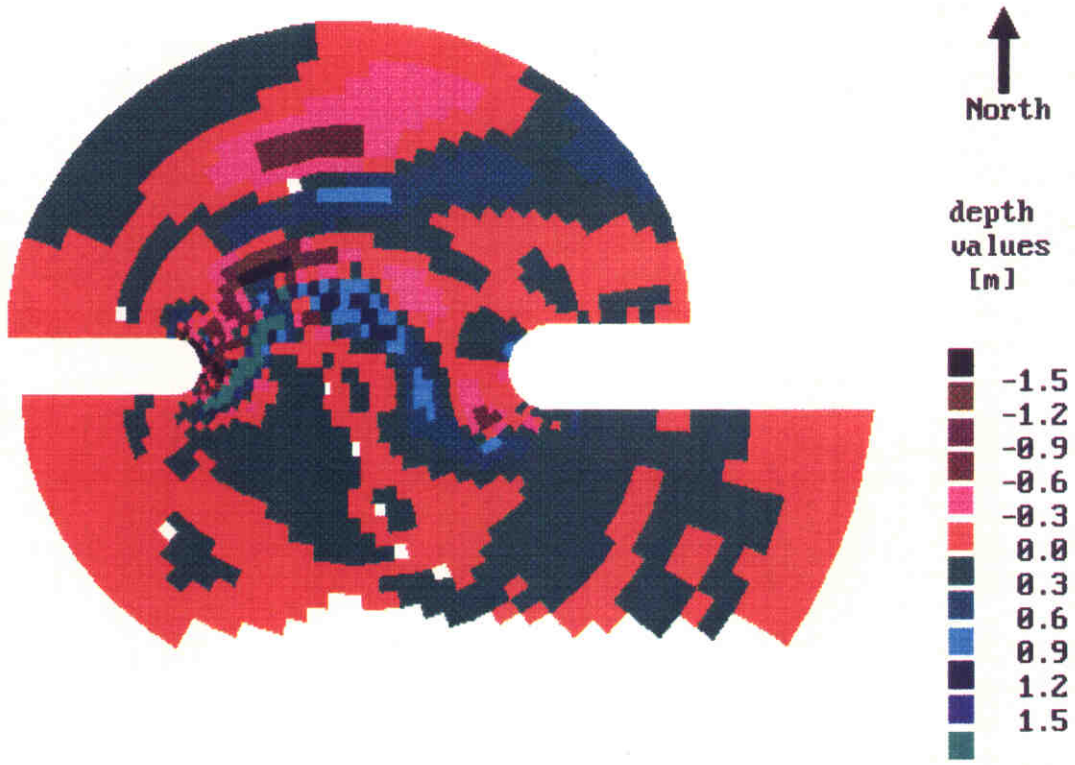

BHS1-SM6

DELFT HYDRAULICS

Difference between computed depth from run SM6 and HS1 after 45 time steps
Influence of the M4 tidal component at the boundary

Kustgenese Project

DELFT HYDRAULICS

h840.50

Fig.6.3

bed level change after 45 steps
effect of higher tidal component

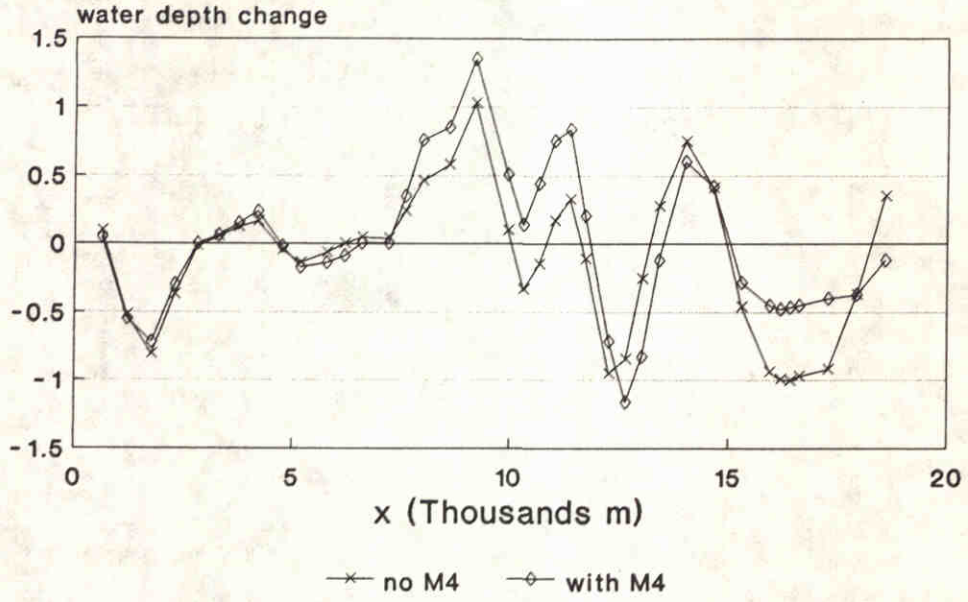

zoutkamplaag

bed level change after 45 steps
effect of higher tidal component

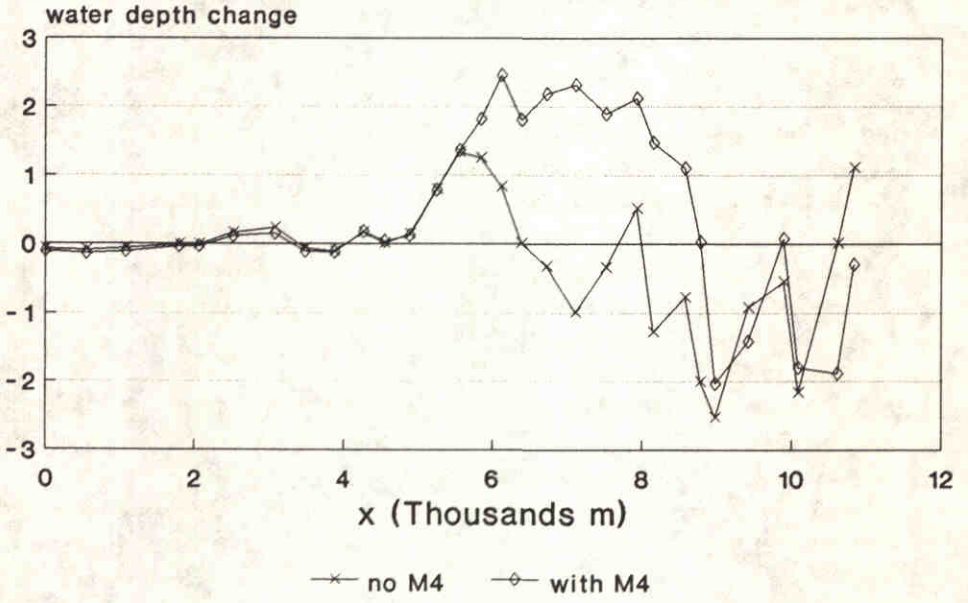

pinkgat

Water depth change from run SM6 and HS1 top: along Zoutkamplaag channel Bottom: along Pinkgat channel		
	Kustgenese Project	
DELFT HYDRAULICS	h840.50	Fig.6.4

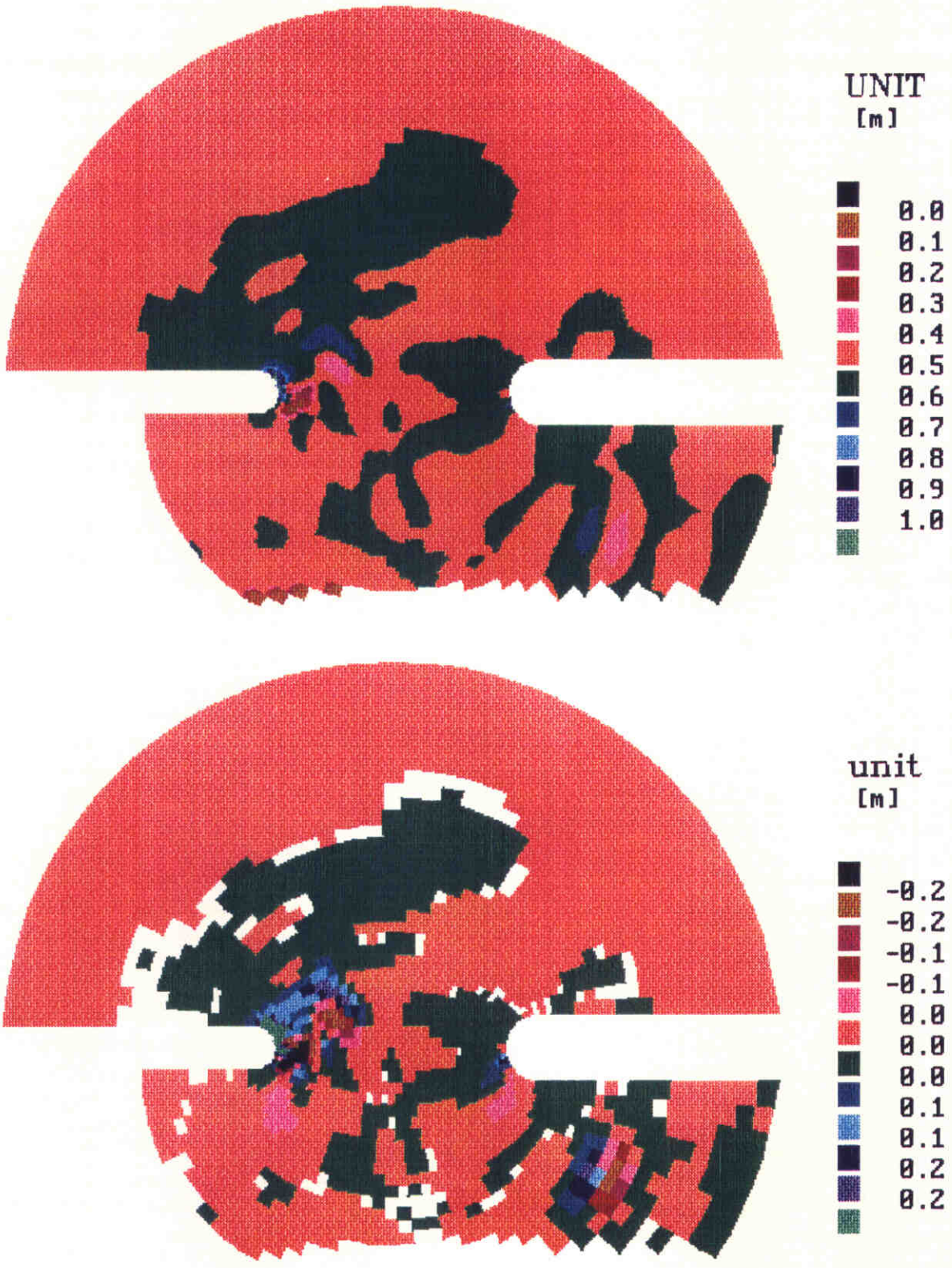

Effect of bed level sink
top: difference between depth from run D01 and SM4
Bottom: deviation from the averaged difference

Kustgenese Project

DELFT HYDRAULICS

h840.50

Fig.6.5

main office
Rotterdamseweg 185
p.o. box 177
2600 MH Delft
The Netherlands
telephone (31) 15 - 56 93 53
telefax (31) 15 - 61 96 74
telex 38176 hydel-nl

location ' De Voorst'
Voorsterweg 28, Marknesse
p.o. box 152
8300 AD Emmeloord
The Netherlands
telephone (31) 5274 - 29 22
telefax (31) 5274 - 35 73
telex 42290 hylvo-nl